# ABSTRACT

NEWNAM, ROBERT PRUETT. High Capacity Heat Exchangers for Recirculating $^{18}F$ Radionuclide Production Targets. (Under the direction of Dr. J.M. Doster).

North Carolina State University in conjunction with Bruce Technologies Inc. is developing recirculating water targets for the cyclotron production of high yields of $^{18}F$ fluoride for PET radiopharmaceuticals. Flourine-18 is commonly produced through proton irradiation of $^{18}O$ enriched water by the $^{18}O(p,n)^{18}F$ reaction. Heat deposited in the target fluid by the proton beam is proportional to the $^{18}F$ produced, thus production is often limited by the targets ability to reject heat. For power levels above 3 kW, boiling batch targets with local cooling can become impractical due to excessive $^{18}O$ water volumes. One potential solution is a recirculating target system where the target water velocity is sufficient to prevent boiling. In this design the heated fluid travels through an external heat exchanger of sufficient capacity to remove the heat, and then through a pump which returns the cooled fluid to the target. A high-flow/low-volume pump and a high-capacity/low-volume heat exchanger are essential to the overall performance of the recirculating target. In this work, two different types of heat exchangers are considered. Laboratory testing was conducted on a small shell and tube heat exchanger that removed nearly 6 kW of heat at flows provided by a miniature regenerative turbine pump. Laboratory testing was also conducted on a small cross flow heat exchanger with measured performance of 7.4 kW and predicted peak performance approaching 10 kW.

# High Capacity Heat Exchangers for Recirculating $^{18}F$ Radionuclide Production Targets

By

**Robert Pruett Newnam**

A thesis submitted to the Graduate Faculty of
North Carolina State University
in partial fulfillment of the
requirements for the Degree of
Master of Science

**Nuclear Engineering**

Raleigh, North Carolina
2007

## Approved By:

| | |
|---|---|
| Dr. M. Bourham | Dr. T. Gerig |
| Dr. M. Haider | Dr. B. Wieland |

Dr. J.M. Doster
Chair of Advisory Committee

# Biography

Robert Pruett Newnam was born on April 22, 1982 to Susan and Barry Newnam. He was raised in Canton, NC and graduated from Pisgah High School in 2000. Following graduation from high school, he started his collegiate studies at UNC-Asheville. He then transferred after two years to North Carolina State University, where he graduated Magna Cum Laude in Mechanical Engineering, May of 2004. He received a Master of Science in Nuclear Engineering from North Carolina State University in May 2007. After graduation he is beginning a career in the United States Navy.

# Acknowledgements

First I would like to thank all the members of my graduate committee. In particular, I would like to thank Dr. Doster for his support and guidance. I would also like to thank Dr. Wieland for his support and interest in my work. Additional thanks go to Matt Stokely for his support in constructing a viable lab and his help throughout my research. I would also like to thank Mark Humphrey for his drafting support and cooperation. Furthermore, I would like thank Dr. Bida for his continued support of the research performed by the North Carolina State University Department of Nuclear Engineering. I also appreciate the support of the Duke Physics machine shop for the fabrication of various items used in my research.

# Contents

# List of Figures

# List of Tables

# List of Symbols and Abbreviations

$a_0$ – 51.35

$a_1$ – -0.0137

$a_2$ – $5.115 \cdot 10^{-6}$

$a_3$ – -25.12

$a_4$ – 0.03927

$A_t$ – Total non-finned surface area of primary side tubes, $m^2$

$A_{t,finned}$ – Total finned surface area of primary side tubes, $m^2$

$A_x$ – Channel cross sectional area, $m^2$

$A_{x,c,x}$ – Inner cross sectional area of each channel, $m^2$

$A_{x,p}$ – Inner cross sectional area of each primary side tube, $m^2$

$A_{x,p,x}$ – Inner cross sectional area of each channel, $m^2$

$A_{x,t}$ – Inner cross sectional area of connection tubes, $m^2$

$C_1$ – 0.453634, table defined variable, constant

$C_{p,\,i}$ – Primary side specific heat capacity, kJ/kg·K

$C_{p,o}$ – Secondary side specific heat capacity, kJ/kg·K

$c_s$ – Input variable

$c_z$ – Table defined variable, $f(z_r)$

D – Fin diameter, m

$D_h$ – Channel hydraulic diameter, m

$d_h$ – Fin hydraulic diameter, m

$D_i$ – Channel ID, m

$D_i$ – Inner diameter of tubes, m

$D_{i,p}$ – Primary side tube ID, m

$D_{i,p,x}$ – Primary side channel ID, m

$D_{i,s}$ – Secondary side supply line ID, m

$D_{i,s,x}$ – Secondary side channel ID, m

$D_{i,t}$ – Connection tube ID, m

$d_{in}$ – Tube OD, m

$D_o$ – Outer diameter of tubes, m

$d_{out}$ – Tube OD, for smooth tubes, m

$f_{c,x}$ – Friction factor, for cold side channels of cross flow heat exchanger

$f_p$ – Friction factor, for shell and tube heat exchanger tubes

$f_{p,x}$ –Friction factor, for hot side channels of cross flow heat exchanger

$f_s$ – Friction factor, for cold side supply tubes

$f_t$ – Friction factor, for connection tubes

G – Volumetric flow rate, LPM

H – Channel height, m

h – Fin height, m

$h_c$ – Convective heat transfer coefficient, $W/m^2 \cdot K$

$h_{c,p}$ – Primary side convective heat transfer coefficient, $W/m^2 \cdot K$

$h_{c,p}$ – Primary side convective heat transfer coefficient, $W/m^2 \cdot K$

$h_{c,s}$ – Secondary side convective heat transfer coefficient, $W/m^2 \cdot K$

$h_{c,s}^{finned}$ – Finned secondary side heat transfer coefficient, $W/m^2 \cdot K$

$h_i$ – Primary side convective heat transfer coefficient, $W/m^2 \cdot K$

$h_o$ – Secondary side convective heat transfer coefficient, $W/m^2 \cdot K$

k – Fluid thermal conductivity, W/m·K

$K_{c,x}$ – Cross flow secondary side forms loss coefficient

$k_p$ – Primary side fluid thermal conductivity, W/m·K

$k_p$ – Primary side fluid thermal conductivity, W/m·K

$K_p$ – Primary side forms loss coefficient

$K_{p,x}$ – Primary side forms factor for cross flow heat exchanger

$k_s$ – Secondary side fluid thermal conductivity, W/m·K

$K_s$ – Secondary side supply line forms losses

$K_t$ – Connection tube forms loss coefficient

$l$ – Characteristic fin length, m

$L_{c,x}$ – Secondary side channel length, m

$L_p$ – Primary side tube length, m

$L_{p,x}$ – Primary side channel length, m

$L_s$ – Secondary side supply line length, m

$L_t$ – Connection tube length, m

m – 0.563446, table defined variable, constant

$\dot{m}_i$ – Primary side mass flow rate, kg/s

$\dot{m}_o$ – Secondary side mass flow rate, kg/s

n – Constant, 0.4 for a heated fluid and 0.3 for a cooled fluid

$N_B$ – Number of baffles

$N_{c,p}$ – Number of primary side channels

$N_{c,s}$ – Number of secondary side channels

$N_t$ – Number of primary side tubes

Pr – Prandtl number

$Pr_p$ – Primary side fluid prandtl number

$Pr_p$ – Primary side fluid prandtl number

$Pr_s$ – Secondary side fluid prandtl number

$P_{supply}$ – Secondary side header pressure, psig or Pa

$P_w$ – Wetted perimeter, m

Q – Heat transfer rate, kW

Re – Reynolds Number, valid for heat exchanger and supply tubes

$Re_d$ – Secondary side Reynolds number based on $d_{out}$

$Re_{d,max}$ – Maximum Reynolds number corresponding to $V_{c,max}$

$Re_l$ – Secondary side Reynolds number based on *l*

$R_{f,i}$ – Primary side fouling factor, $m^2 \cdot K/W$

$R_{f,o}$ – Secondary side fouling factor, $m^2 \cdot K/W$

$S_l$ – $S_T$ – $S_D$ – Tube Pitch, equal, m

$S_{f\delta}$ – Distance between tube bases, m

ShellD – Shell ID, m

$S_p$ – Fin length plus fin width, m

$\bar{S}$ – Tube pitch ratio

t – Primary side tube wall thickness, m

$T_{in,\,i}$ – Primary side inlet temperature, $T_{sat}$ @ $P_{sat}$, K

$T_{in,\,o}$ – Secondary side inlet temperature, K

$T_{out,\,i}$ – Primary side outlet temperature, K

$T_{out,\,o}$ – Secondary side outlet temperature, K

UA – Overall heat transfer coefficient, W/K

$V_c$ – Speed of secondary side fluid across tube bundle, m/s

$V_{c,max}$ – Maximum occurring velocity in secondary side, m/s

$V_{c,x}$ – Velocity through secondary side channels, m/s

$V_p$ – Velocity through primary side tubes, m/s

$V_{p,x}$ – Velocity through primary side channels, m/s

$V_s$ – Supply line fluid velocity, m/s

$V_t$ – Velocity through connection tubes, m/s

W – Channel width, m

$z_r$ – Number of tubes in widest row

$\delta$ – Fin width, m

$\Delta P_c$ – Secondary side pressure drop, Pa

$\Delta P_h$ – Primary side pressure drop, Pa

$\Delta P_{HX}$ – Heat exchanger pressure drop, Pa

$\Delta P_p$ – Change in pressure across the pump, kPa

$\Delta P_{pressurizer}$ (G) – Pressure drop vs. flow correlation for pressurizer

$\Delta P_s$ – Supply line pressure drop, Pa

$\Delta P_{target}$ (G) – Pressure drop vs. flow correlation for target

$\Delta T_{lm}$ – Log mean temperature difference, K

$\eta_f$ – Fin efficiency, constant, 95%

$\mu_p$ – Primary side fluid viscosity, $N{\cdot}s/m^2$

$\mu_s$ – Secondary side fluid viscosity, $N{\cdot}s/m^2$

$\rho_p$ – Primary side fluid density, $kg/m^3$

$\rho_s$ – Secondary side fluid density, $kg/m^3$

$\Omega$ – Rotational speed of motor, RPM

# Chapter 1

# Introduction

## 1.1 Background

Imaging techniques used in modern medicine provide quality, *in vivo* pictures of internal human anatomy as well as biochemical and physiological processes. These techniques record geometrical and functional information. Positron Emission Tomography (PET) is an imaging technique that captures metabolic activity within the body. PET is particularly useful in the detection of cancer.

PET imaging is based upon the detection of radionuclide decay from radiopharmaceuticals injected into a patient's blood stream. One such radiopharmaceutical is the sugar 2-deoxy-2-[$^{18}$F]fluoro-D-glucose ($^{18}$FDG), which is bonded with the fluorine-18 ($^{18}$F) isotope. Once a patient has been injected with $^{18}$FDG, the radiopharmaceutical is dispersed throughout the body. Cancerous areas, which have high metabolic rates, will accumulate a higher percentage of $^{18}$FDG. Subsequently, these areas will have elevated concentrations of the $^{18}$F radioisotope from the metabolically trapped radiopharmaceutical. [11]

The radioisotope fluorine-18 ($^{18}$F) decays by positron emission with a half life of 109.7 minutes. The positron slows down over a short distance before combining with an electron, resulting in the emission of two 511 keV annihilation photons 180° apart. Using a coincidence counter, the photons can then be recorded and the emission point computed. This information is then used to create a 3-dimensional image. [11]

Fluourine-18 is commonly produced with cyclotrons through the $^{18}$O(p,n)$^{18}$F reaction. In typical production targets liquid $H_2{}^{18}O$ is bombarded with protons of energy 2.4 MeV or greater. Due to the small reaction cross section, several thousand incident

protons are necessary to produce one $^{18}F$ radionuclide [6]. Therefore, this process produces large amounts of waste heat as the protons deposit their kinetic energy in the target water. A major challenge in target design is the efficient removal of this waste heat.

## 1.2 Purpose

The recirculating target is one design under consideration for the production of the $^{18}F$ radionuclide. Common to all $^{18}F$ water targets, large amounts of waste heat is deposited in the target fluid during operation. Therefore, a common problem for all designs is effective target cooling. A recirculating target pumps the heated fluid to an external heat exchanger where the heat is transferred to a low temperature heat sink. A typical design constraint for recirculating targets is that the target water remains below the boiling point at all times. Figure 1 shows the general layout of the recirculating target system.

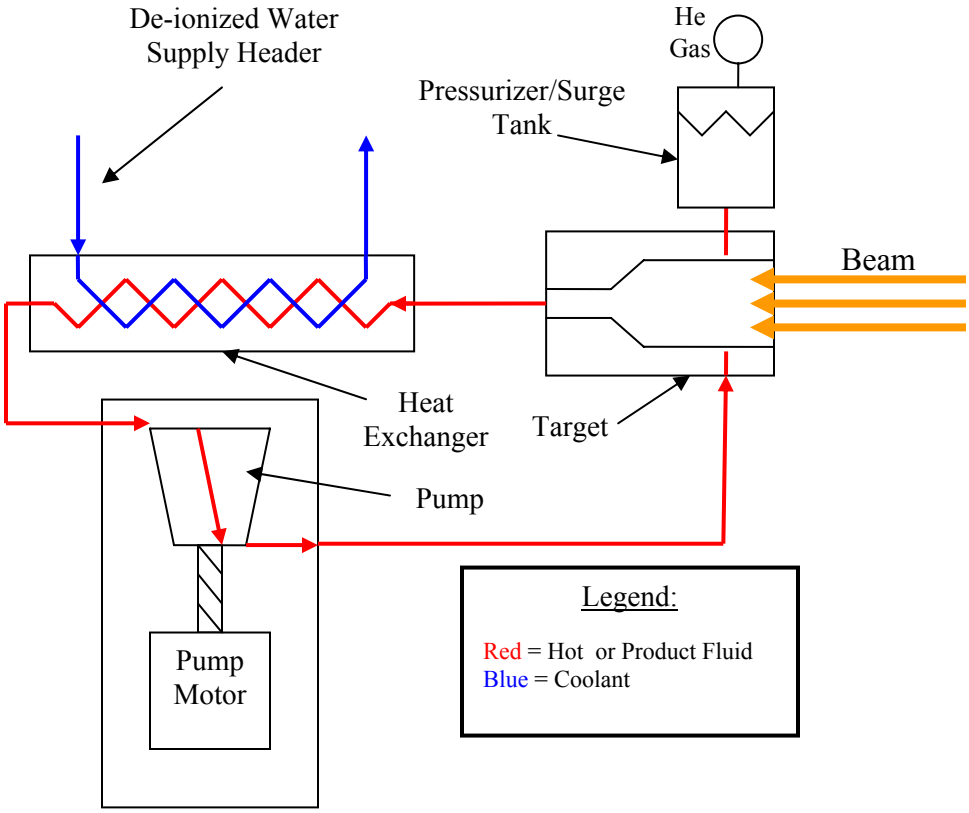


Figure 1: General layout of recirculating target system

A first generation recirculating target design incorporated a two-pass, plate-type heat exchanger as the primary heat sink [1]. This heat exchanger had multi pass flow channels with the intent of increasing surface area and heat transfer efficiency. The heat exchanger was tested at heat transfer rates up to 4.5 kW, but weighed in excess of 20 pounds and had an internal target water volume of 17 mL. It was discovered that this heat exchanger had misaligned plates that reduced its effectiveness. Even so, the design still fell short of the overall goals of the recirculating target system. When considering weight alone, this design was by no means compact. The design goals for the recirculating target are heat transfer rates in excess of 10 kW with minimum weight and volume. It is unlikely that the two pass plate-type heat exchanger has the necessary capacity, or can be easily implemented in a recirculating target system. Figure 1 shows a picture of the first generation plate-type heat exchanger. [1]

Figure 2: First generation two pass plate-type heat exchanger [1]

New designs are required to expand the options available for providing efficient, compact, and high capacity heat removal for the recirculating target system. Three goals are essential to the success of a new heat exchanger design. These goals include: having a small primary or "product" side volume, physical dimensions that allow for easy implementation into an integrated target design, and a heat removal rate of 10 kW. Two

competing heat exchanger designs are considered in this work, a counter flow shell and tube heat exchanger, and a compact cross flow heat exchanger. The specific aims of this research are:

- Design, optimize and test a compact shell and tube heat exchanger compatible with the regenerative turbine pump and the integrated recirculating target system
- Design, optimize and test a compact cross flow heat exchanger compatible with the regenerative turbine pump and the integrated recirculating target system
- Simulate the performance of the integrated recirculating target system with the selected heat exchanger under different operating conditions and heat loads

Cross flow heat exchangers are more commonly used for compact designs, whereas shell and tube heat exchangers are commonly found in larger more robust applications such as cooling industrial machinery oils. Shell and tube heat exchangers are suitable for this application because they are easily implemented into industrial settings, and are relatively cheap to construct and repair. This study discusses the design, simulation, and selection of both types of heat exchangers. It also serves as research tool to successfully compare these designs for their potential integration into the recirculating target system. [5, 8]

## 1.3 Related Research

Currently, North Carolina State University in conjunction with Bruce Technologies, Inc. is developing two innovative target systems for increased production of the $^{18}F$ radionuclide. One of these target systems is the recirculating target design. The other is a thermosyphon batch target.

The thermosyphon target uses boiling in combination with condensing heat transfer to cool the enriched water during bombardment. This is accomplished by incorporating a condensing region within the target directly above the beam strike. Jetting on the backside of the target combined with cooling channels within the target body, are used as the low temperature heat sink. This target design is self regulating in that the condensing height adjusts automatically according to the heat load. Practical thermosyphon target designs have been simulated with heat rejection rates up to 3 kW. [10]

## 1.4 Heat Exchanger Design Parameters

New heat exchanger designs must be compatible with existing components such as the regenerative turbine pump and recirculating target bodies. The current regenerative turbine pump is being redesigned and is expected to have improved performance. Therefore, if a heat exchanger can successfully fulfill all design objectives with the flow rates delivered by the current pump, the design objectives should also be satisfied with the redesigned pump. Independent of heat exchanger geometry, the main objective for a new heat exchanger is to deliver the maximum heat transfer with the smallest possible primary side volume.

The secondary side inlet temperature for this study is set by the cooling water supply to the Duke CS-30 Cyclotron. At different production locations this value will likely change. Also, the design goals for the recirculating target system are a 10+ kW operational load. If lower loads are desired it may become economical to design a lower capacity heat exchanger or change the number of heat exchangers in the system, thus minimizing excess volume. Table 1 gives the design objectives and constraints for the new heat exchangers.

Table 1: Design Constraints and Objectives

| | |
|---|---|
| **Primary Side Restrictions:** | |
| Primary Side Volume: | **≤ 10 mL (Without Manifolds)** |
| Heat Transfer Rate: | **10 kW** |
| Primary Side Pressure: | **≤ 500 psia** |
| Pump Characteristics: | ***Turbine Pump Performance Curve*** |
| **Secondary Side:** | |
| Pressure Head: | **75 psig** |
| Inlet Temperature, De-Ionizer: | **68 °F** |
| Supply Line ID: | **3/8 in** |
| Supply Line Length: | **20 ft** |

# Chapter 2

# Compact Shell and Tube Heat Exchanger

## 2.1 Description

A shell and tube heat exchanger is comprised of a large outer shell (typically cylindrical) with a series of staggered or in-lined tubes inside the shell. One fluid flows within the tubes, while the second fluid flows through the shell over the outside of the tube bundle. In practice, the hot or cold fluid can be contained in either the inside or the outside of the tubes. For example, in a steam condenser the cold fluid flows on the inside of the tubes and the steam is allowed to pass over the tubes and condense. Alternately, the hot fluid can flow on the inside of the tubes and the cold fluid can flow on the outside as with industrial oil coolers. [5, 8]

After setting which side of the heat exchanger will be the primary side (the hot fluid) and the secondary side (the cold fluid), it is necessary to select either a counter or parallel flow configuration. In counter flow heat exchangers, the primary and secondary sides flow in opposite directions, whereas in parallel flow heat exchangers both sides flow in the same direction. Counter flow promotes a higher log mean temperature difference between the primary and secondary side, thus promoting more efficient heat transfer. Using counter flow typically reduces necessary area and/or flow velocity required to produce a desired heat transfer rate. As a result, counter flow designs are the most commonly used. Figure 2 shows the flow paths in a typical counter flow shell and tube heat exchanger.

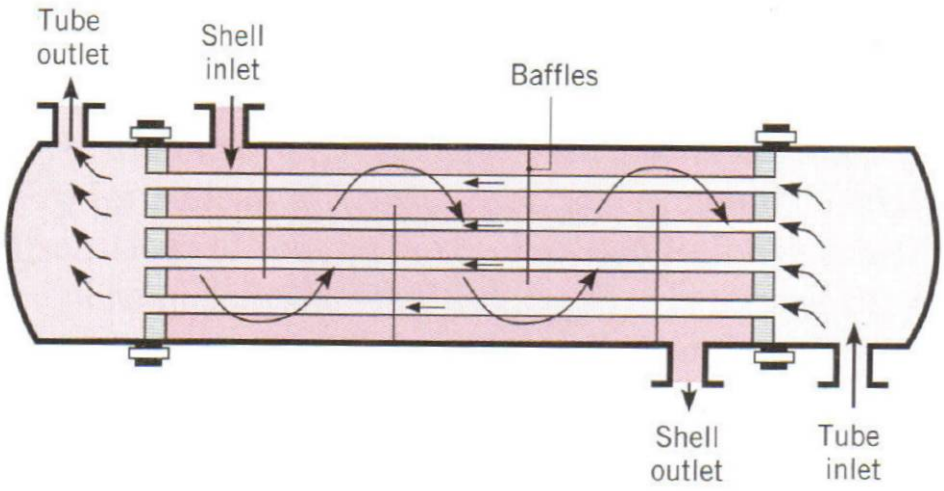


Figure 3: General operation of a counter flow shell and tube heat exchanger [8]

## 2.2 Reason for Consideration

A shell and tube heat exchanger is an ideal design for this study. By setting the inside of the tubes as the primary side, it is possible to maintain a small product volume. The primary side or product side fluid is expensive (typically $50/mL) and consists of enriched $^{18}O$ water. It is desirable to keep this volume as small as possible in the event of spills or contamination and to maintain a minimum inventory. The volume on the shell side is typically larger by design and in comparison to the tube side will easily accommodate high flows. Because the coolant flow available for the recirculating target system is much larger than the necessary primary flow, it makes sense to use the shell side of the heat exchanger for cooling. Furthermore, the actual dimensions of a shell and tube heat exchanger vary widely depending on the numbers of tubes, tube diameters, and tube lengths. Different component dimensions can be evaluated based upon their performance and compatibility with regards to the integrated recirculating target. In summary, a shell and tube heat exchanger is an extremely versatile platform for compact designs.

## 2.3 Design

### 2.3.1 Methodology and Theory

In order to determine an optimal shell and tube heat exchanger design, it is necessary to simulate different combinations of tube/shell dimensions and orientations. To accurately simulate the performance of a shell and tube heat exchanger requires evaluating several processes. First, tube quantity, diameter, thickness, and length must be selected along with shell size and flow orientation. Then, assuming a primary flow rate, pressure drops across the heat exchanger and other devices in the system must be determined. Since a specific pump had been selected for the integrated target system, its performance data was included in the model.

For both primary and secondary sides of the heat exchanger, heat transfer characteristics are dependent on flow rate, tube diameter, and the number of tubes. Because pressure drop is a concern for the product side of the heat exchanger, it is not practical to include fins or slots in the tubing to increase surface area. Due to the high pressure head available on the secondary side, it is possible to fin the outside of the tubes to increase turbulence and surface area. Finning the outside of the tubes will likely have a minimal affect, as in most shell and tube heat exchangers the majority of thermal resistance exists on the primary side. This study explores the advantages and disadvantages of both finned and smooth tube bundles. [9]

The following sections outline the steps necessary to simulate the performance of a shell and tube heat exchanger. Included in these sections are the equations used for the models and an explanation of the steps taken to code a FORTRAN program that predicts the performance of a shell and tube heat exchanger. In the program, fluid properties are considered for a range of 500 psia to atmospheric pressure. It should be noted that enriched $^{18}O$ water and the de-ionized water have similar properties to tap water. Therefore, all primary and secondary side fluid properties are taken from standard fluids and thermodynamics tables for water.

The initial use of this code was to predict heat exchanger performance as a function of tube and shell dimensions so that optimal configurations could be determined. Later, this program was modified and used to simulate the integrated recirculating target with a specific heat exchanger design as well as to simulate the performance of a lab

testing apparatus. Modifications include accounting for pressure drops associated with smaller diameter tubes, the target, a circulation heater, and the pressurizer.

## I. Primary Side

As mentioned previously, a prototype regenerative turbine pump had been selected for the integrated recirculating target. The pump had been tested in previous work as well as used for a feasibility study of the recirculating target design. The current pump incorporates a horizontal shaft with two seals and two bearings on the shaft. The impeller and shaft are made of stainless steel. The impeller uses opposing double rows of vanes that produce screw-type fluid flow through the body of the pump. As the impeller rotates the pressure increases in a series of small pressure impulses. Because fluid pressure is gradually increased the effects of collapsing bubbles in a two phase mixture are greatly reduced. The added versatility of being able to run two phase mixtures is necessary in the event that localized boiling occurs in the system and the mixture is transported through the pump before condensing. [14]

Future modifications of the regenerative turbine pump include a change in the main drive. The current shaft driven design couples the pump impeller directly to the electric driving motor. This design requires shaft seals that are prone to failure after extended use. To eliminate the shaft seals, a magnetic drive is being designed that will eliminate direct coupling between the pump and the driving motor. Also, work will be completed on optimizing the size, dimensions and orientation of the impeller to maximize performance at moderate pump speeds. General dimensions of the current pump base are 5.03 cm high, 5.03 cm deep, and 3.18 cm long with an impeller diameter of 2.79 cm. The impeller has 20 notches, thus 20 vanes on each side. Figure 3 shows the general layout and assembly of the regenerative turbine pump and impeller. [1]

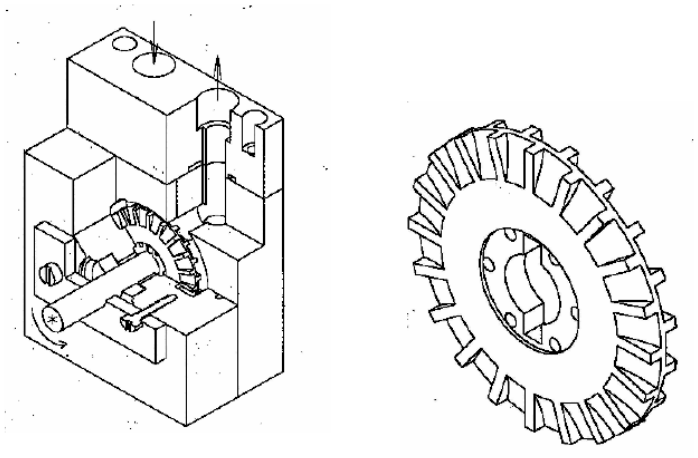

Figure 4: Regenerative turbine pump assembly and impeller [1]

The performance characteristics of the regenerative turbine pump were obtained in a previous study and consist of a correlated equation in terms of pump speed, volumetric flow rate, and pressure drop across the pump. This correlation is assumed accurate for use in this research and supplies the basis for establishing a reasonable range of flow rates and pressure drops for the integrated recirculating target design. The following correlation was adopted. [1]

$$\Delta P_p = a_0 + a_1\Omega + a_2\Omega^2 + a_3 G + a_4 G^2 \tag{1}$$

This correlation allows the differential pressure across the pump to be calculated for any flow rate at a given pump speed. The pressure drop across the pump is set by the rest of the flow system which could include the heat exchanger, connecting tubing, the target, a circulation heater, and the pressurizer. The flow rate and the pressure drop are related by the following equations.

Fluid velocity through heat exchanger tubes

$$V_p = \frac{G}{1000\left(L/m^3\right) * 60\left(s/\min\right) * N_t A_{x,p}} \tag{2}$$

Fluid velocity through primary side supply tubing

$$V_t = \frac{G}{1000\left(L/m^3\right) * 60\left(s/\min\right) A_{x,t}} \tag{3}$$

Reynolds number for flow inside tubes

$$\mathrm{Re} = \frac{\rho\, V D_i}{\mu} \tag{4}$$

Colebrook Formula: ε = 1.524E-6 m for Drawn Tubing:

*(Considered valid for Connection and Heat Exchanger tubing)*

$$\frac{1}{\sqrt{f}} = 1.14 - 2.0 \times \log\left[\frac{\varepsilon}{D_i} + \frac{9.35}{\mathrm{Re}\sqrt{f}}\right] \tag{5}$$

The primary side pressure drop can be expressed in terms of the primary side velocities as

$$\Delta P_h = \left(\frac{f_p L_p}{D_{i,p}} + K_p\right)\frac{\rho_p V_p^2}{2} + \left(\frac{f_t L_t}{D_{i,t}} + K_t\right)\frac{\rho_p V_t^2}{2} + \Delta P_{pressurizer}(G) + \Delta P_{target}(G) \tag{6}$$

The primary side pressure drop is then equal to the differential pressure produced by the regenerative turbine pump

$$\Delta P_h = \Delta P_p \tag{7}$$

Combining equations (1) – (7) yields a single non-linear equation in the unknown variable G. For a given set of dimensions the primary side flow rate can be solved iteratively at any pump speed. Once the primary side fluid flow rate has been determined, the convective heat transfer coefficient may be obtained from the Dittus-Boelter correlation. [3]

$$h_{c,p} = \left(\frac{k_p}{D_i}\right) \cdot 0.023 \cdot \mathrm{Re}^{0.8} \cdot \mathrm{Pr}_p^{0.3} \tag{8}$$

## II. Secondary Side

The secondary side consists of fluid flow over the tube bundle. Water from a fixed high pressure supply source is injected through the shell wall perpendicular to the tube bundle. The water is then routed across the tube bundle by a series of baffles, which for design purposes are assumed to be present roughly every three shell ID lengths along the heat exchanger. The baffles cause the fluid to flow both perpendicular and parallel to the tube bundle while inside the shell. Once the water has traversed the entire tube bundle it exits at the end through the shell wall.

Due to the tortuous path that the supply water must travel, simply modeling the flow as a simplified tube is not sufficient. Pressure drop correlations were found for both finned and smooth tube bundles in a triangular lattice or "staggered" configuration. When calculating the total pressure drop across the secondary side, the pressure drop resulting from one pass across the tube bundle is multiplied by the number of passes caused by the baffles. Furthermore, it should be noted that the pressure drop correlations found for staggered smooth and finned tube bundles were obtained for large industrial sized shell and tube heat exchangers such as condensers or feed water heaters. A correlation for small tube bundles was not available. Therefore, the size scale in which this study uses these correlations may be outside of their data range such that their accuracy could be affected. Figure 4 shows the dimensional parameters needed to establish a secondary side model and an example of a staggered tube bundle design. [7]

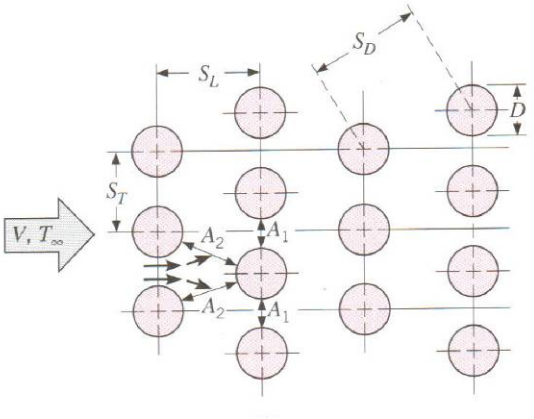


Figure 5: Staggered tube bundle profile [8]

A relatively constant fluid speed throughout the tube bundle is desired in order to evenly distribute heat transfer and to minimize pressure drop. One way to regulate these fluid velocities is to set $S_T$ and $S_D$ equal. This in turn causes $S_L$ to be equal to $(3/4)^{0.5} * S_T$. For design purposes $S_T$ and $S_D$ are set to be 25% larger than the tube OD for the smooth tube bundle, and 20% larger than the fin OD of the finned tube bundle. This spacing was found to offer the best heat transfer while minimizing excess pressure drop. [8]

***Finned Tubing:***

Incorporating fins on the outside of the tubing is one way to increase heat transfer area on the secondary side. It also promotes turbulence in the fluid flow which can

increase heat transfer. However, finned tubes can result in higher pressure drop and may be difficult to include due to fabrication and availability issues.

The fin diameter was set to be 20% larger than the tube OD. Fin width and spacing was defined to be equal at 1 mm for all tube sizes which allows maximum area while remaining reasonably easy to construct. These dimensions were found to offer a 12 to 18% increase in tube surface area in the range of tube sizes for this study. Fins also increase secondary side pressure drop by an average of 8.3% based on tube count and bundle dimensions when compared to a smooth tube bundle.

The following correlation for finned tube bundles was used to determine the pressure drop per pass across the bundle and the secondary side pressure drop. Figure 5 illustrates some of the defined fin dimensions and variables. [7]

$$d_{in} = D_i + 2t \tag{8}$$

$$l = \frac{\left(D^2 - d_{in}^2\right)N_f}{2L\beta} + \frac{\left(D^2 - d_{in}^2\right)N_f}{2d_{in}L\beta}\sqrt{0.785\left(D^2 - d_{in}^2\right)} \tag{9}$$

$$d_h = \frac{2\left[S_{f\delta}\left(S_1 - d_{in}\right) - 2\delta h\right]}{2h + S_{f\delta}} \tag{10}$$

$$c_s = 5.4\left(\frac{l}{d_h}\right)^{0.3} \tag{11}$$

The Reynolds number specific to the finned tube bundle is defined as [7]

$$\mathrm{Re}_l = \frac{\rho_s V_c l}{\mu_s} \tag{12}$$

The pressure drop across a finned tube bundle is defined as [7]

$$\Delta P_{HX} = c_z c_s \,\mathrm{Re}_l^{-0.25}\, z_r \frac{\rho_s V_c^2}{2}\left(N_B + 1\right) \tag{13}$$

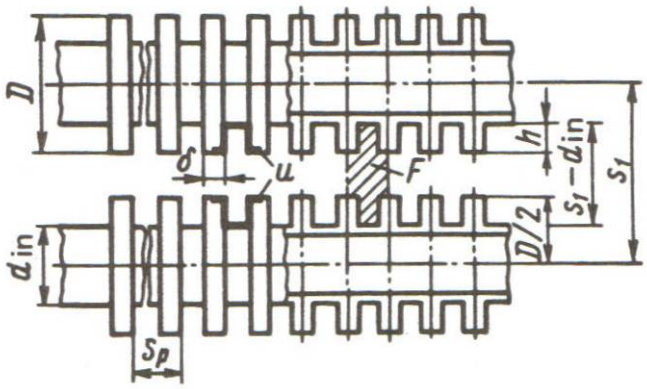


Figure 6: Finned tubing dimensions [7]

It is also necessary to include pressure drops associated with the secondary side supply lines. A mass balance between the shell and the supply line provides a relationship between the shell velocity and the supply line velocity.

The shell diameter for smooth or finned tube bundles is defined as

$$ShellD = z_r \cdot S_T \tag{14}$$

The following equations define the mass balance for supply line and shell

$$\rho_s\left(\frac{\pi D_{i,s}^2}{4}\right)V_s = \rho_s\left(\frac{\pi\left(ShellD^2 - \frac{N_t}{(S_p)}\left[(S_p-\delta)D^2 + \delta D_f^2\right]\right)}{4}\right)V_c$$

$$\Rightarrow D_{i,s}^2 V_s = \left(ShellD^2 - \frac{N_t}{(S_p)}\left[(S_p-\delta)D^2 + \delta D_f^2\right]\right)V_c$$

$$\Rightarrow V_s = \frac{\left(ShellD^2 - \frac{N_t}{(S_p)}\left[(S_p-\delta)D^2 + \delta D_f^2\right]\right)}{D_{i,s}^2}\cdot V_c \tag{15}$$

The pressure drop for the secondary side supply lines is defined as

$$\Delta P_s = \left(\frac{f_s L_s}{D_{i,s}} + K_s\right)\frac{\rho_s V_s^2}{2} \tag{16}$$

The total pressure drop across the secondary side of the shell and tube heat exchanger with finned tubes is

$$\Delta P_c = \Delta P_{HX} + \Delta P_s \tag{17}$$

Because the supply pressure from the cooling water manifold is considered a gauge pressure reading and the secondary side is dumped to atmospheric pressure, the total pressure drop across the secondary side of the heat exchanger can be equated to the secondary side pressure head.

$$\Delta P_c = P_{supply} \tag{18}$$

Combining equations (8) – (18) yields a single non-linear equation in the one unknown variable $V_c$ which can be solve iteratively for given dimensions. Once the secondary side fluid velocity has been determined, the convective heat transfer coefficient can be solved using the Grimison Correlation for smooth tube bundles.

The maximum velocity across the tube bundle is defined as [8]

$$V_{c,MAX} = \frac{S_T}{S_T - d_{in}} V_c \tag{19}$$

The Reynolds number associated with the maximum velocity is then defined as [8]

$$\mathrm{Re}_{d_{in},MAX} = \frac{\rho_s V_{c,MAX} d_{in}}{\mu_s} \tag{20}$$

The Grimison correlation for a convective heat transfer coefficient across a smooth tube pack is defined as [8]

$$h_{c,s} = \frac{k_s}{d_{in}} \cdot 1.13 C_1 \mathrm{Re}^m_{d_{in.},MAX} \mathrm{Pr}_s^{1/3} \tag{21}$$

The variables $C_1$ and m are constants based on tube bundle dimensions. Because the tube bundle dimensions are set proportionally, these constants do not change unless the proportionality changes. The following equation is necessary to correct the convective heat transfer coefficient to include the effects of finned tubing. [8]

$$h_{c,s}^{finned} = h_{c,s}\left[1 - \frac{A_{t,\,finned}}{A_t}\left(1 - \eta_f\right)\right] \tag{22}$$

The fin efficiency $\eta_f$, is a function of the fin dimensions and is available from the literature.

***Smooth Tubing:***

A different pressure drop correlation is required when considering smooth tubing.

The tube pitch ratio is defined as [7]

$$\bar{s} = \frac{(S_T - d_{out})}{(S_D - d_{out})} \tag{23}$$

The Reynolds number for the smooth tube bundle is defined as [7]

$$\mathrm{Re}_d = \frac{\rho_s V_c d_{out}}{\mu_s} \tag{24}$$

The mass balance for the supply line and shell is defined as

$$\rho_s \left( \frac{\pi D_{i,s}^2}{4} \right) V_s = \rho_s \left( \frac{\pi \left( ShellD^2 - N_t d_{out}^2 \right)}{4} \right) V_c$$

$$\Rightarrow D_{i,s}^2 V_s = \left( ShellD^2 - N_t d_{out}^2 \right) V_c \tag{25}$$

$$\Rightarrow V_s = \frac{\left( ShellD^2 - N_t \cdot d_{out}^2 \right)}{D_{i,s}^2} \cdot V_c$$

The pressure drop across a smooth tube bundle is defined as [7]

$$\Delta P_{HX} = \left[ \left\{ 3.2 + 0.66(1.7 - \bar{s})^{1.5} + \left( 13.1 - 9.1 \cdot \frac{S_1}{d_{out}} \right) \left[ 0.8 + 0.2(1.7 - \bar{s})^{1.5} \right] \right\} \mathrm{Re}_d^{-0.27} (z_p + 1) \right] \cdot \frac{\rho_s V_c^2}{2} (N_B + 1) \tag{26}$$

The pressure drops associated with the tube bundle and supply lines are added together, as in equation (17). Equation (18) then relates the secondary side pressure drop to the supply pressure head.

Combining equations (16) – (18) and (23) – (26) yields a single non-linear equation with one unknown variable $V_c$ which can be solved iteratively. Given the secondary side fluid velocity, the convective heat transfer coefficient can be solved using the Grimison Correlation for smooth tube bundles. In the absence of fins the Grimison correlation can be used directly without any correction factors. Solving equations (19) – (21) yields the convective heat transfer coefficient for the secondary side assuming smooth tubes. [8]

## III. Heat Transfer

To calculate the heat transfer rate it is first necessary to evaluate the primary and secondary side flow rates. Given the flow rates, convective heat transfer coefficients are calculated. Using this information and the known inlet temperatures, a system of equations can be established to solve for the heat transfer rate.

Primary side mass flow rate

$$\dot{m}_i = \rho_p N_t A_{x,p} V_p \tag{27}$$

Secondary side mass flow rate

$$\dot{m}_o = \rho_s A_{x,s} V_s \tag{28}$$

Primary side heat balance

$$\begin{aligned} \dot{Q} &= \dot{m}_i C_{p,i} (T_{in,i} - T_{out,i}) \\ \Rightarrow T_{out,i} &= T_{in,i} - \dot{Q} \big/ \dot{m}_i C_{p,i} \end{aligned} \tag{29}$$

Secondary side heat balance

$$\begin{aligned} \dot{Q} &= \dot{m}_o C_{p,o} (T_{out,o} - T_{in,o}) \\ \Rightarrow T_{out,o} &= T_{in,o} + \dot{Q} \big/ \dot{m}_o C_{p,o} \end{aligned} \tag{30}$$

The overall heat transfer coefficient can then be obtained from

$$\frac{1}{UA} = \frac{1}{h_i A_i} + \frac{R_{f,i}}{A_i} + \frac{\ln(D_o / D_i)}{2\pi k L} + \frac{R_{f,o}}{A_o} + \frac{1}{h_o A_o} \tag{31}$$

Fouling factors for the primary and secondary side are defined to be 0.000176 $m^2 \cdot K/W$ for water flowing inside tubes, or across finned/smooth tube bundles [9]. For the small tube diameters considered in this work, any fouling that occurs would likely stop the fluid flow. Due to the relative cleanliness of the production environment it is appropriate to exclude fouling from these calculations. Because the secondary side header is supplied with de-ionized water, no significant fouling is expected to occur on the exterior of the tubes as well.

Log mean temperature difference is defined as

$$\Delta T_{lm} = \frac{(T_{in,i} - T_{out,o}) - (T_{out,i} - T_{in,o})}{\ln\left((T_{in,i} - T_{out,o}) / (T_{out,i} - T_{in,o})\right)} \tag{32}$$

which gives for the heat transfer rate across the heat exchanger

$$Q = UA\Delta T_{lm} \tag{33}$$

Combining equations (27) – (33) yields a single non-linear equation with one unknown variable Q which can be solved iteratively.

### 2.3.2 Program Flowchart

A FORTRAN program was written to predict the performance of the shell and tube heat exchanger using the methods and models described previously. Brent's Algorithm was used to iteratively solve the non linear equations. Figure 6 gives the program flowchart. The program includes fitted correlations for fluid properties.

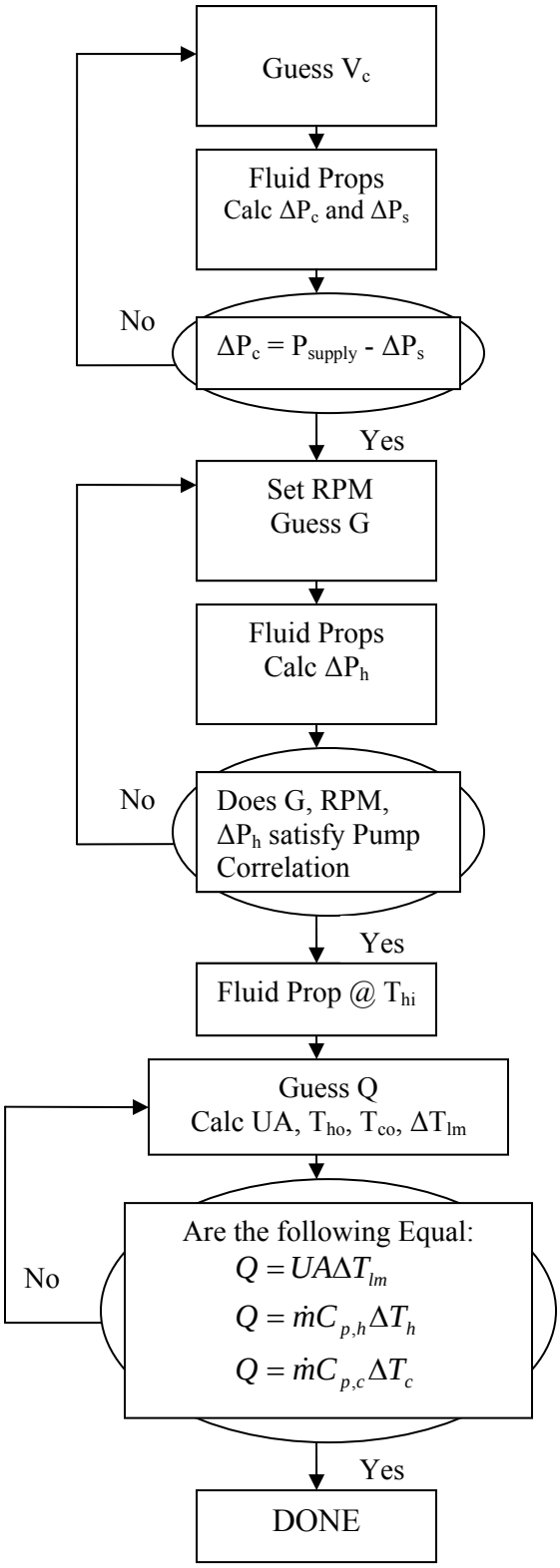


Figure 7: General program flowchart

### 2.3.3 Materials

The integrated recirculating target system must be constructed of materials that are compatible with radiopharmaceuticals and their production environment. Copper is a standard choice for heat exchanger construction due to its high thermal conductivity. Unfortunately, copper results in product chemical impurities and also activates after long exposures to radiation fields. Stainless steel, a common choice for use with radiopharmaceutical production hardware does not cause chemical impurities and does not easily activate in radiation fields. Because of this, stainless steel is the likely choice for constructing the heat exchanger. Stainless steel suffers however from a relatively low thermal conductivity, though these effects can be minimized by using thin walled tubing. Heat exchanger designs were simulated with both 316 SS and copper. This serves to show a spread of performance characteristics based solely on tube material. [1]

### 2.3.4 Optimization

Primary side tube dimensions have a direct impact on the performance of a shell and tube heat exchanger. In order to select the best dimensions, combinations of tube quantity, length and diameter within design constraints must be checked for overall performance. Optimization is based upon a set pump speed that is moderate, sustainable, and representative of anticipated operating conditions during production. The pump speed selected was 5500 RPM, which is about 75% capacity. Constraints set on primary side volume and heat transfer were also used to eliminate any combinations that did not meet requirements. Tube length is the major contributor to overall heat exchanger size. Therefore, tube length must be considered for physical size restrictions even though it may be the most important factor except for tube wall thickness in overall heat transfer performance.

Optimization of the heat exchanger does not require simulation of the entire integrated recirculating target system. Therefore, during heat exchanger optimization only the pressure drops associated with the primary and secondary sides of the heat exchanger and the connection tubes and fittings were evaluated. Large diameter/low pressure drop tubes were considered with short lengths for the primary side. This represents the minimum flow restriction that the heat exchanger could encounter in use with the regenerative turbine pump and is a baseline to create the largest spectrum of flow rates that the pump can provide.

It is also of interest to examine configurations composed of multiple parallel and series compact shell and tube heat exchangers. An advantage of parallel heat exchangers is the potential reduction in overall foot print of the integrated system. Series heat exchangers may be configured to essentially act as connective piping between the target chamber and pump, thereby reducing overall system volume. Parallel and series designs will be evaluated to determine which orientation yields better heat transfer rates.

The number of tubes is set by the number that can be uniformly spaced within a one inch diameter shell. Table 2 shows the range of design variables considered for the shell and tube heat exchanger.

Table 2: Design Variables

| | **Single Heat Exchanger** |
|---|---|
| **Tube ID (cm) =** | $0.15 \leq D_i \leq 0.25$ |
| **Tube Length (cm) =** | $4.0 \leq L \leq 12.0$ |
| **Tube Wall Thickness (cm/in) =** | 0.0254 / 0.010 |
| **Number of Tubes =** | 4,7,14,23 |
| **Total Tube Volume (mL) =** | $\leq 5.0$ |
| **Shell ID (cm/in) =** | $\leq 2.54$ / 1.00 |

The optimization routine calculates heat exchanger performance over the full range of the design variables. The tube ID and length are changed in increments of 0.01 cm and 1.0 cm respectively. The design objective is maximum heat transfer rate for a given system pressure. The inlet temperature is set to 96% of the saturation temperature at the specified system pressure. In practice, a heat exchanger would not operate with a bulk fluid temperature at or close to saturation to prevent localized boiling at some point in the system. Table 3 shows the results for finned tubes made from both 316 stainless steel and copper. Likewise, Table 4 shows the same data for smooth tubing.

Table 3: Four heat exchanger designs with finned 316 SS and copper tubes

| Optimization Summary for Finned Tubes | | | | | | | | | |
|---|---|---|---|---|---|---|---|---|---|
| *All Designs are Counter Flow* | | | | | | | | | |
| | | Design 1 | | Design 2 | | Design 3 | | Design 4 | |
| | | *Single Heat Exchanger at a Pump Speed of 5500 RPM* | | | | | | | |
| Tube ID (in/cm) = | | 0.0945 | 0.2400 | 0.0945 | 0.2400 | 0.0630 | 0.1600 | 0.0591 | 0.1500 |
| Tube Length (in/cm) = | | 4.7244 | 12.0000 | 4.7244 | 12.0000 | 4.7244 | 12.0000 | 4.7244 | 12.0000 |
| Tube Wall Thickness (in/mm) = | | 0.0100 | 0.2540 | 0.0100 | 0.2540 | 0.0100 | 0.2540 | 0.0100 | 0.2540 |
| Fin Height (in/mm) = | | 0.0114 | 0.2908 | 0.0114 | 0.2908 | 0.0083 | 0.2108 | 0.0079 | 0.2008 |
| Fin Thickness (in/mm) = | | 0.0394 | 1.0000 | 0.0394 | 1.0000 | 0.0394 | 1.0000 | 0.0394 | 1.0000 |
| Fin Gap (in/mm) = | | 0.0394 | 1.0000 | 0.0394 | 1.0000 | 0.0394 | 1.0000 | 0.0394 | 1.0000 |
| Tube Pitch (in/mm) = | | 0.1717 | 4.3620 | 0.1717 | 4.3620 | 0.1245 | 3.1620 | 0.1186 | 3.0120 |
| Shell ID (in/cm) = | | 0.5495 | 1.3958 | 0.5495 | 1.3958 | 0.4980 | 1.2648 | 0.6641 | 1.6867 |
| Number of Tubes = | | 4 | | 7 | | 14 | | 23 | |
| Total Tube Volume (mL) = | | 2.17 | | 3.80 | | 3.38 | | 4.88 | |
| Primary Flow Rate (LPM) = | | 2.52 | | 2.56 | | 2.55 | | 2.57 | |
| Secondary Flow Rate (LPM) = | | 2.25 | | 1.74 | | 3.36 | | 3.58 | |
| System: | | 316 Stainless Steel Tubing Heat Transfer (kW) | | | | | | | |
| Press. (psia): | Sat. / Inlet Temp. (°F) | *Single Heat Exchanger* | | | | | | | |
| 500 | 467.01 / 448.32 | 7.69 | | 10.25 | | 15.66 | | 18.22 | |
| 400 | 444.60 / 426.816 | 7.19 | | 9.56 | | 14.62 | | 17.03 | |
| 300 | 417.35 / 400.66 | 6.57 | | 8.72 | | 13.35 | | 15.56 | |
| 200 | 381.90 / 366.53 | 5.75 | | 7.61 | | 11.66 | | 13.62 | |
| 100 | 327.82 / 314.71 | 4.52 | | 5.95 | | 9.11 | | 10.68 | |
| 50 | 281.02 / 269.78 | 3.49 | | 4.56 | | 6.98 | | 8.21 | |
| 25 | 239.15 / 229.58 | 2.63 | | 3.41 | | 5.20 | | 6.15 | |
| 15 | 213.03 / 204.51 | 2.08 | | 2.69 | | 4.10 | | 4.87 | |
| System: | | Copper Tubing Heat Transfer (kW) | | | | | | | |
| Press. (psia): | Sat. / Inlet Temp. (°F) | *Single Heat Exchanger* | | | | | | | |
| 500 | 467.01 / 448.32 | 9.08 | | 11.59 | | 17.67 | | 20.12 | |
| 400 | 444.60 / 426.816 | 8.48 | | 10.81 | | 16.50 | | 18.80 | |
| 300 | 417.35 / 400.66 | 7.75 | | 9.85 | | 15.05 | | 17.18 | |
| 200 | 381.90 / 366.53 | 6.78 | | 8.59 | | 13.14 | | 15.02 | |
| 100 | 327.82 / 314.71 | 5.31 | | 6.69 | | 10.23 | | 11.76 | |
| 50 | 281.02 / 269.78 | 4.07 | | 5.11 | | 7.80 | | 9.01 | |
| 25 | 239.15 / 229.58 | 3.05 | | 3.80 | | 5.79 | | 6.73 | |
| 15 | 213.03 / 204.51 | 2.41 | | 2.99 | | 4.54 | | 5.30 | |

Table 4: Four heat exchanger designs with smooth 316 SS and copper tubes

| Optimization Summary for Smooth Tubes | | | | | | | | |
|---|---|---|---|---|---|---|---|---|
| *All Designs are Counter Flow* | | | | | | | | |
| | | Design 5 | | Design 6 | | Design 7 | | Design 8 | |
| | | *Single Heat Exchanger at a Pump Speed of 5500 RPM* | | | | | | | |
| Tube ID (in/cm) = | | 0.0945 | 0.2400 | 0.0945 | 0.2400 | 0.0630 | 0.1600 | 0.0591 | 0.1500 |
| Tube Length (in/cm) = | | 4.7244 | 12.0000 | 4.7244 | 12.0000 | 4.7244 | 12.0000 | 4.7244 | 12.0000 |
| Tube Wall Thickness (in/mm) = | | 0.0100 | 0.2540 | 0.0100 | 0.2540 | 0.0100 | 0.2540 | 0.0100 | 0.2540 |
| Tube Pitch (in/mm) = | | 0.1431 | 3.6350 | 0.1431 | 3.6350 | 0.1037 | 2.6350 | 0.0988 | 2.5100 |
| Shell ID (in/cm) = | | 0.4580 | 1.1632 | 0.4580 | 1.1632 | 0.4150 | 1.0540 | 0.6324 | 1.6064 |
| Number of Tubes = | | 4 | | 7 | | 14 | | 23 | |
| Total Tube Volume (mL) = | | 2.17 | | 3.80 | | 3.38 | | 4.88 | |
| Primary Flow Rate (LPM) = | | 2.52 | | 2.56 | | 2.55 | | 2.57 | |
| Secondary Flow Rate (LPM) = | | 3.28 | | 2.32 | | 4.88 | | 5.14 | |
| System: | | 316 Stainless Steel Tubing Heat Transfer (kW) | | | | | | | |
| Press. (psia): | Sat. / Inlet Temp. (°F) | *Single Heat Exchanger* | | | | | | | |
| 500 | 467.01 / 448.32 | 7.52 | | 9.70 | | 13.83 | | 16.75 | |
| 400 | 444.60 / 426.816 | 7.03 | | 9.06 | | 12.94 | | 15.67 | |
| 300 | 417.35 / 400.66 | 6.43 | | 8.27 | | 11.83 | | 14.34 | |
| 200 | 381.90 / 366.53 | 5.64 | | 7.23 | | 10.36 | | 12.58 | |
| 100 | 327.82 / 314.71 | 4.44 | | 5.67 | | 8.14 | | 9.91 | |
| 50 | 281.02 / 269.78 | 3.43 | | 4.36 | | 6.27 | | 7.65 | |
| 25 | 239.15 / 229.58 | 2.58 | | 3.27 | | 4.70 | | 5.75 | |
| 15 | 213.03 / 204.51 | 2.05 | | 2.58 | | 3.72 | | 4.56 | |
| System: | | Copper Tubing Heat Transfer (kW) | | | | | | | |
| Press. (psia): | Sat. / Inlet Temp. (°F) | *Single Heat Exchanger* | | | | | | | |
| 500 | 467.01 / 448.32 | 8.84 | | 10.90 | | 15.38 | | 18.33 | |
| 400 | 444.60 / 426.816 | 8.27 | | 10.18 | | 14.38 | | 17.16 | |
| 300 | 417.35 / 400.66 | 7.56 | | 9.29 | | 13.15 | | 15.69 | |
| 200 | 381.90 / 366.53 | 6.62 | | 8.11 | | 11.51 | | 13.76 | |
| 100 | 327.82 / 314.71 | 5.19 | | 6.34 | | 9.03 | | 10.82 | |
| 50 | 281.02 / 269.78 | 3.99 | | 4.85 | | 6.92 | | 8.33 | |
| 25 | 239.15 / 229.58 | 2.99 | | 3.62 | | 5.18 | | 6.25 | |
| 15 | 213.03 / 204.51 | 2.36 | | 2.85 | | 4.08 | | 4.94 | |

Note that the optimum tube IDs for both the finned and smooth tube bundles are the same. This is because the greatest resistance to heat transfer occurs on the primary side, minimizing the fin effectiveness. Furthermore, all designs display maximum

performance with the longest tube lengths tested. This is because for any set number of tubes, the longer tube length increases inside and outside surface area.

Both optimization routines compare 316 stainless steel and copper tubes. Though 316 SS tubes will be used in the prototype, the results show an average increase in heat transfer of 12.5% with copper tubes. The results also show an average increase in heat transfer of 7.1% with finned tubes. Table 5 shows the average heat transfer per unit volume for each of the four designs with both finned and smooth tubes.

Table 5: Average heat transfer per unit volume for the optimized designs

| | Average kW/mL for 316 Stainless Steel Tubes | | | |
|---|---|---|---|---|
| Finned Tubes | Design 1 | Design 2 | Design 3 | Design 4 |
| | 2.30 | 3.04 | 4.64 | 5.43 |
| | | | | |
| Smooth Tubes | Design 5 | Design 6 | Design 7 | Design 8 |
| | 2.25 | 2.89 | 4.13 | 5.02 |

The results of the design study show that the use of a low thermal conductivity metal such as 316 SS does not greatly reduce the performance of these heat exchangers. Results also show that finned tubes do not offer substantial increases in performance. Due to the complications in design and construction of finned tubes, their use is considered impractical for this application. The optimization also indicates that heat exchangers with higher numbers of tubes out perform other designs. It should be noted however, that in order to meet volume restrictions, the tube IDs can become small. In fact, tube IDs less than 1.5 mm or 0.059" are probably outside what is reasonable for construction.

## 2.4 Fabrication of Prototype

The design study identified heat exchanger characteristics such as tube quantity, tube diameter and length, the shell diameter, and even the materials to be used. The design study however does not address the mechanical requirements necessary to build and assemble the heat exchanger.

### 2.4.1 Custom Construction

Contracting with either the NCSU or Duke Medical Center machine shops to fabricate the prototype heat exchanger was considered. However, there are a number of

issues related to custom fabrication. While the shell of the heat exchanger is simple to construct, construction of the tube bundle requires aligning and inserting baffles and is significantly more involved. If finned tubes are used, this process would be even more complicated. In addition, it would be difficult to attach thin wall tubes to the bulk heads of the heat exchanger. Brazing thin tubes in the arrangement required is problematic and requires specialized furnaces, materials, and experience. Furthermore, the availability of suitable tubing sizes could reduce the overall effectiveness of the proposed designs.

Insuring a sealed boundary at the inlet and outlet points of the primary side that will reliably separate the primary and secondary sides is difficult on this size scale. If this cannot be performed correctly, the heat exchanger will not function properly. Based on these considerations, it was decided to seek out an established shell and tube heat exchanger manufacturer to build the prototype.

### 2.4.2 Purchase Part

Exergy, LLC specializes in the design and construction of compact shell and tube heat exchangers. They have over ten different standard off-the-shelf designs that can be purchased. Of interest to this work are their 10 series, shell and tube heat exchangers. The 10 Series incorporates Exergy's smallest tube sizes of 0.094" OD with 0.010" wall thickness. This series has a general shell ID of 10 mm. All tube bundles consist of 7 staggered smooth tubes. The difference between the models in the 10 series shell and tube heat exchangers are the tube lengths. Tube lengths offered include 4, 8, and 12". Their corresponding primary side volumes are approximately 2, 4, and 6 mL. [4]

The Exergy 10 Series shell and tube heat exchangers are similar in size and configuration to the design 6 shell and tube heat exchanger considered in this study. Both heat exchanger designs use an array of 7 staggered smooth tubes. The smallest of the 10 Series heat exchangers has a tube length of 10.2 cm which is slightly shorter than design 6 tube length of 12 cm. Tube ID for the optimized design was set to be 2.4 mm whereas the 10 Series heat exchangers use 1.9 mm tubes. Shell diameters for both are around 10 to 12 mm. Tube pitch for the optimized design was 3.64 mm and for the 10 Series is 3.00 mm, both of which are 25% larger than the tube OD.

All 10 series shell and tube heat exchangers are made of 316 SS. Stainless steel is desirable for durability, longevity, and can be used with radiopharmaceuticals. In the

next section, the performance of these three shell and tube heat exchangers will be simulated. From this analysis a prototype selection will be made.

## 2.5 Simulation and Selection of Exergy LLC Design

Exergy LLC located in Garden City, NY is a producer of high efficiency heat exchangers with over twenty-five years of experience. Their specialty is compact shell and tube heat exchangers for both sanitary and non sanitary applications. [4]

### 2.5.1 Simulation of 10 Series Shell and Tube Heat Exchangers

The 10 Series shell and tube heat exchanger produced by Exergy LLC is very similar to design 6 evaluated in the previous section. Therefore, the basic methodology needed to evaluate the thermal and hydraulic performance of these heat exchangers has already been established. Simple modifications to the existing code were necessary to incorporate specific characteristics of the 10 Series heat exchangers such as tube pitch, baffle positioning and count, and shell size. After making these adjustments, the performance of these heat exchangers was simulated to consider their use with the existing recirculating pump and the secondary side characteristics set forth for this study. These heat exchangers can be operated in either parallel or counter flow. For maximum performance only the counter flow arrangement is evaluated.

To better establish the performance range of the 10 Series heat exchangers, it was necessary to simulate and compare all three models in the series. In addition to their thermal and hydraulic performance, the physical dimensions of these heat exchangers will be considered for integration into the recirculating target system. All of the 10 Series are essentially compact, but their lengths vary by multiples of 4". It should be noted that on the recommendation of Exergy's design engineer, no fouling should be considered in the simulation of their heat exchangers. In their experience with small tube sizes there is little chance of significant fouling that does not render the primary side tubes clogged. Figure 7 shows the Exergy 10 Series model 00268-3 shell and tube heat Exchanger. [4]

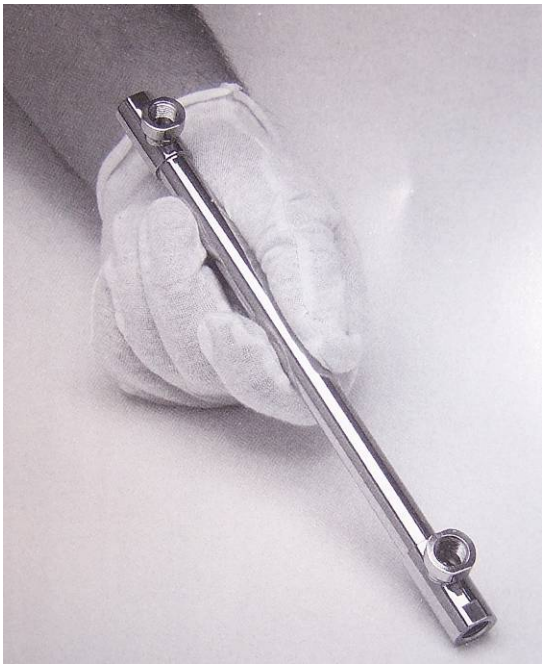

Figure 8: Exergy model 00268-3 shell and tube heat exchanger [5]

Exergy uses Nickel-Chromium brazing to connect the primary side tubes to the inlet and outlet bulk heads. Specialized furnaces are used to heat and treat both the brazing and the bulk heads. Though this process does render a reliable product, it does have its limitations. The brazing is susceptible to thermal stressing and has a tendency to crack if stretched. Stretching can occur when a high temperature difference exists between the tube and bulk heads. To reduce the risk of cracking, Exergy imposes a limit on the maximum average temperature difference (MATD) its heat exchangers should experience during operation. [4]

The MATD is defined to be the difference between the averages of the primary and secondary side inlet and outlet fluid temperatures. [4]

$$MATD = \left( \frac{T_{h,i} + T_{h,o}}{2} \right) - \left( \frac{T_{c,i} + T_{c,o}}{2} \right) \tag{34}$$

Exergy recommends the MATD should not exceed 125 °F. This MATD value is somewhat conservative and limits the overall performance of the heat exchanger. However, even with this limit Exergy predicts around 4.2 kW for their smallest heat exchanger at the expected flow rates of the integrated target system. Adding the MATD limit to the design calculations requires that the simulation iterates to find a primary inlet temperature that satisfies the MATD limit. This is easily done beginning with a set

primary inlet temperature and then decreasing it in intervals until the MATD limit has been met. Figure 8 shows the modified programming logic that includes the MATD calculations.

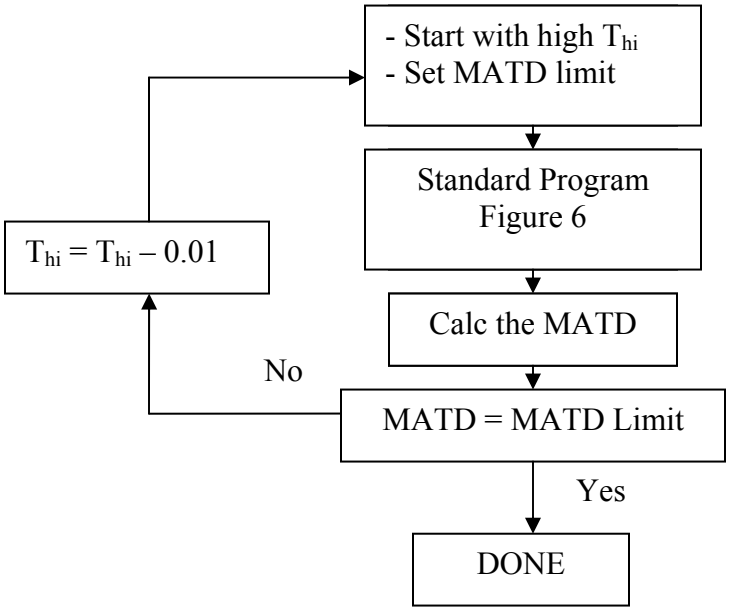


Figure 9: Program logic with MATD

The Exergy 10 Series shell and tube heat exchangers are also subject to absolute pressure and temperature limits. These limits represent the ranges of operation that the manufacturer will warranty their parts as well as possible operational limits. Table 6 shows the manufacturer specified operating limits. The only operating limit of concern to this work is the MATD.

Table 6: Exergy 10 series operating limitations [4]

| | | |
|---|---|---|
| Maximum operating pressure for shell side: | 1,000 | psi |
| Maximum operating pressure for tube side: | 1,500 | psi |
| Maximum operating temperature: | 800 | °F |
| Maximum average temperature difference: | 125 | °F |

Each of the three heat exchangers was evaluated at three MATD levels for flow rates corresponding to pump speeds between 3,000 and 10,000 RPM. This upper limit for the pump speed is outside the proposed operational window for the recirculating pump. However during lab testing the pump was ran at these speeds even though it would not be used at that capacity with the integrated system. As future pumps will have

higher capacity and reliability, operating the pump at higher RPM simulates performance at the anticipated higher flow rates. Since the performance of the heat exchangers is directly related to the supplied flow rates, a more efficient and higher capacity pump is essential to maximize their performance.

A baseline comparison of the three Series 10 heat exchangers was performed at a pump speed of 5500 RPM. Table 7 gives the dimensions and simulated performance of the 10 Series heat exchangers at approximately the same primary side flow rate for three different MATD levels.

Table 7: Dimensions and performance results for the Exergy 10 series shell and tube heat exchangers

| **Simulation Summary for Exergy 10 Series Shell and Tube Heat Exchanger** | | | | | | | |
|---|---|---|---|---|---|---|---|
| *All Calculations for Counter Flow* | | | | | | | |
| | | 00268-2 | | 00268-1 | | 00268-3 | |
| | | *Single Heat Exchanger* | | | | | |
| Tube ID (in/cm) = | | 0.0748 | 0.1900 | 0.0748 | 0.1900 | 0.0748 | 0.1900 |
| Tube Length (in/cm) = | | 4.0157 | 10.2000 | 7.9921 | 20.3000 | 12.0079 | 30.5000 |
| Tube Wall Thickness (in/mm) = | | 0.0100 | 0.2540 | 0.0100 | 0.2540 | 0.0100 | 0.2540 |
| Tube Pitch (in/mm) = | | 0.1181 | 3.0000 | 0.1181 | 3.0000 | 0.1181 | 3.0000 |
| Shell ID (in/cm) = | | 0.4331 | 1.1000 | 0.4331 | 1.1000 | 0.4331 | 1.1000 |
| Number of Tubes = | | 7 | | 7 | | 7 | |
| Total Tube Volume (mL) = | | 2.01 | | 4.00 | | 6.00 | |
| Heat Exchanger ΔP (psi) = | | 3.79 | | 3.94 | | 4.07 | |
| Primary Flow Rate (LPM) = | | 3.47 | | 3.45 | | 3.45 | |
| Secondary Flow Rate (LPM) = | | 12.57 | | 6.64 | | 4.22 | |
| System: | | 316 Stainless Steel Tubing<br>Heat Transfer (kW) | | | | | |
| MATD (°F) | Pressure (psi) | *Single Heat Exchanger* | | | | | |
| 125 | 100 | 4.40 | | 8.45 | | 12.35 | |
| 100 | 100 | 3.34 | | 6.34 | | 9.27 | |
| 75 | 100 | 2.33 | | 4.42 | | 6.43 | |

Additional simulations were performed at pump speeds from 3000 to 10000 RPM, which correspond to approximate primary side flow rates of 1.8 to 7.8 LPM respectively for all models. Figure 9 displays the thermal performance for all three models at an MATD of 125 °F. Figure 10 displays the simulated pressure drop vs. flow for all three models.

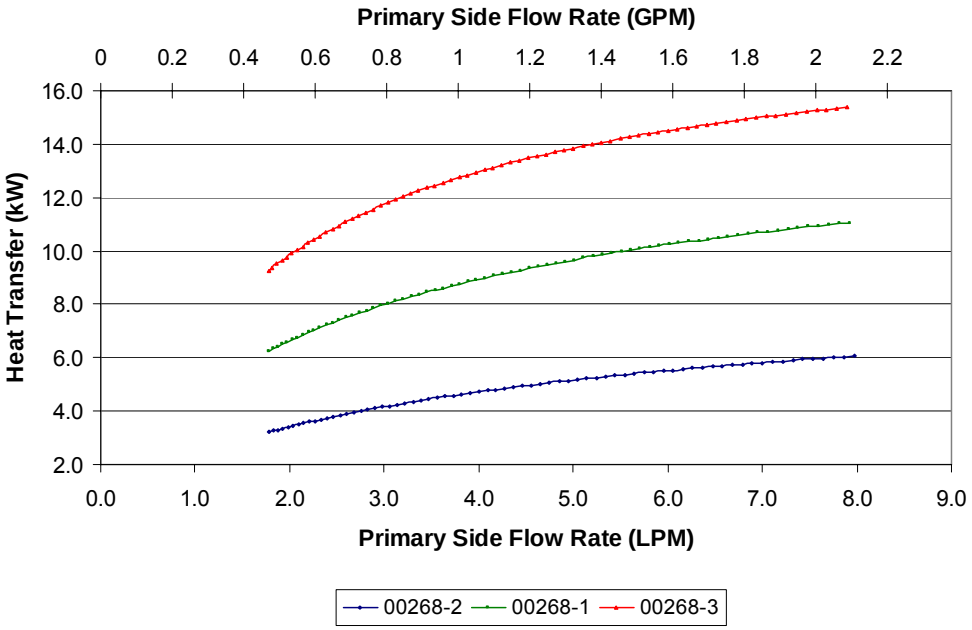


Figure 10: Exergy 10 Series Thermal Performance

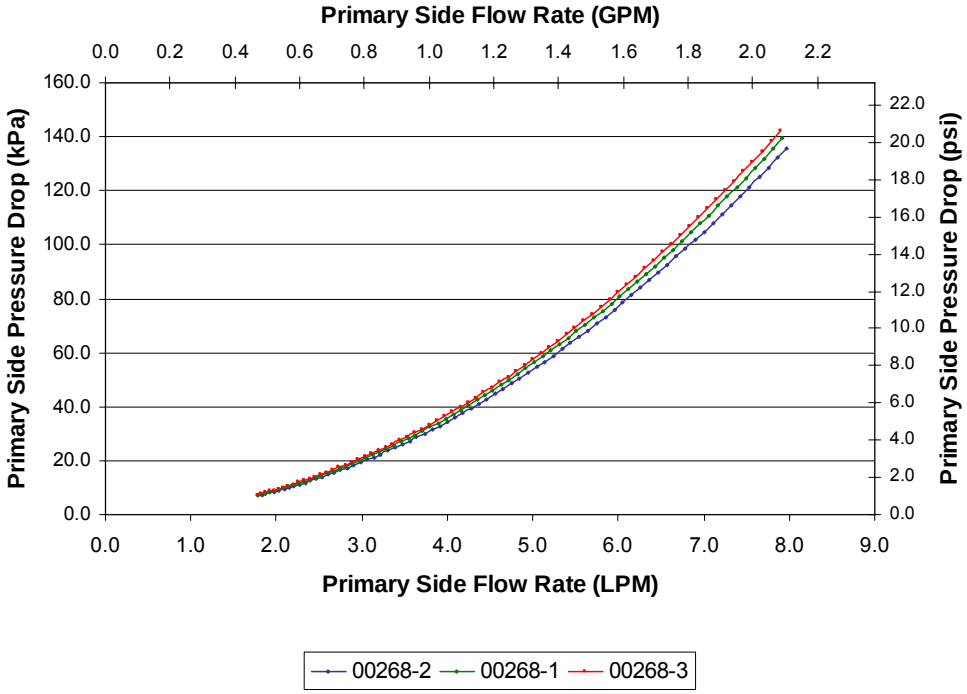


Figure 11: Exergy 10 Series Pressure Drop vs. Flow

It can be seen that the performance of these models differs greatly as a result of the different tube lengths. Though the model with the longest tubes out performs the other models, the ratio of heat transfer rate to primary side volume (load density), provides a better metric for gauging heat exchanger efficiency. As stated previously, the main objective for the selected heat exchanger is to transfer the maximum amount of heat with the smallest volume. Table 8 shows the load density for all of the 10 Series shell and tube heat exchangers.

Table 8: Load density of Exergy 10 series

| | Exergy 10 Series Model Number | | |
|---|---|---|---|
| MATD | 00268-2 | 00268-1 | 00268-3 |
| (°F) | kW/mL at ≈ 3.45 LPM | | |
| 125 | 2.19 | 2.12 | 2.06 |
| 100 | 1.66 | 1.59 | 1.54 |
| 75 | 1.16 | 1.11 | 1.07 |

It can be seen that the 00268-2 model has the greatest load densities for all MATD levels. This is due to higher secondary flow rates compared to the other models.

The optimized designs mentioned in previous sections are very similar in size to the Exergy 10 series shell and tube heat exchangers. Though the MATD was not considered previously, it may be that such a limiting factor would be present if the heat exchanger were custom built.

### 2.5.2 Selection of Prototype Shell and Tube Heat Exchanger

Selection of the prototype shell and tube heat exchanger is based on both physical size and performance. If the 12" model 00268-3 were used, it would require large spaces to be included between the pump and target body. Furthermore, it may be wasting primary side volume if low heat loads are desired. If model 00268-2 were used with its 4" tubes, it would fit neatly into the layout of the integrated target system and would have capacity to remove nearly 6 kW. This model also gives versatility to the builder when the integrated system becomes commercially available. For example, if the builder needs to supply a target with a 4 kW capacity, then only one 00268-2 heat exchanger is necessary. If the builder needs to supply a target with an 8 kW capacity, then either two 00268-2 heat exchangers can be used in the same system or one 00268-1 heat exchanger can be used.

Due to its versatility, the model 00268-2 heat exchanger was selected for the prototype shell and tube heat exchanger. Figure 11 shows a picture of the Exergy LLC model 00268-2 shell and tube heat exchanger beside a standard writing pen.


Figure 12: Exergy LLC model 00268-2 shell and tube heat exchanger

Manifolds for the 10 Series heat exchangers are simple pipe fittings. The calculated volume per manifold for the model 00268-2 heat exchanger is ≈ 0.4 mL.

### 2.5.3 Parallel vs. Series Orientation

It is of interest to evaluate the performance of a set of identical heat exchangers placed in either a parallel or series orientation. In both configurations, the secondary sides of the heat exchangers will be considered independent. This means that each heat exchanger will have equivalent secondary side pressure drop and flow rate. Depending on the component layout, it may be advantageous to place two heat exchangers in series in order to use them for both heat removal and as connective piping to other components. A parallel configuration may have advantages if increased heat transfer is required but physical space is limited. Figure 12 shows the general orientation of both a parallel and series set of heat exchangers.

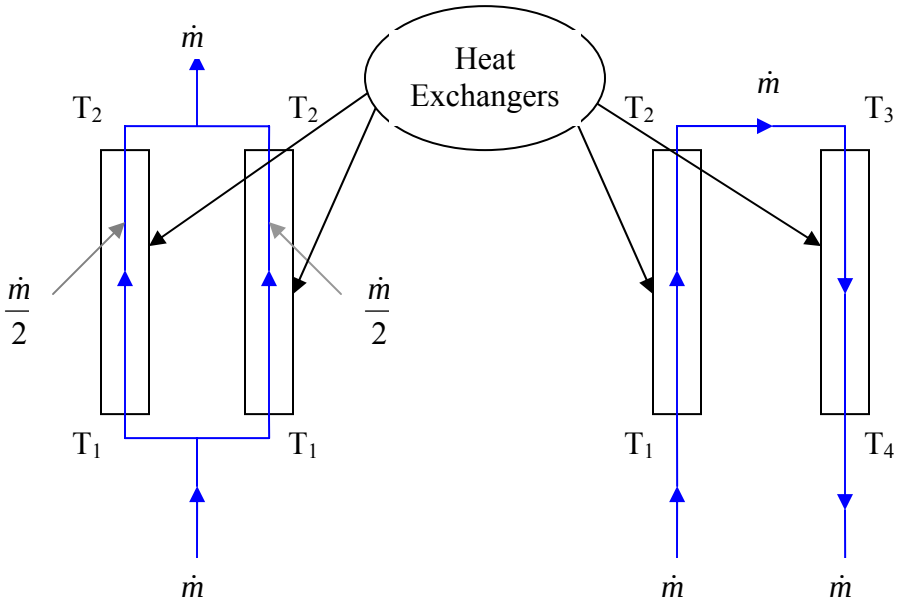


Figure 13: Parallel and series orientation

In a parallel orientation the mass flow rate is cut in half before entering each heat exchanger. Furthermore, the inlet and outlet temperature for each heat exchanger are identical. For a series orientation, both heat exchangers have the same mass flow rate but the inlet and outlet temperatures are different with the outlet temperature of the first heat exchanger serving as the inlet temperature for the second heat exchanger. A simulation of each system was performed to determine the orientation with the higher heat transfer. Figure 13 and 14 show the results for two model 00268-2 heat exchangers in parallel and series at 3 different MATD levels.

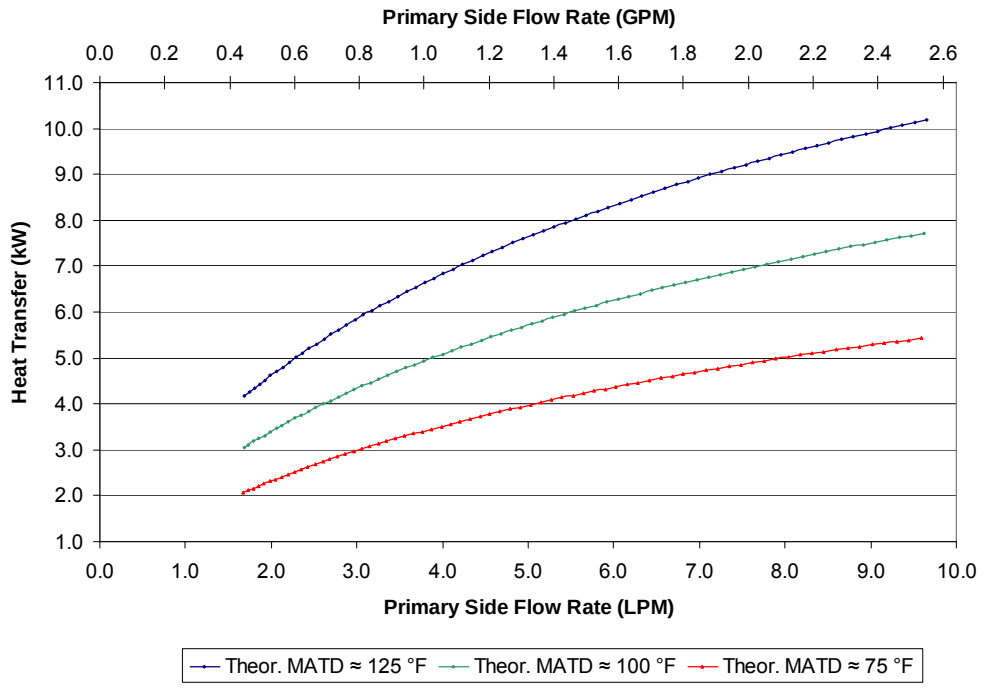


Figure 14: Two Exergy model 00268-2 heat exchangers in parallel

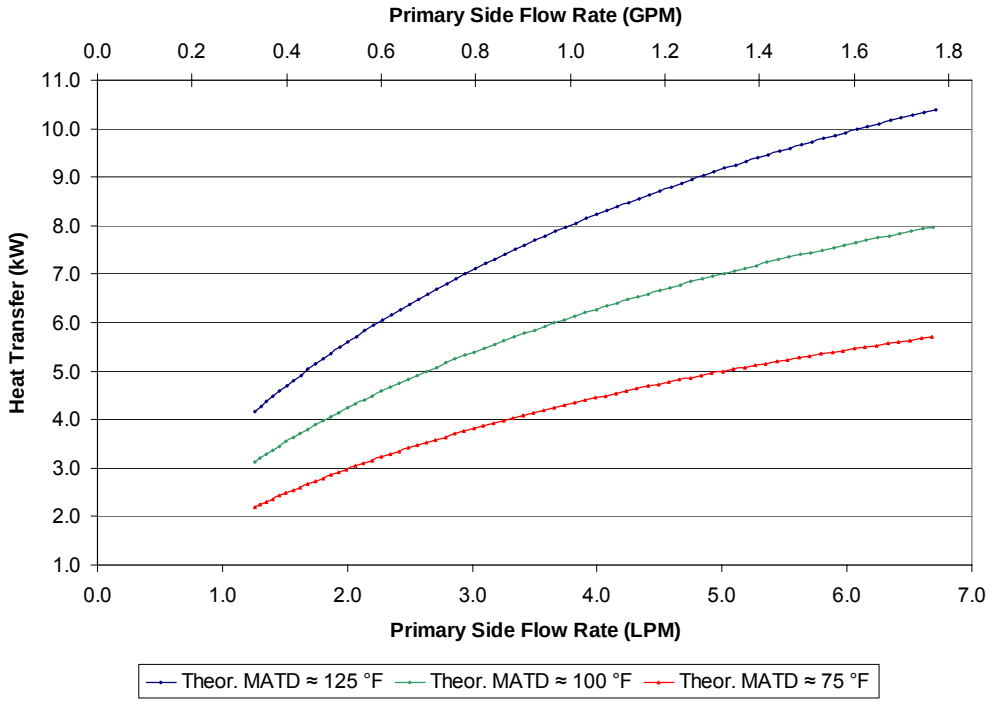


Figure 15: Two Exergy model 00268-2 heat exchangers in series

It can be seen that the series orientation yields a higher heat transfer rate than the parallel orientation by around 0.2 kW. There is a trade off between high inlet temperatures versus high flow rates. Having high inlet temperatures for both heat exchangers (parallel orientation) allows both to be run at the MATD limit. Having high flow rates for both heat exchangers (series orientation) yields a higher primary convective heat transfer coefficient, at the cost of higher system pressure drop. Both orientations are viable alternatives to be used with the integrated target system. If maximum heat transfer is desired, the series orientation should be used.

## 2.5 Experimental Tests

Bench top experiments were performed on an Exergy model 00268-2 heat exchanger to validate the simulation results. The original regenerative turbine pump was used to drive the primary side of the heat exchanger. This pump was designed to supply high pressure head and flow rates with minimal internal volume. The measured pump performance curves were also used as a basis for the simulated results. For the secondary side, the building water supply stepped up by a 0.5 hp FLOTEC utility pump was used to simulate expected supply pressures from a test facility de-ionized water supply. Secondary water conditions were held constant with a supply pressure of 62 psig and a temperature of 80 °F. The heat source came from an adjustable 0 to 9 kW WATLOW circulation heater. The primary side flow rate was recorded by a calibrated 0 to 3 psi Rosemont ΔP pressure transducer. A ΔP vs. Flow rate correlation was also established for the secondary side of the Exergy heat exchanger that was then used to calculate the heat transfer rate for the secondary side.

Independent tests were conducted to gather the pressure drop vs. flow data. An Omega 0 to 75 psi ΔP pressure transducer was used to record pressure drops and a Rosemont 0 to 3 psi ΔP pressure transducer was used to record flow rates.

Automated data collection was performed using LabVIEW and a series of Field point modules. LabVIEW was able to record all necessary temperatures and pressures throughout the system. Figure 15 and 16 show the laboratory equipment and the LabVIEW control screen.

Figure 16: Overview of laboratory equipment

Figure 17: Snapshot of shell and tube heat exchanger with testing instrumentation

LABVIEW was configured with a visual interface that served as both operational controls and as a system layout schematic. Figure 17 shows the on-screen LabVIEW controls schematic.

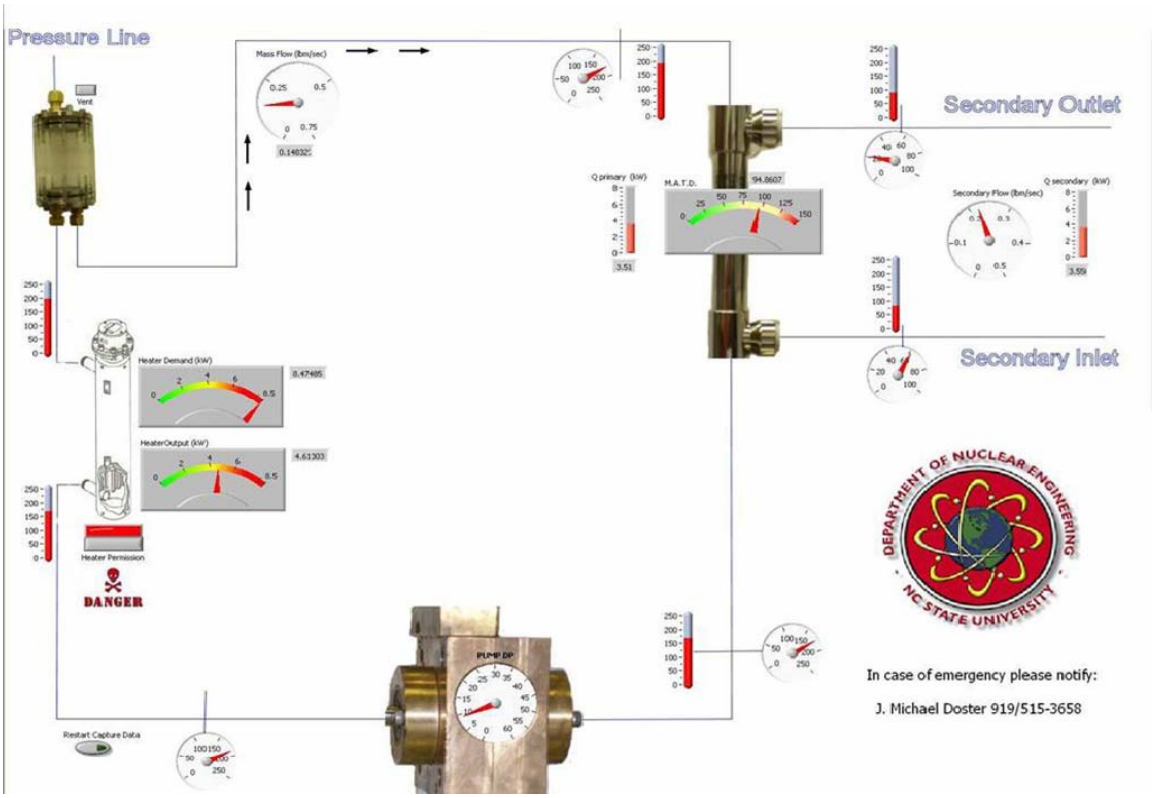


Figure 18: Screen shot of LabVIEW controls schematic for the shell and tube system

Before the data was taken the entire system was allowed to warm up for over an hour. This served to allow all system components to reach equilibrium. Data was collected in increments of 500 RPM with the regenerative turbine pump. Each time the pump speed was increased, the heater output was increased to maintain a steady MATD level. Data was collected over a time period of 15 to 20 seconds at a sampling rate of 4 samples per second. This data was then averaged to represent the data point for that speed setting.

## 2.6 Results

Data gathered from the experiments were compared to the theoretical model established earlier in this study. Of interests is heat transfer vs. primary side flow rate, the total system pressure drop vs. primary side flow rate, and heat exchanger primary side pressure drop vs. primary side flow rate. Figure 18 displays the thermal performance data.

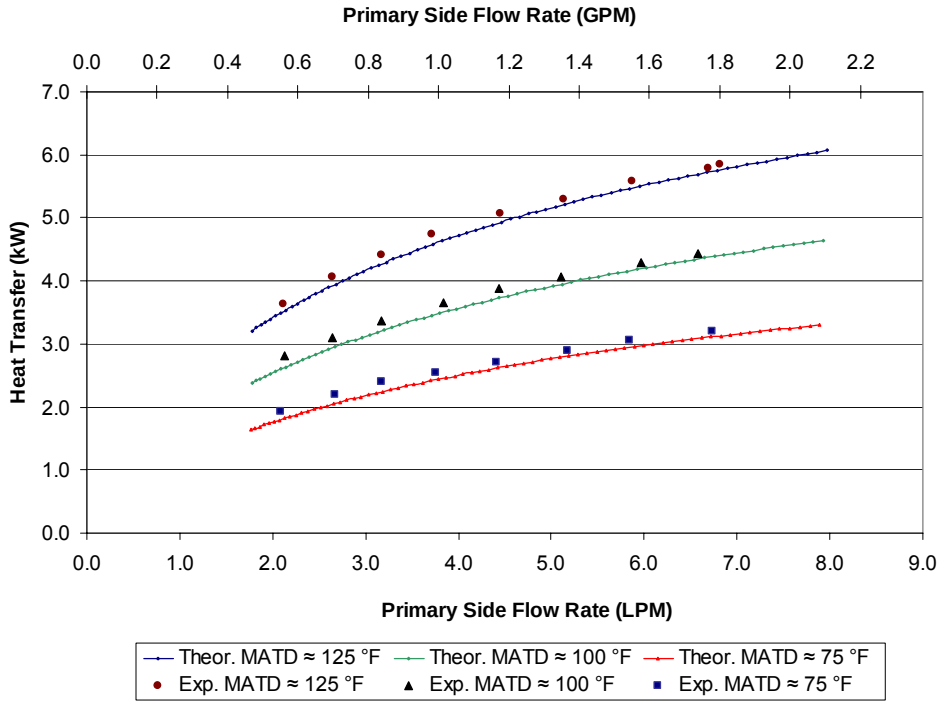


Figure 19: Exergy model 00268-2 thermal performance results

From Figure 18 it can be seen that the experimental data match the simulation results well for all three test MATD levels, though the simulation results consistently under predict heat exchanger performance by a small amount. Because the slope of the simulation and experimental data are close to the same, it appears that the primary side model is accurately predicting heat transfer as the primary side flow rate increases. Therefore, the difference between the simulated and measured results is likely due to under predicting the secondary side thermal performance. This is possibly due to minor dimensional discrepancies between the actual tube pitch and what was measured directly from the heat exchanger. Exact tube pitch dimensions were not attainable due to their proprietary nature.

It should also be noted that variations in the slope of the experimental data is most likely due to inadequacies with the regenerative turbine pump. Throughout the tests variations in pump speed caused ± 0.024 LPM fluctuations in primary side flow rate. This is because of the type of electrical motor that is used for the first generation regenerative turbine pump. This issue has been addressed and will be solved for the integrated recirculating target system.

The experimental results have shown the simulation models are capable of simulating the thermal performance of the combined heat exchanger and regenerative turbine pump. It should also be noted that the simulation and experimental results show a strong relation between primary side flow rate and heat transfer rate. This is because the majority of the thermal resistance is in the primary side heat transfer coefficient. Table 9 shows the thermal resistance values at different primary side flow rates. It can be seen that the primary side resistance is reduced by both higher temperatures and higher flow rates. It should also be noted that wall resistance is slightly reduced by higher temperatures. These results imply performance of the integrated target system can be improved if a higher capacity pump can be developed.

Table 9: Heat transfer resistance for Exergy 00268-2 shell and tube heat exchanger

| Exergy 10 Series Model 00268-2 Shell and Tube Heat Exchanger | | | | | | |
|---|---|---|---|---|---|---|
| MATD (°F) | Primary Side Flow Rate (LPM) | Primary Side Resistance | Primary Side Fouling | Wall Resistance | Secondary Side Fouling | Secondary Side Resistance |
| | | K/W | | | | |
| 125 | 1.98 | 0.0134 | 0.0 | 0.0037 | 0.0 | 0.0032 |
| | 2.98 | 0.0098 | 0.0 | 0.0037 | 0.0 | 0.0032 |
| | 4.00 | 0.0078 | 0.0 | 0.0037 | 0.0 | 0.0032 |
| | 5.04 | 0.0065 | 0.0 | 0.0037 | 0.0 | 0.0032 |
| | 6.05 | 0.0056 | 0.0 | 0.0037 | 0.0 | 0.0032 |
| | 7.00 | 0.0050 | 0.0 | 0.0037 | 0.0 | 0.0032 |
| 100 | 1.97 | 0.0149 | 0.0 | 0.0037 | 0.0 | 0.0032 |
| | 3.05 | 0.0106 | 0.0 | 0.0037 | 0.0 | 0.0032 |
| | 3.98 | 0.0086 | 0.0 | 0.0037 | 0.0 | 0.0032 |
| | 5.02 | 0.0072 | 0.0 | 0.0037 | 0.0 | 0.0032 |
| | 6.02 | 0.0062 | 0.0 | 0.0037 | 0.0 | 0.0032 |
| | 7.07 | 0.0055 | 0.0 | 0.0037 | 0.0 | 0.0032 |
| 75 | 2.02 | 0.0165 | 0.0 | 0.0038 | 0.0 | 0.0032 |
| | 3.03 | 0.0120 | 0.0 | 0.0038 | 0.0 | 0.0032 |
| | 4.05 | 0.0095 | 0.0 | 0.0038 | 0.0 | 0.0032 |
| | 4.99 | 0.0081 | 0.0 | 0.0038 | 0.0 | 0.0032 |
| | 6.10 | 0.0069 | 0.0 | 0.0038 | 0.0 | 0.0032 |
| | 7.04 | 0.0062 | 0.0 | 0.0038 | 0.0 | 0.0032 |

The thermal resistance values of the previous table show that a higher MATD reduces thermal resistance in primary side convection and tube conductivity. Further simulation shows that heat transfer is enhanced at higher system temperatures. For an MATD limited heat exchanger, it is necessary to increase the secondary side temperature

along with the primary side in order to increase system temperature and maintain a constant MATD. Table 10 shows data simulated for various system temperatures at an MATD of 125 °F, flow rates are varied from 1.75 to 8.20 LPM.

Table 10: Simulated heat transfer results for the shell and tube heat exchanger at different system temperatures at an MATD of 125 °F

| | | | | Average Values | | |
|---|---|---|---|---|---|---|
| **Peak Heat Transfer Rate (kW)** | **Peak Primary Side Inlet Temperature (°F)** | **Required System Pressure (Approx.) psia** | **Secondary Side Inlet Temperature (°F)** | **Interior Convective Resistance (W/°K)** | **Tube Wall Conductivity Resistance (W/°K)** | **Exterior Convective Resistance (W/°K)** |
| | | | | | | |
| 6.07 | 234.7 | 23 | 82.2 | 0.0080 | 0.0037 | 0.0032 |
| 6.26 | 244.6 | 28 | 91.2 | 0.0078 | 0.0037 | 0.0030 |
| 6.63 | 264.3 | 39 | 109.2 | 0.0073 | 0.0036 | 0.0027 |
| 6.81 | 274.1 | 46 | 118.2 | 0.0071 | 0.0036 | 0.0026 |
| 6.99 | 283.9 | 54 | 127.2 | 0.0070 | 0.0036 | 0.0024 |
| 7.17 | 293.7 | 63 | 136.2 | 0.0068 | 0.0036 | 0.0023 |
| 7.34 | 303.5 | 73 | 145.2 | 0.0066 | 0.0035 | 0.0022 |
| 7.51 | 313.3 | 84 | 154.2 | 0.0065 | 0.0035 | 0.0021 |
| 7.68 | 323.1 | 96 | 163.2 | 0.0063 | 0.0035 | 0.0020 |
| 7.84 | 332.9 | 110 | 172.2 | 0.0062 | 0.0035 | 0.0019 |
| 8.00 | 342.6 | 125 | 181.2 | 0.0061 | 0.0035 | 0.0018 |
| 8.15 | 352.2 | 142 | 190.2 | 0.0060 | 0.0034 | 0.0017 |
| 8.30 | 361.9 | 160 | 199.2 | 0.0059 | 0.0034 | 0.0017 |
| 8.45 | 371.6 | 180 | 208.2 | 0.0058 | 0.0034 | 0.0016 |
| 8.59 | 381.2 | 202 | 217.2 | 0.0057 | 0.0034 | 0.0015 |

From the previous table, it can be seen that thermal resistances decrease as system temperatures increase. The increase in temperatures causes the viscosity of water to decrease for both the primary and secondary sides. This in turn causes the Reynolds numbers to increase. Since the convective heat transfer coefficients are strongly dependent on the Reynolds numbers, the increased temperatures also increase the convection coefficients for both sides. Furthermore, the thermal conductivity values for 316 SS increase with temperature as well. All of these variables combined promote higher heat transfer rates. Note the increase in secondary side temperature that is required to maintain a constant MATD. From this simulation it can be determined that higher heat transfer rates may be achievable if system temperatures are increased. Though doing so will likely increase stress on other devices in the system.

Figures 20, 21 and 22 show the pressure drop vs. primary side flow rate for both the entire testing apparatus and the primary side of the heat exchanger as well as the pressure drop vs. flow data for the secondary side of the heat exchanger.

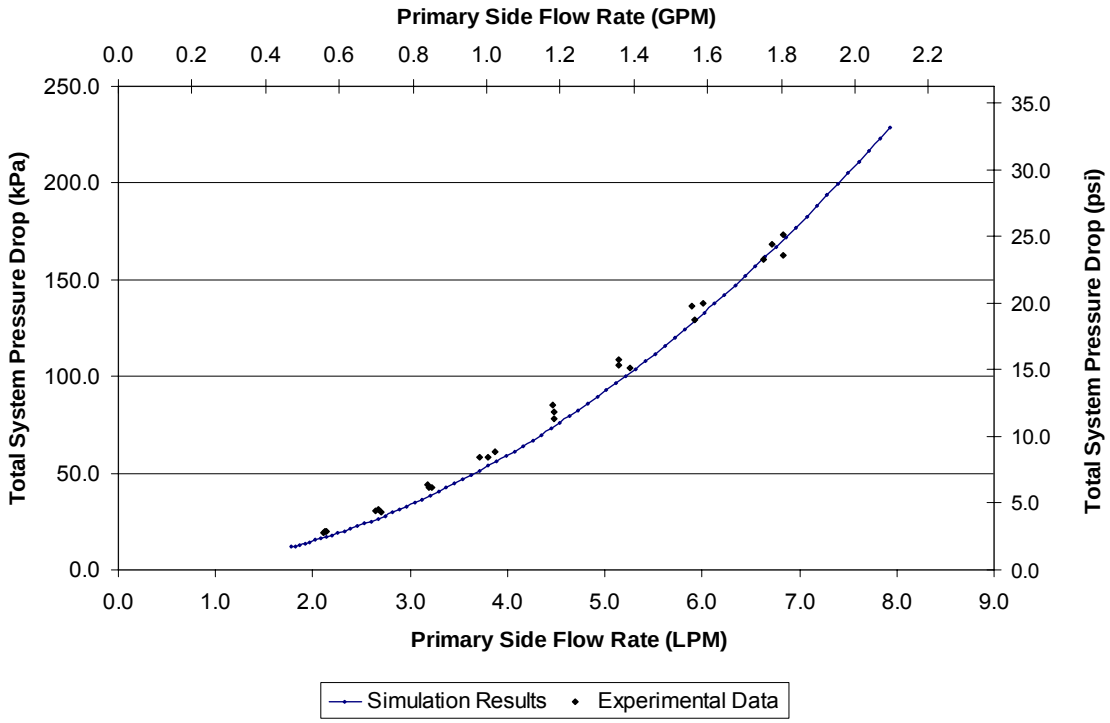


Figure 20: Testing apparatus pressure drop vs. flow

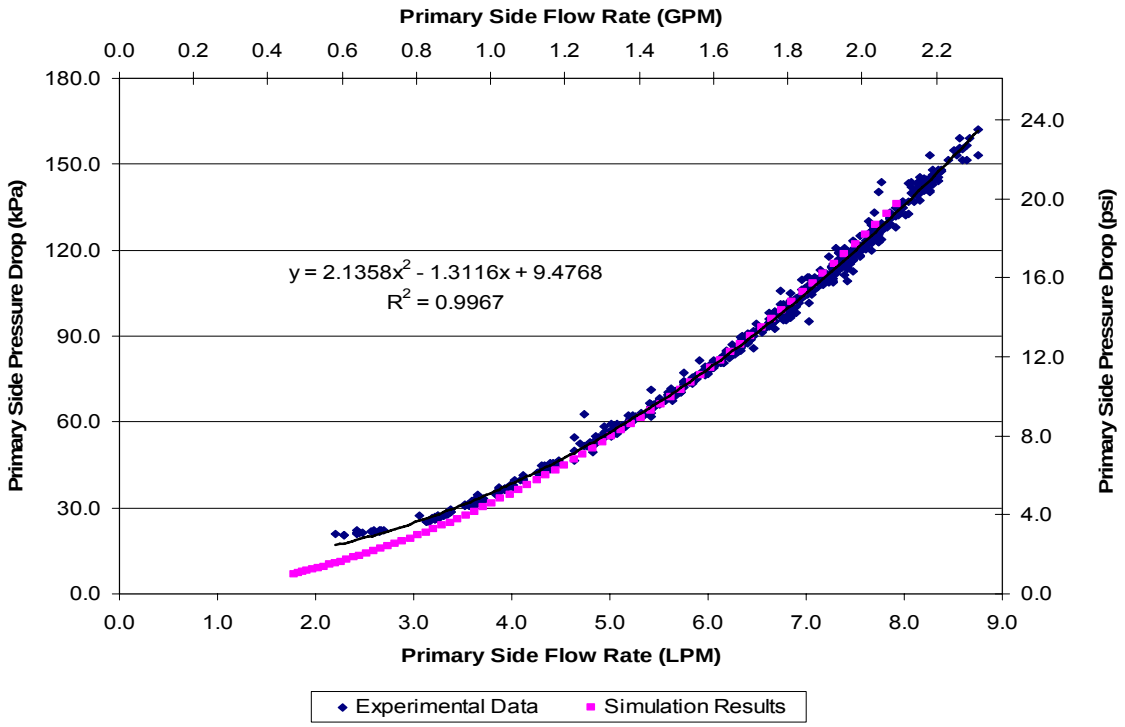


Figure 21: Exergy model 00268-2 primary side pressure drop vs. flow results

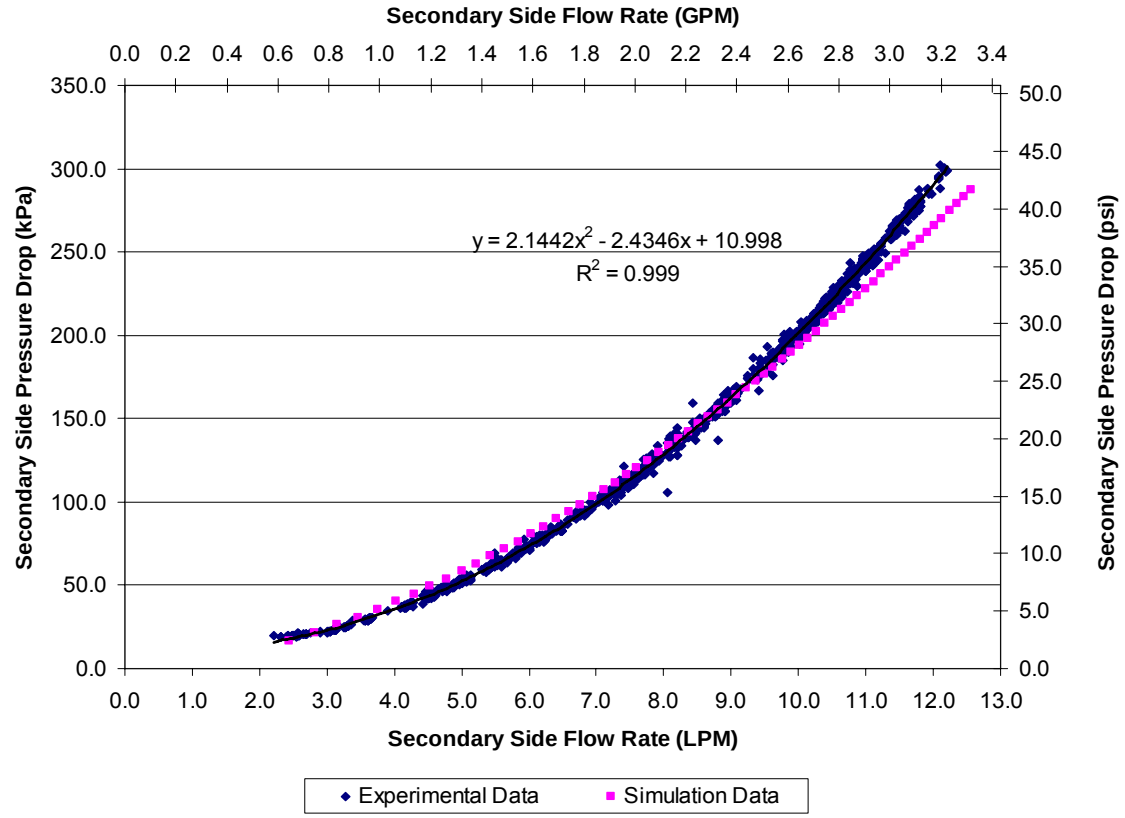


Figure 22: Exergy model 00268-2 secondary side pressure drop vs. flow results at 64.7 °F

Figure 20 displays the experimental and simulation pressure drop vs. flow results for the testing apparatus. It can be seen that the model predicts a slightly lower pressure drop at flow rates below 6 LPM and is in the middle of the experimental data at higher flow rates. This discrepancy is present because at these low flow rates the forms factors are functions of velocity.

Figure 21 shows the results of the ΔP vs. flow test for the primary side of the Exergy 00268-2 shell and tube heat exchanger. The theoretical model does predict slightly lower pressure drop values amounting to less than 1 psi at flow rates between 2 to 4 LPM, but is accurate at higher flow rates. This is most likely due to forms factors.

Figure 22 displays the experimental results for the secondary side pressure drop vs. secondary side flow rate. It can be seen that the theoretical model under predicts the secondary side pressure drop at flow rates above 10 LPM and is very close at lower flow rates. Future uses of the Exergy model 00268-2 simulation will likely include this correlated function for the hydraulic performance of the secondary side.

# Chapter 3

# Compact Cross Flow Heat Exchanger

## 3.1 Description

A cross flow heat exchanger refers to designs in which the hot and cold fluids are passed perpendicular to one another without making physical contact. Heat is conducted through a media between the two fluids. In order to maximize the performance of a cross flow heat exchanger the wall resistance must be minimized by using extremely thin walled channels. Minimizing the conduction resistance also makes the heat exchanger performance independent of the conduction material. Increased performance is also obtained by maximizing the convective properties of a high flow, low temperature secondary side.

Cross flow heat exchanger designs include flow between two flat plates, while other designs use molded rectangular or bored circular channels. Many cross flow heat exchangers have nearly identical primary and secondary side geometries, therefore they operate well in situations where the primary and secondary side flow characteristics are similar with a high temperature difference between sides, yet still benefit if the secondary side has larger flow rates as this will minimize heat transfer resistance on the secondary side. By minimizing wall resistance cross flow heat exchangers are very efficient and are a strong choice for use in compact designs. [9]

A common characteristic among cross flow heat exchangers is the intricate flow paths used to increase heat transfer. As stated above, most flow paths are contained between two plates, or a series of channels perpendicular to one another. Designing a series of individual channels increases heat transfer surface area. Designs exist which incorporate over 3000, 100 - 150 μm square channels on a 1 $cm^2$ surface [2, 12]. In this configuration the flow is basically passing through a fine screen mesh, where the pressure drops are minimal, the convective heat transfer coefficients are high and wall resistance is

at a minimum. Designs such as these are ideal, but extremely difficult and expensive to fabricate. Other, more practical designs such as the use of a series of bored circular channels are very effective while remaining relatively easy to design and fabricate. Figure 23 shows the general size and shape of a cross flow heat exchanger.

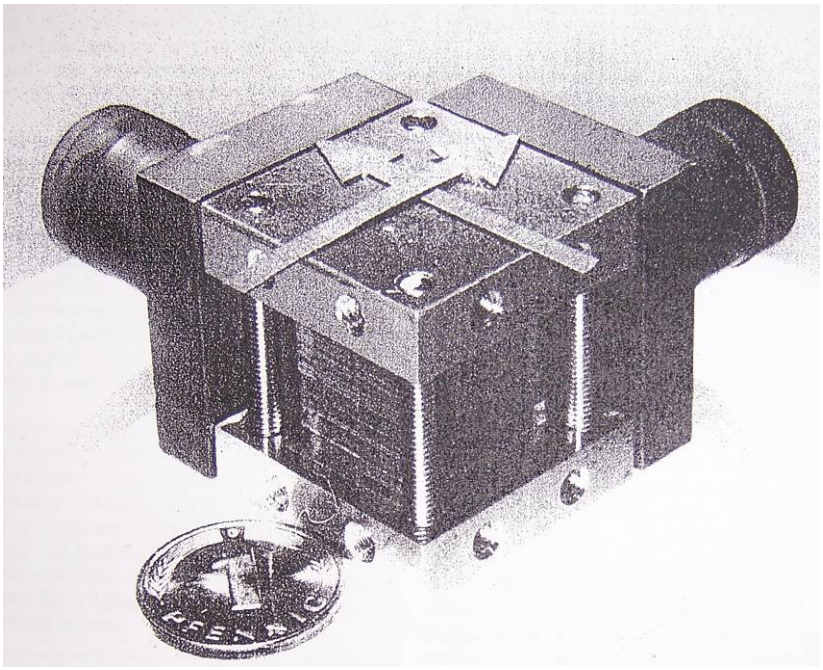

Figure 23: Cross flow heat exchanger [12]

## 3.2 Reason for Consideration

Cross flow heat exchangers are ideal for compact designs. They use small channels and wall thicknesses to maximize heat transfer rates. Furthermore, if constructed as a one-piece part, a cross flow heat exchanger can handle larger thermal stress than other designs. The cross flow designs that will be considered in this study consist of either rigidly bonded plates, or machined and tapped channels in a solid core.

A compact cross flow heat exchanger is another option for use with the integrated recirculating target design. In particular, a solid block cross-flow design is simple and reliable. This design would require a solid piece of metal stock to be shaped into a cube, into which the coolant channels can be bored directly. The material choice for this design will be based on heat transfer rates, machinability, and compatibility with the integrated target design and the production of the $^{18}F$ radionuclide.

## 3.3 Design

### 3.3.1 Methodology and Theory

In order to determine an optimal cross flow heat exchanger design, it is necessary to simulate different combinations of channel height, width (or diameter) and length, as well as the wall thickness. Assuming a primary flow rate, pressure drops across the heat exchanger and other devices in the system must be determined. As with the simulation/optimization of the shell and tube heat exchanger the correlated performance data for the regenerative turbine pump was included in the model.

The following sections outline the steps necessary to simulate the performance of a cross flow heat exchanger. Included in these sections are the equations used for the models and an explanation of the steps taken to code a FORTRAN program that predicts the performance of a cross flow heat exchanger. In the program, fluid properties are considered for a range of 500 psi to atmospheric pressure. It should be noted that enriched $^{18}O$ water and the de-ionized water have similar properties to tap water. Therefore, all primary and secondary side fluid properties are taken from standard fluids and thermodynamics tables for water.

As with the shell and tube heat exchanger, the initial use of this code was to predict heat exchanger performance as a function of tube and shell dimensions so that optimal configurations could be determined. Later, this program was modified and used to simulate a specific sized cross flow heat exchanger in use with the integrated recirculating target as well as simulate the performance of a lab testing apparatus. Modifications include accounting for pressure drops associated with smaller diameter tubes, the target, a circulation heater, and the pressurizer.

### I. Primary Side

The regenerative turbine pump was assumed to provide the flow to the cross flow heat exchanger. The $\Delta P$ created by the pump must be equated to the pressure drop across the primary side loop. As before, changing the pump speed correlates to different primary side pressure drops and flow rates. The primary side flow rate and the pressure drop are related by the following equations.

The fluid velocity through primary side heat exchanger channels is

$$V_{p,x} = \frac{G}{1000\left(L/m^3\right) * 60\left(s/\min\right) * N_{c,p} A_{x,p,x}} \tag{36}$$

The fluid velocity through the primary side supply tubing is defined by equation (3). The primary side pressure drop is defined as

$$\Delta P_h = \left(\frac{f_{p,x} L_{p,x}}{D_{i,p,x}} + K_{p,x}\right)\frac{\rho_p V_{p,x}^2}{2} + \left(\frac{f_t L_t}{D_{i,t}} + K_t\right)\frac{\rho_p V_t^2}{2} + \Delta P_{pressurizer}(G) + \Delta P_{target}(G) \tag{37}$$

The primary side pressure drop is then equal to the differential pressure produced by the regenerative turbine pump as defined by equation (7)

Combining Equations (1), (3) – (5), (7) and (36) – (37) yields a single non-linear equation with one unknown iterative variable G. For a given set of dimensions the flow through the channels can be solved iteratively at any pump speed.

## II. Secondary Side

The secondary side is operated at the constant inlet pressure and temperature listed earlier. The inlet temperature is held constant at 68 °F with a 75 psig or 517.107 kPa head pressure. Pressure losses will occur both in the connection lines and the secondary side of the heat exchanger. The outlet is considered to be at atmospheric pressure. The following equations relate the secondary side pressure drops and flow rates.

A mass balance between the secondary side channels and supply lines gives

$$V_s = V_{c,x}\left(\frac{A_{x,s}}{A_{x,c}}\right) \tag{38}$$

The total pressure drop for the secondary side of the cross flow heat exchanger is

$$\Delta P_c = \left(\frac{f_s L_s}{D_{i,s}} + K_s\right)\frac{\rho_s V_s^2}{2} + \left(\frac{f_{c,x} L_{c,x}}{D_{i,c,x}} + K_{c,x}\right)\frac{\rho_s V_{c,x}^2}{2} \tag{39}$$

Combining Equations (1), (4) – (5), (18) and (38) – (39) yields a non-linear equation with one unknown variable $V_c$. For a given set of dimensions the flow through the channels can be solved iteratively for any secondary side header pressure.

## III. Heat Transfer

In order to model the heat transfer capabilities of the cross flow heat exchanger, it is necessary to calculate the mass flow rates and convective heat transfer coefficients for the primary and secondary sides. To use a log mean temperature difference requires the outlet temperatures of both the primary and secondary sides. The only known temperatures for either side are the inlet temperatures. A system of equations must be created that relates the heat transfer rate to the exit temperatures. The following equations are necessary to solve for the heat transfer rate.

Once the primary and secondary side fluid velocities have been determined, the convective heat transfer coefficient can be obtained from the Dittus-Boelter correlation.

$$h_c = \left(\frac{k}{D_i}\right) \cdot 0.023 \cdot \mathrm{Re}^{0.8} \cdot \mathrm{Pr}_s^n \tag{40}$$

The primary side mass flow rate is

$$\dot{m}_i = \rho_p N_{c,p} A_{x,p,x} V_p \tag{41}$$

Similarly, the secondary side mass flow rate is given by

$$\dot{m}_o = \rho_s N_{c,s} A_{x,s,x} V_s \tag{42}$$

For the cross flow heat exchanger the overall heat transfer coefficient is given by

$$\frac{1}{UA} = \frac{1}{h_c A_i} + \frac{R_{f,i}}{A_i} + \frac{t}{kA_i} + \frac{R_{f,o}}{A_o} + \frac{1}{h_c A_o} \tag{43}$$

Such that the heat transfer rate across the heat exchanger is

$$\dot{Q} = F \cdot UA\Delta T_{lm} \tag{44}$$

Where F is a correction factor for cross flow heat exchangers and is illustrated in Figure 24.

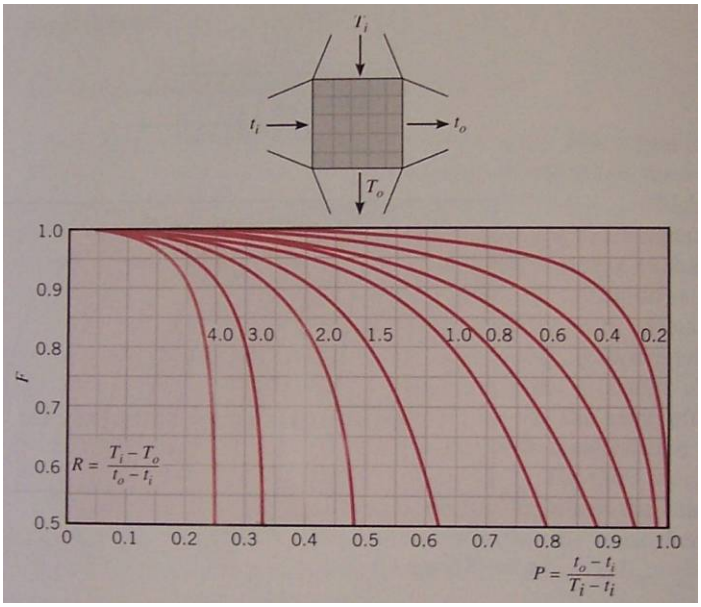


Figure 24: Correction factors for a single-pass, cross-flow heat exchanger with both fluids unmixed [8]

Fouling factors for the primary and secondary side are set to zero. Fouling factors are not relevant for small channels because any fouling that occurs would immediately clog the channels. Therefore, it is not necessary to include the effects of fouling in the calculations. [4]

Combining equations (29), (30), (32) and (41) – (44) yields a non-linear equation with one unknown variable Q which can be solved iteratively. As before, if the pump speed is changed the primary side characteristics change. The secondary side characteristics are essentially constant due to fixed inlet conditions, though the secondary $\Delta T$ will change if the pump speed changes. As with the shell and tube heat exchanger, the equations described in this section were implemented in a FORTRAN program and solved.

### 3.3.3 Rectangular Micro-Channels

Previous authors have measured the performance of micro cross flow heat exchangers that incorporate the use of small rectangular channels [2, 12]. These heat exchangers contained thousands of micro channels having dimensions 100 μm X 78 μm X 1 cm, with wall thicknesses around 25 μm and yielded heat transfer rates of 19.2 kW at a log mean temperature difference of 138.2 °F and a total volume of 1 mL. Figure 25 shows the rectangular micro channels.

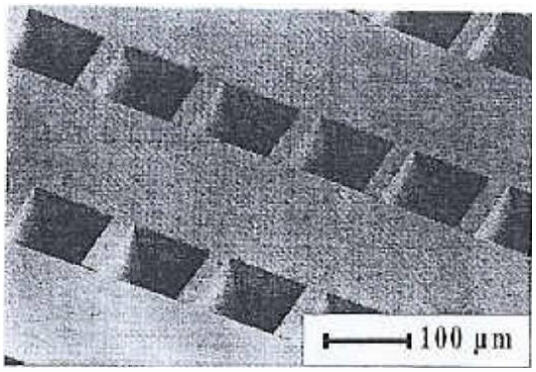


Figure 25: Rectangular micro channels [2]

To model the micro cross flow heat exchanger with rectangular channels the hydraulic diameter defined with equations (45) – (46) is used to replace the standard circular channel diameter in the previous equations. [3]

$$P_w = 2*(H+W) \tag{45}$$

$$D_h = \frac{4*A_x}{P_w} \tag{46}$$

### 3.3.4 Materials

As with the shell and tube heat exchanger, materials selected for the cross flow heat exchanger must be compatible with radiopharmaceuticals, their production environment and have adequate heat transfer properties. As before, stainless steel is a good choice to fulfill these requirements.

There are several types of stainless steel. Most are not free machining, which means they cannot be easily drilled or milled. The most common stainless steel is 316 SS. In general, 316 SS is formed and welded into the geometry desired. The material selected for the compact cross flow heat exchanger must be machinable, as the channels will be bored through solid stock. The exterior surfaces will then be machined to accommodate inlet and exit manifolds. To satisfy these requirements, 304 SS was chosen as the heat exchanger material. It has essentially the same thermal properties as 316 SS, is compatible with radiopharmaceuticals and can be machined to the desired specifications.

### 3.3.5 Operational and Fabrication Limitations

In comparison to the Exergy shell and tube heat exchanger the micro cross flow heat exchanger is tiny. The shell and tube heat exchanger, which had 1.9 mm or 1900 μm ID tubes, experienced clogging and eventually fouling in some situations. This was observed during experimental tests, where debris from the heater passed through the heat exchanger. Even though the debris did not hinder the performance of the shell and tube heat exchanger, a filter was installed to alleviate the problem for future tests. The same debris would have clogged the micro cross flow heat exchanger.

Although the integrated target should not see large amounts of heavy debris or sludge during operation, there will be some crud build up in the target after prolonged use. This crud may not clog the shell and tube heat exchanger but if present in the micro cross flow heat exchanger with square channels of 150 μm per side would likely create fouling issues and perhaps even clog some channels after extended operation.

There are challenges associated with fabrication of the micro cross flow heat exchanger as well. The common fabrication method is diffusion bonding. This is a technology intensive process that is not easily accessible and is likely expensive.

Though the micro cross flow heat exchanger will likely be impractical, it is useful to predict the performance of a generalized micro heat exchanger design. These predictions can be compared to results in the literature to validate the computational models and provide reference designs for the integrated recirculating target system.

There are also fabrication issues associated with the circular channel cross flow heat exchanger. The channels can only be bored in set increments and the smaller diameter channels must be drilled further apart if drilled deep. Upon consultation with the Duke University Physics machine shop, it was determined that 1/8” holes were the smallest diameter that could be drilled by a conventional drill bit and maintain reasonable tolerances at a depth of around 2 inches. The relationship between depth and tolerance are from drill bit “wander” and the possibility of drill bit breakage as it bores through the stock. The smaller the drill bit, the sooner wandering begins, and thus the less depth can be achieved. Consultation with the Duke University Physics machine shop indicated the depth limit in 304 SS is around 2” for a 0.125” diameter drilled hole with a wall thickness limit of 0.0625”.

Further research found EDM or Electrical Discharge Machining processes that can bore small circular channels into hard machining materials. This process, known as

"Deep Hole" or "Plunging" EDM allows smaller diameter channels to be bored deeper with better precision than using a conventional drill bit. This added precision also allows for smaller wall thicknesses to be incorporated into a design. Though there are limitations to EDM, it is possible to create 0.030" diameter channels with 0.010" wall thicknesses. For a prototype design it was recommended that a 0.040" channel diameter with a 0.020" wall thickness be constructed. This is mainly due to inexperience with using an EDM for these purposes in 304 SS. [15]

### 3.3.6 Optimization and Simulation

Design of the circular channel cross flow heat exchanger is constrained by the fabrication limits placed on channel diameter, depth and wall thickness. The micro rectangular channel cross flow heat exchanger is simply not practical to build, but its design should be considered for future reference.

To maximize exposure between the primary and secondary channels, the channel arrays were selected to be cubic. The MATD used with the shell and tube heat exchanger was used as a practical measure of how hard the heat exchanger was operated and serves as a good measure of comparison between the shell and tube and cross flow heat exchanger designs. Table 11 shows the dimensions and results of simulating these designs at moderate pump speed of 5500 RPM.

Table 11: Four cross flow heat exchanger designs made of 304 SS

| Simulation Summary for Cross Flow Heat Exchangers | | | | | | | | | |
|---|---|---|---|---|---|---|---|---|---|
| | | Design 1 | | Design 2 | | Design 3 | | Design 4 | |
| | | *Single Heat Exchanger* | | | | | | | |
| Circular Channel Diameter (in/cm) = | | 0.125 | 0.318 | 0.040 | 0.102 | 0.030 | 0.076 | ----- | ----- |
| Square Channel Side Length (in/μm) = | | ----- | ----- | ----- | ----- | ----- | ----- | 5.906E-05 | 150 |
| Channel Length (in/cm) = | | 1.600 | 4.064 | 1.600 | 4.064 | 1.600 | 4.064 | 0.394 | 1.000 |
| Wall Thickness (in/mm) = | | 0.063 | 1.588 | 0.020 | 0.508 | 0.010 | 0.254 | 9.843E-04 | 2.500E-02 |
| Number of Primary Side Channels = | | 21 | | 136 | | 300 | | 3192 | |
| Number of Secondary Side Channels = | | 28 | | 153 | | 325 | | 3249 | |
| Primary Side Volume (mL) = | | 6.76 | | 4.48 | | 5.56 | | 0.72 | |
| Primary Flow Rate (LPM) = | | 3.50 | | 3.51 | | 3.54 | | 3.62 | |
| Primary Side ΔP (psi) = | | 2.33 | | 2.82 | | 2.29 | | 2.25 | |
| Secondary Flow Rate (LPM) = | | 13.34 | | 12.18 | | 13.29 | | 12.72 | |
| System: | | 304 Stainless Steel Body<br>Heat Transfer (kW)<br>*Single Heat Exchanger* | | | | | | | |
| MATD (°F) | Pressure (psia) | | | | | | | | |
| 250 | 200 | 2.24 | | 7.84 | | 13.42 | | 31.90 | |
| 200 | 200 | 1.70 | | 5.94 | | 10.16 | | 25.01 | |
| 150 | 200 | 1.19 | | 4.13 | | 7.00 | | 17.50 | |
| 100 | 200 | 0.72 | | 2.48 | | 4.15 | | 10.20 | |

It can be seen that the performance of design 1 is far less than the others. It should also be noted that design 4 has by far the greatest performance. The reason for the extreme difference in performance is mostly due to wall thickness. It is also apparent that design 4 is far more efficient that the other designs, with primary side volume of only 0.72 mL. This is nearly 10% of the volume of design 1, yet it transfers around 14 times the amount of heat. Tables 12 and 13 show the load densities and the heat transfer resistance values for the four designs which further explain the performance differences in these designs.

Table 12: Load densities for four cross flow heat exchanger designs

| Compact Cross Flow Heat Exchangers | | | | |
|---|---|---|---|---|
| MATD | Design 1 | Design 2 | Design 3 | Design 4 |
| (°F) | kW/mL at a flow rate of ≈ 3.54 mL | | | |
| 250 | 0.33 | 1.75 | 2.41 | 44.42 |
| 200 | 0.25 | 1.33 | 1.83 | 34.83 |
| 150 | 0.18 | 0.92 | 1.26 | 24.37 |
| 100 | 0.11 | 0.55 | 0.75 | 14.21 |

Table 13: Heat transfer resistance for four cross flow heat exchanger designs

| Heat Transfer Resistance Comparison for all Cross Flow Heat Exchangers at an MATD of 200 °F | | | | | | |
|---|---|---|---|---|---|---|
| MATD (°F) | Primary Side Flow Rate (LPM) | Primary Side Resistance | Primary Side Fouling | Wall Resistance | Secondary Side Fouling | Secondary Side Resistance |
| | | K / W | | | | |
| Design 1 | 2.02 | 0.0412 | 0.0000 | 0.0225 | 0.0000 | 0.0158 |
| | 3.04 | 0.0298 | 0.0000 | 0.0225 | 0.0000 | 0.0158 |
| | 3.97 | 0.0242 | 0.0000 | 0.0225 | 0.0000 | 0.0158 |
| | 5.00 | 0.0201 | 0.0000 | 0.0225 | 0.0000 | 0.0158 |
| | 5.99 | 0.0174 | 0.0000 | 0.0225 | 0.0000 | 0.0158 |
| | 7.03 | 0.0154 | 0.0000 | 0.0225 | 0.0000 | 0.0158 |
| Design 2 | 0.01 | 0.0129 | 0.0000 | 0.0042 | 0.0000 | 0.0059 |
| | 0.01 | 0.0095 | 0.0000 | 0.0042 | 0.0000 | 0.0059 |
| | 0.01 | 0.0077 | 0.0000 | 0.0042 | 0.0000 | 0.0059 |
| | 0.01 | 0.0064 | 0.0000 | 0.0042 | 0.0000 | 0.0059 |
| | 0.01 | 0.0056 | 0.0000 | 0.0042 | 0.0000 | 0.0059 |
| | 0.00 | 0.0049 | 0.0000 | 0.0042 | 0.0000 | 0.0059 |
| Design 3 | 1.98 | 0.0085 | 0.0000 | 0.0014 | 0.0000 | 0.0037 |
| | 2.98 | 0.0062 | 0.0000 | 0.0014 | 0.0000 | 0.0037 |
| | 4.00 | 0.0050 | 0.0000 | 0.0014 | 0.0000 | 0.0037 |
| | 5.03 | 0.0042 | 0.0000 | 0.0014 | 0.0000 | 0.0037 |
| | 6.03 | 0.0036 | 0.0000 | 0.0014 | 0.0000 | 0.0037 |
| | 6.97 | 0.0033 | 0.0000 | 0.0014 | 0.0000 | 0.0037 |
| Design 4 | 1.99 | 0.0034 | 0.0000 | 0.0001 | 0.0000 | 0.0018 |
| | 3.00 | 0.0025 | 0.0000 | 0.0001 | 0.0000 | 0.0018 |
| | 4.02 | 0.0020 | 0.0000 | 0.0001 | 0.0000 | 0.0018 |
| | 4.97 | 0.0017 | 0.0000 | 0.0001 | 0.0000 | 0.0018 |
| | 5.98 | 0.0015 | 0.0000 | 0.0001 | 0.0000 | 0.0018 |
| | 7.03 | 0.0013 | 0.0000 | 0.0001 | 0.0000 | 0.0018 |

There is a large difference in wall resistance between each design. Table 12 shows that design 4 has wall resistance orders of magnitude less than the other designs. Design 1 has the worst performance and subsequently the highest wall resistance. Designs 2 and 3 however present a compromise between the ideal and the practical. It is possible to fabricate these two designs, and they offer reasonable performance. Of these two designs, design 3 is a better choice for optimal output. Design 3 offers 70% more heat transfer and a 66% decrease in wall resistance in comparison to design 2. However, for a prototype either design will serve as proof of principle and validation of modeling techniques. Figure 26 shows expected performance for designs 2 and 3 at an MATD level of 200 °F.

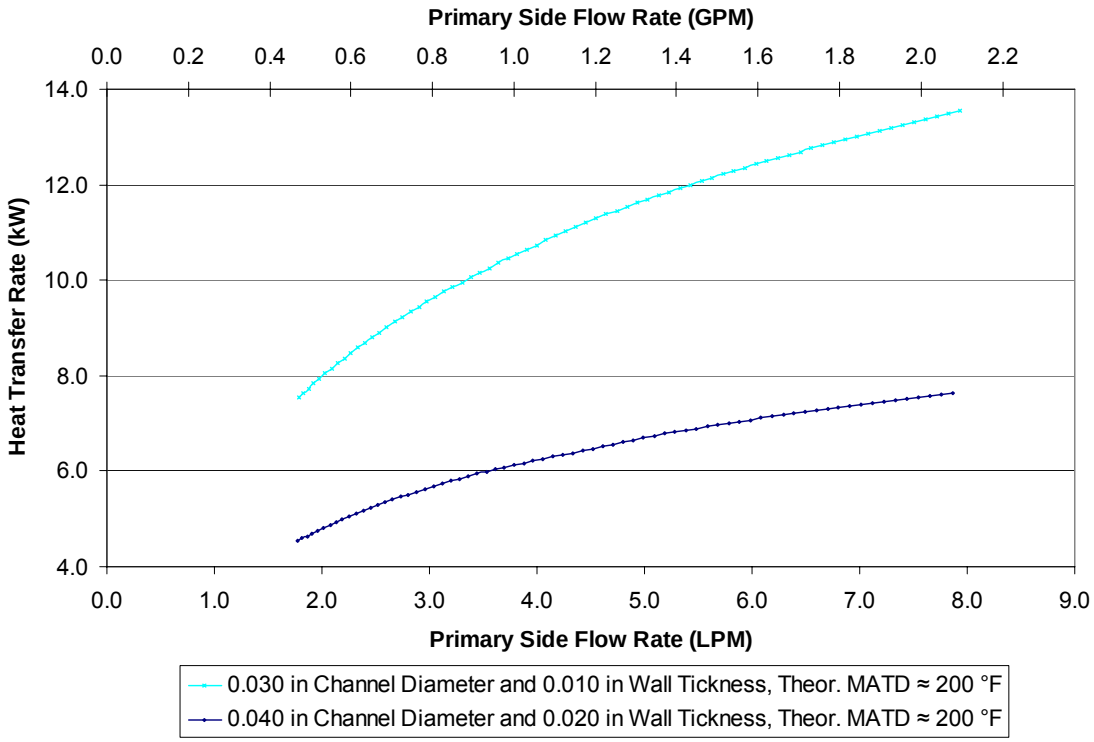


Figure 26: Designs 2 and 3 thermal simulation results

It can be seen from the figure that the slope of the thermal performance curves for design 3 is much higher than for design 2. This is because the decrease in wall resistance causes the performance of the heat exchanger to be more responsive to primary side flow rate.

## 3.4 Selection and Fabrication of Prototype

A prototype circular channel cross flow heat exchanger was designed and constructed to validate the computational models used in this study. Based upon recommendations from Xactwire EDM out of Waukesha, WI, design 2 with 0.040" bored holes and 0.020" wall thickness was the most feasible selection for a first of a kind prototype. Xactwire EDM believes it would be possible to construct a heat exchanger with 0.030" bored holes and 0.010" wall thicknesses after gaining experience fabricating this prototype design.

After Xactwire EDM bored the channels for the primary and secondary sides, the body of the heat exchanger was shipped to the Duke University Physics machine shop. At Duke, the final machining of the heat exchanger along with the construction of the

manifolds was completed. Figure 27 displays a dimensioned drawing for the design 2 cross flow heat exchanger. Figures 28 and 29 show two different views of the constructed cross flow heat exchanger.

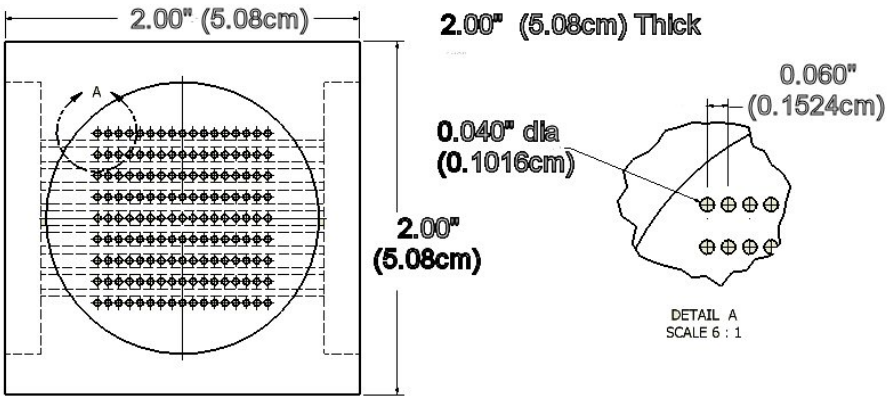


Figure 27: Dimensioned drawing of the design 2 cross flow heat exchanger (courtesy of Mark Humphrey)

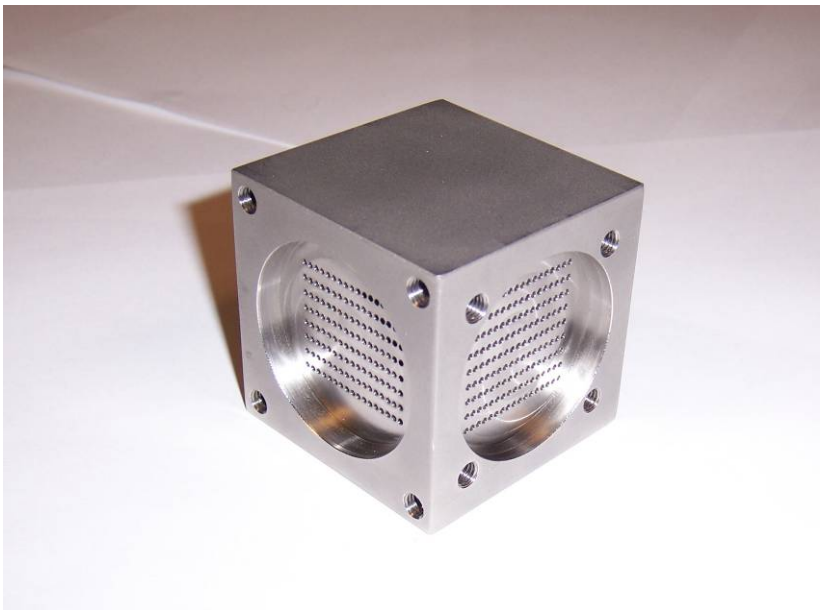

Figure 28: Corner view showing primary and secondary sides

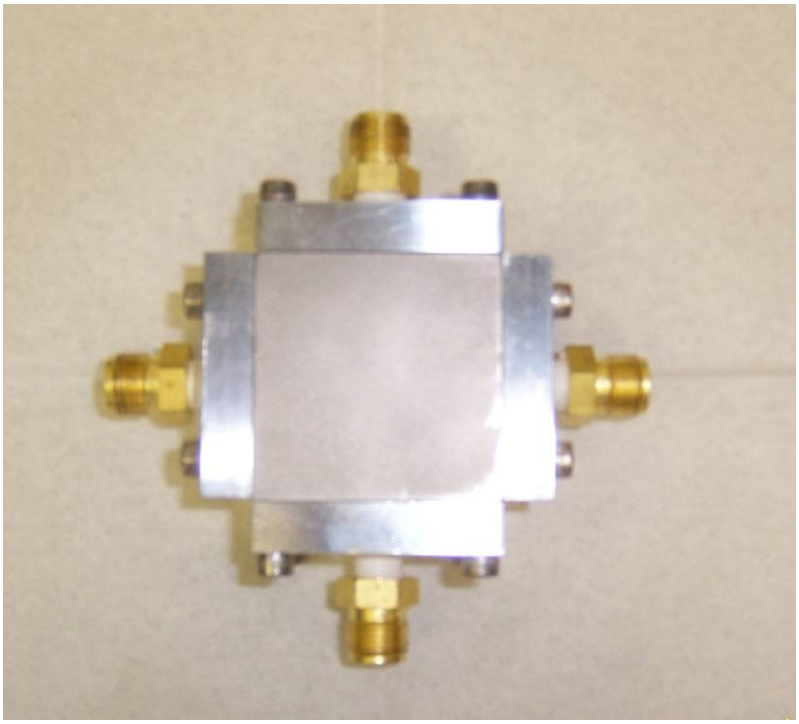

Figure 29: Assembled view with manifolds and fittings attached

## 3.5 Prototype Manifold Design

In order to maintain a low primary side volume, it is necessary to engineer low pressure drop, low volume manifolds. It would be simple to create an open chamber manifold that would evenly disperse fluid to all channels, but this design could quickly lead to a 5+ mL volume. It makes more sense to create a manifold that keeps the tubing connections as close to the heat exchanger channels as possible.

The prototype manifold design uses one connection point and then splits the stream into four separate paths which are directed to the four quadrants on the front of the heat exchanger channel array. Figures 30 and 31 show a construction drawing and a picture of the constructed manifold.

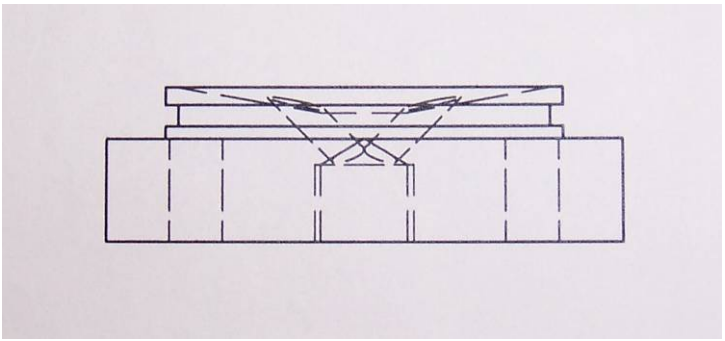

Figure 30: Side view drawing of manifold (courtesy of Mark Humphrey)

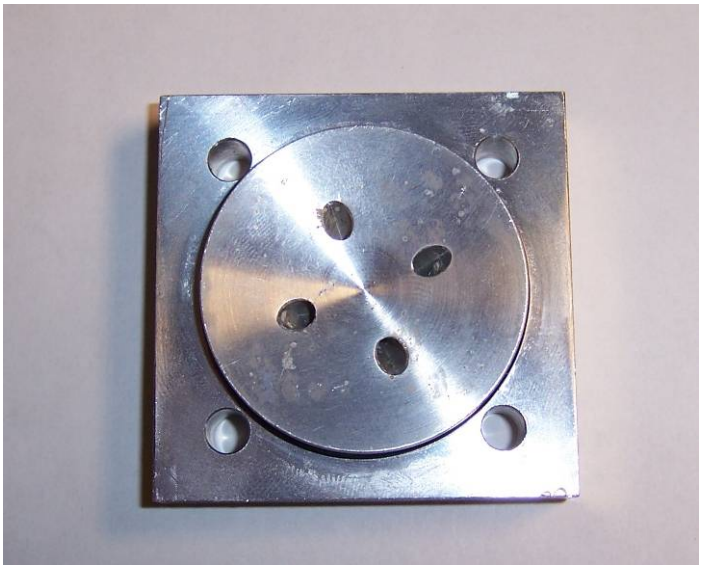

Figure 31: Cross flow heat exchanger manifold

This manifold design has a calculated volume of ≈ 2 mL. Therefore, together the manifolds will add 4 mL to the primary side volume. For the prototype cross flow heat exchanger this means the total primary side volume is around 8.48 mL.

After the manifolds were received simple "shower head" tests were performed to inspect the flow through the heat exchanger. This was necessary prior to testing the cross flow heat exchanger to insure uniform flow through the channels. The test was performed by running water through the heat exchanger horizontally with the exit side open. This allows for visual inspection of the distribution between the channels. Figure 32 shows a picture of the test.


Figure 32: Cross flow heat exchanger flow tests

These simply qualitative tests indicated that flow is reasonably distributed between the channels, with the possibility that there might be slightly higher velocities towards the edges of the channel array. This is most likely due to the angle at which the water exits the manifolds and enters the channels. Optimization of the manifolds may be possible with computational fluid dynamics (CFD) modeling.

An attempt was made to optimize the manifold design using the CFD models contained within COMSOL Multi-physics 3.2b. The design approach was to simulate a quarter symmetry model of the heat exchanger with both the inlet and exit manifolds. However, it was quickly discovered that COMSOL had difficulties in computing 3-dimensional CFD models of this complexity and the optimization study was terminated.

## 3.6 Experimental Tests

As with the shell and tube heat exchanger, experiments were performed to validate the theoretical models with experimental data. The prototype regenerative turbine pump provided flow to the primary loop, and the building water supply held at 62 psig in conjunction with the FLOTEC utility pump was used for the secondary side. A $\Delta P$ vs. flow correlation was established for the secondary side in order to measure secondary side flow rates while in operation. A Rosemont $\Delta P$ 0 to 3 psi pressure

transducer was used to measure the primary side flow rate. Thermocouples were placed throughout the system to record temperatures.

Independent tests were conducted to gather the pressure drop vs. flow data. An Omega 0 to 75 psi ΔP pressure transducer was used to record pressure drops and a Rosemont 0 to 3 psi ΔP pressure transducer was used to record flow rates.

With the shell and tube heat exchanger, the MATD had to be monitored continuously to minimize thermal stresses in the heat exchanger's brazed joints. With the cross flow heat exchanger this is not a concern, and the thermal limit is effectively the 350 °F melting temperature of the O-ring seals. However, the MATD is a good measure of how hard the heat exchanger is being operated and was used to set exertion levels for comparison with the theoretical models and later with the shell and tube heat exchanger. Figure 33 displays the instrumented cross flow heat exchanger. Figure 34 shows the control panel for the cross flow heat exchanger system.

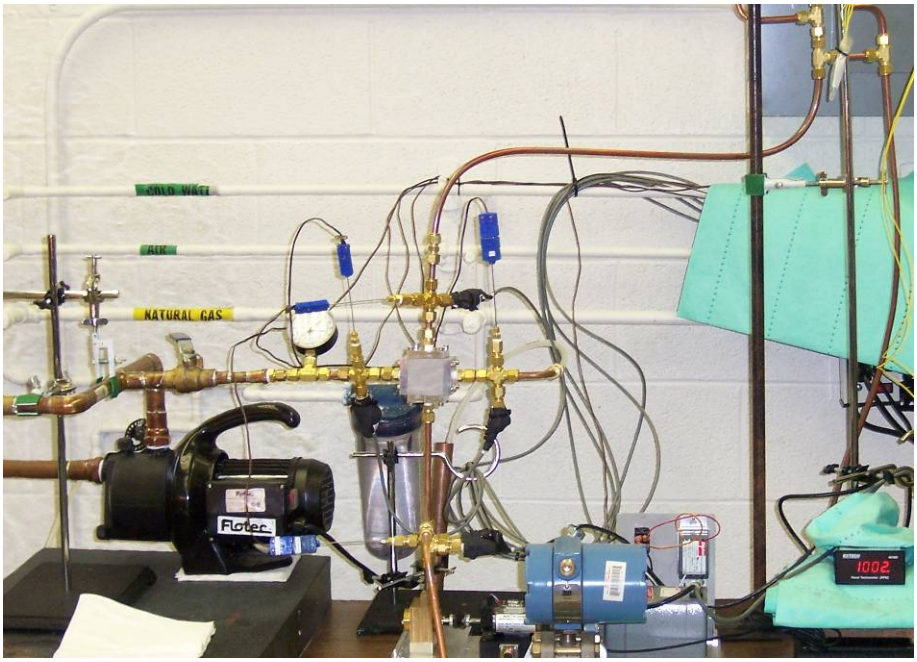


Figure 33: Snapshot of cross flow heat exchanger with testing instrumentation

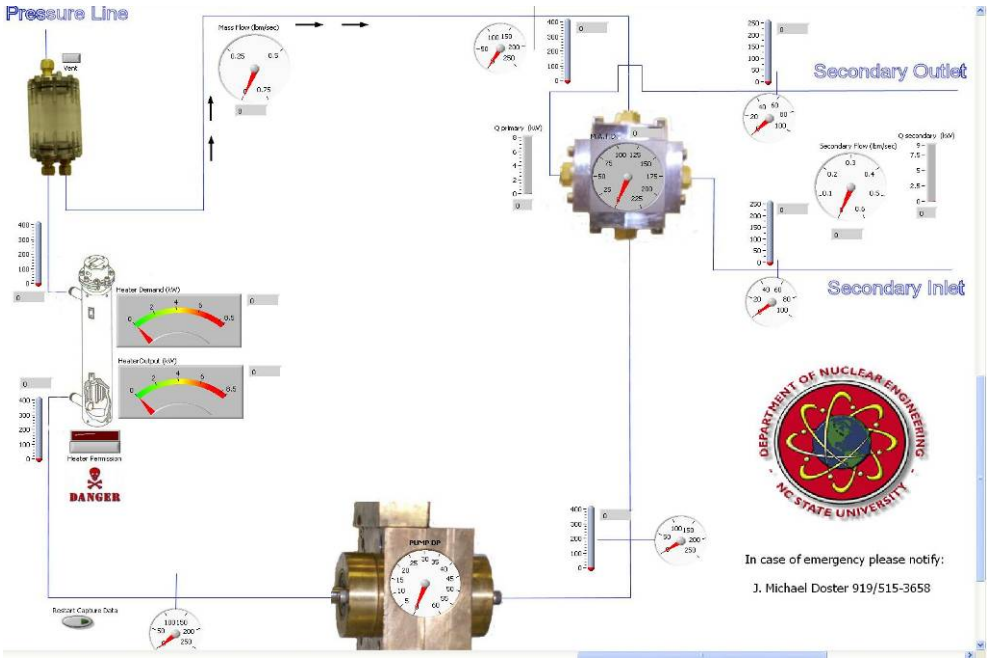


Figure 34: Screen shot of LABVIEW controls schematic for the cross flow system

The system was allowed to warm up for over an hour, and data was collected in increments of 500 RPM with the regenerative turbine pump. Each time the pump speed was increased, the heater output was increased to maintain a steady MATD level. Data was collected over a time period of 15 to 20 seconds at a sampling rate of 4 samples per second. This data was then averaged to represent the data point for that speed setting.

## 3.6 Results

### 3.6.1 Micro Heat Exchanger Model Validation

To validate the model established for the cross flow heat exchanger with rectangular micro-channels, a simulation was made of a known micro heat exchanger that had been experimentally tested. An article was found that described the construction and experimental tests of a micro heat exchanger [12]. The heat exchanger was constructed by compressing thin sheets of copper with grooves machined with thin diamond cutting wheels. Channels were cut to dimensions 100 μm X 78 μm X 14 mm, with a 23 μm wall thickness. The primary and secondary channels were stacked perpendicular on top of each other. The channels were cut on the inside of the foils leaving a 2 mm gap of uncut area on each side. [12]

Results indicate that the experimentally tested heat exchanger worked exceptionally well. It is stated that the inlet conditions for the primary and secondary sides were held nearly constant at 95 °C and 13 °C. At that primary side inlet temperature no pressurization was required to prevent boiling. Furthermore, the primary and secondary side flow rates were maintained equal to one another and varied from 0.25 to 12.5 LPM. Performance measurements indicate that the heat exchanger had peak performance of 19.2 kW with a log mean temperature difference of 59 °K and a volumetric heat transfer coefficient of 324 W/cm$^3$°K. [12]

A model of this micro heat exchanger was developed with primary and secondary side characteristics set accordingly. The flow rate was varied from 0.25 to 12.5 LPM and the heat transfer rate, log mean temperature difference, and volumetric heat transfer coefficient calculated. Figure 35 shows the log mean temperature difference and heat transfer rate for the simulation.

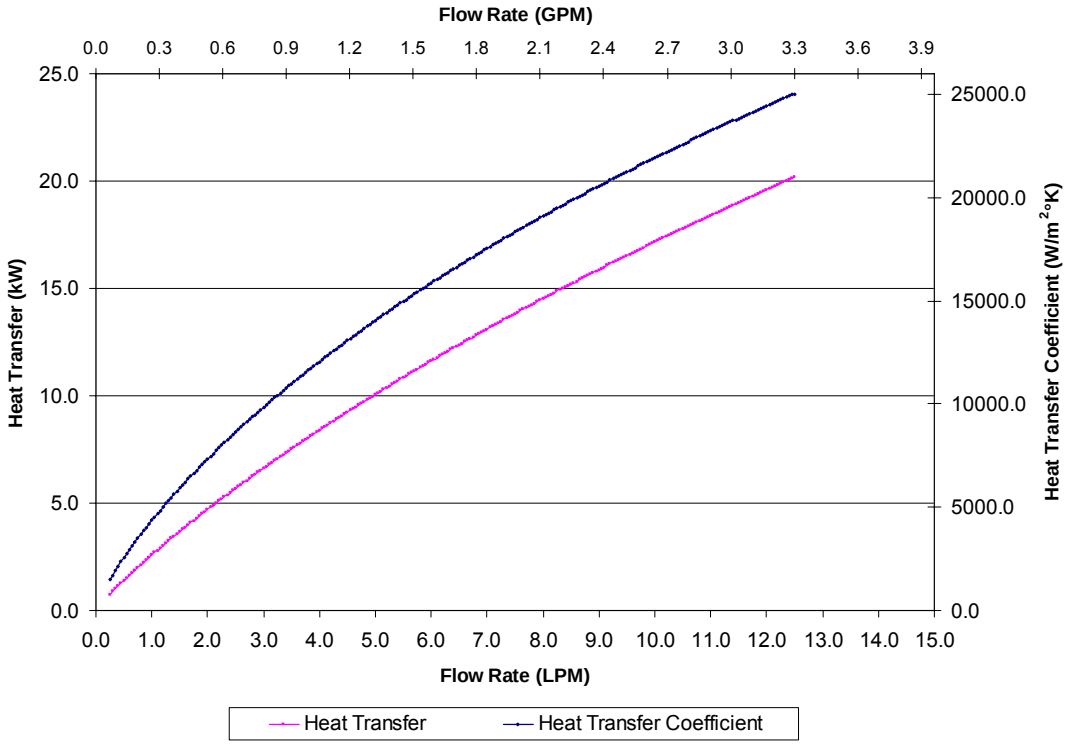


Figure 35: Results for validation of micro cross flow heat exchanger model

Limited numbers are available to compare the modeled results to the experimental data. Table 14 compares the reference experimental data to the simulated data.

Table 14: Comparison of simulation and experimental data for the micro cross flow heat exchanger validation model

| | Reference Experimental Data [12] | | | Simulated Data | | | Relative Error | | |
|---|---|---|---|---|---|---|---|---|---|
| Flow Rate (LPM) | Heat Transfer (kW) | Log Mean Temperature Difference (°K) | Heat Transfer Coefficient ($W/m^2°K$) (Approx.) | Heat Transfer (kW) | Log Mean Temperature Difference (°F) | Heat Transfer Coefficient ($W/m^2°K$) | Heat Transfer (kW) | Log Mean Temperature Difference (°K) | Heat Transfer Coefficient ($W/m^2°K$) |
| | | | | | | | | | |
| 5.0 | 10.0 | -- | 13500 | 10.0 | 52.8 | 14043.5 | 0.5% | -- | 3.9% |
| 10.0 | 16.0 | -- | 19000 | 17.2 | 57.1 | 21926.6 | 6.7% | -- | 13.3% |
| 12.5 | 19.2 | 59.0 | 23000 | 20.2 | 58.5 | 25025.5 | 4.8% | 0.8% | 8.1% |

It can be seen from the previous table that data matches best at low flow rates. Of the data compared, the one available experimental data point of log mean temperature difference matches the closest. It can also be seen that the heat transfer rate and heat transfer coefficient have relative errors that maintain close linearity between data points. From this it may be inferred that the heat transfer coefficient is primarily responsible for differences in the heat transfer rate. There is not enough known about the experimental tests to draw exact conclusions about data discrepancies. However, with a maximum error of 6.7% for the heat transfer rate it can be concluded that the model matches reasonably well.

### 3.6.2 Results of Experimental Tests

Experiments were performed to validate the theoretical models of the circular channel cross flow heat exchanger. Of interest is the heat transfer vs. primary side flow rate, the predicted total system pressure drop vs. primary side flow rate, and the primary side heat exchanger pressure drop vs. primary side flow rate. Figure 36 displays the thermal performance data.

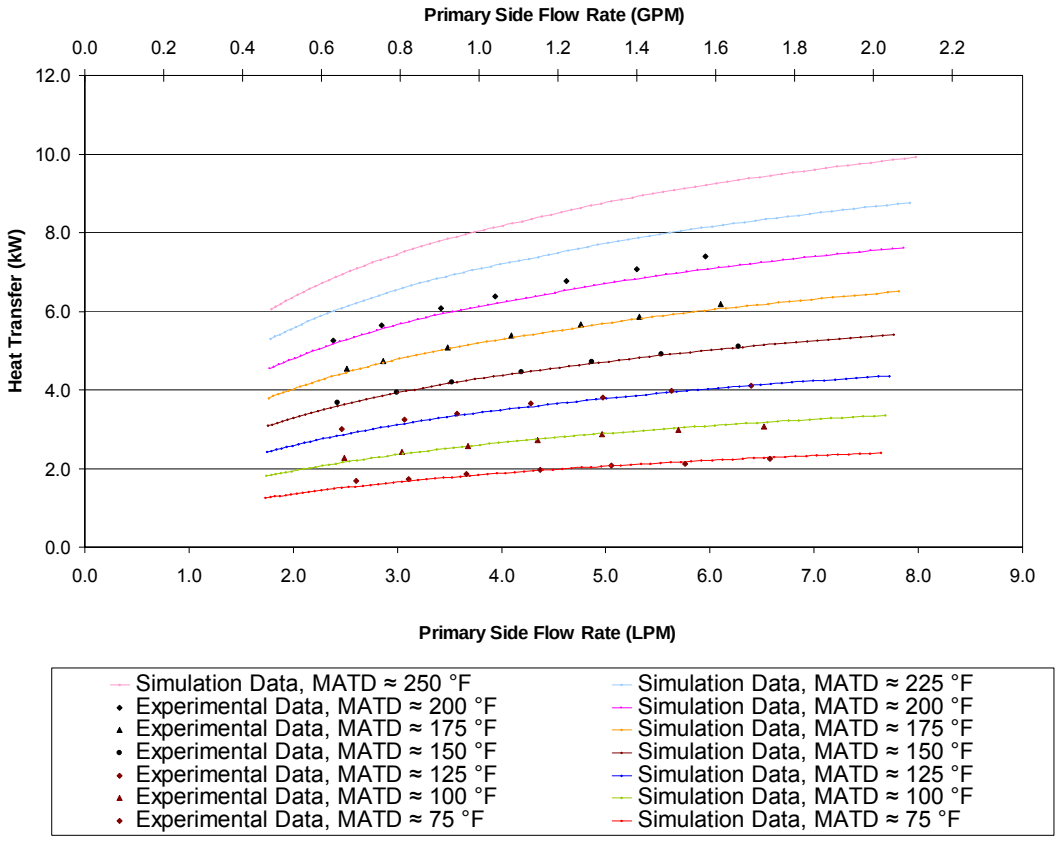


Figure 36: Design 2 thermal performance results

From Figure 36 it can be seen that the experimental data match the theoretical simulation results well across all six tested MATD levels. Similar to the testing of the shell and tube heat exchanger, variations in pump speed caused ± 0.024 LPM fluctuations in the primary side flow rate. Also during the testing of the cross flow heat exchanger the pump experienced seal and bearing failures which caused the pump to run with more vibrations. This could have reduced the performance of the pump as there was also some leaking.

It should be noted that the results show a strong relation between primary side flow rate and heat transfer rate. This is because the heat transfer resistance is the highest on the primary side throughout the experimental primary side flow rate span, but reduces as flow rate increases. Refer to Table 12 for the heat transfer resistance values. Figures 37, 38, and 39 displays the pressure drop vs. primary side flow rate for both the entire testing apparatus and the primary side of the heat exchanger as well as the pressure drop vs. flow data for the secondary side of the heat exchanger.

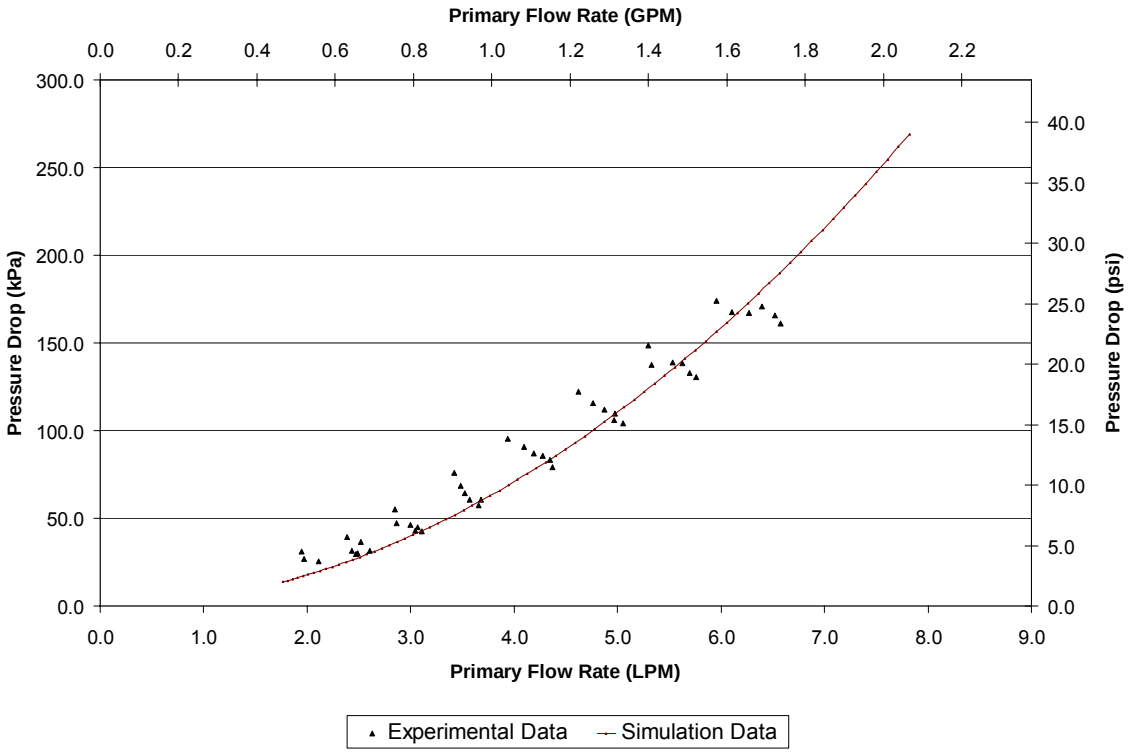


Figure 37: Design 2 testing apparatus pressure drop vs. flow results

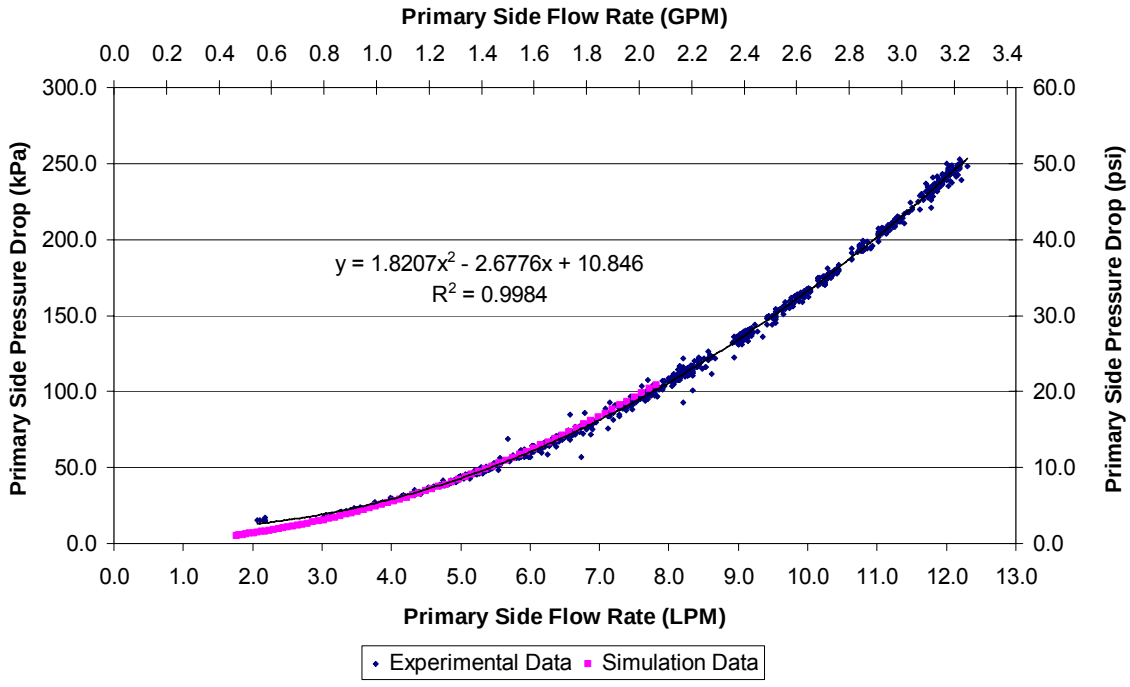


Figure 38: Design 2 primary side pressure drop vs. flow results

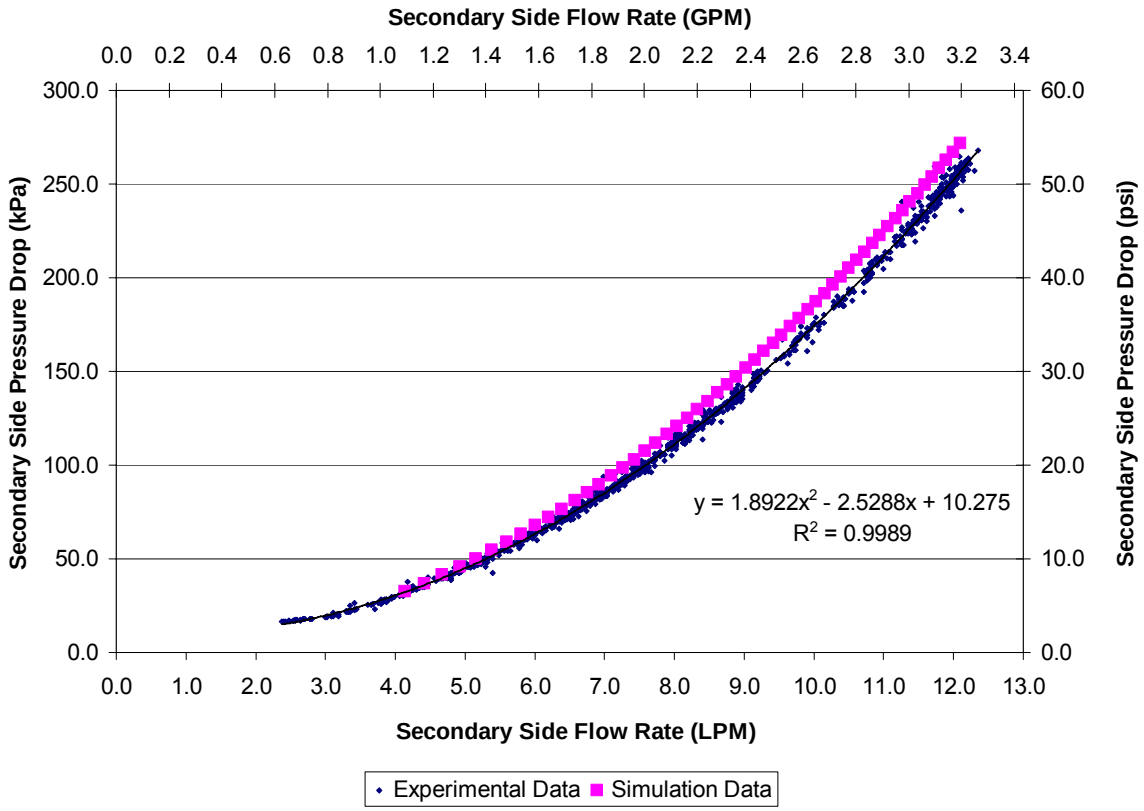


Figure 39: Design 2 secondary side pressure drop vs. flow results, at 64.3 °F

As before, the entire system was simulated and approximate values of forms factors were included in the modeling. For the testing apparatus a forms factor of 14.0 was determined necessary. This is higher than with the shell and tube experiments as the piping changed around the pressurizer and a filter was added to the system.

Figure 37 displays the experimental and simulation pressure drop vs. flow results for the testing apparatus. It can be seen that the model predicts a slightly lower pressure drop at low flow rates and is in the middle of the experimental data at higher flow rates. This is most likely due to the added complexity of the pressurizer connections, and filter present in the cross flow experimental system which was difficult to accurately account for.

Figure 38 shows the results of the ΔP vs. flow test for the primary side of the prototype cross flow heat exchanger. Data was taken over a range of flow rates and shows that the theoretical model adequately predicts pressure drop. The theoretical model does predict slightly lower pressure drop values amounting to less than 1 psi at

flow rates between 2 to 3 LPM, and is in the middle of the data at higher flow rates. This is most likely because the forms factor is not a constant at these lower flow rates.

Figure 39 displays the experimental results for the secondary side pressure drop vs. secondary side flow rate for the constructed cross flow heat exchanger with 0.040" channels and 0.020" channel spacing. It can be seen that the theoretical model predicts a slightly higher pressure drop at all flow rates, though the theoretical data is reasonably close to the experimental data.

# Chapter 4

# Heat Exchanger Selection and Integrated System Simulation

## 4.1 Purpose

The performance of several integrated target systems was simulated upon selection of a prototype heat exchanger design. Unlike the test apparatus, the final integrated system will have small diameter and shorter length connective tubes. There will also be additional devices added to the system such as a miniature pressurizer and the target chamber. These additional devices plus smaller tubing will increase pressure drop and decrease flow rates, as well as contribute to the overall system volume. Furthermore, the performance characteristics of the regenerative turbine pump will be considered valid for this preliminary evaluation of the system. The regenerative turbine pump will be simulated in a practical range of operation. This limits pump speed to between 4000 and 6000 RPM.

## 4.2 Heat Exchanger Selection

Two heat exchangers have been designed, simulated, and experimentally tested. Laboratory experiments show that the models established to simulate the thermal performance of these heat exchangers are accurate. It is now possible to select which built design would best suit the needs of the prototype integrated recirculating target system. It is also useful to determine if construction of a cross flow heat exchanger with smaller channel diameter and channel spacing such as the design 3 cross flow heat exchanger discussed in this study would further benefit the integrated recirculating target system performance. The design 3 cross flow heat exchanger has 0.030" diameter

channels and 0.010" channel spacing. It is also useful to compare the model 00268-1 shell and tube heat exchanger, the next larger of the Exergy 10 Series.

One major concern for the integrated recirculating system is physical dimensions. The shell and tube heat exchanger has the smallest footprint of the two built designs. It is 4.9 inches long, 0.6 inches wide, 1 inch tall and weighs 0.35 pounds. The Exergy model 00268-1 shell and tube heat exchanger is roughly twice as long and heavy. The Cross flow heat exchanger has rough dimensions of 2.5 inches cubed with a weight of around 2 pounds. The design 3 cross flow heat exchanger would have similar physical dimensions. With the manifolds, both built heat exchangers require even more space to be added to the system. But even with manifolds, the shell and tube heat exchanger is the smallest. Figure 40 shows both heat exchangers with manifolds.

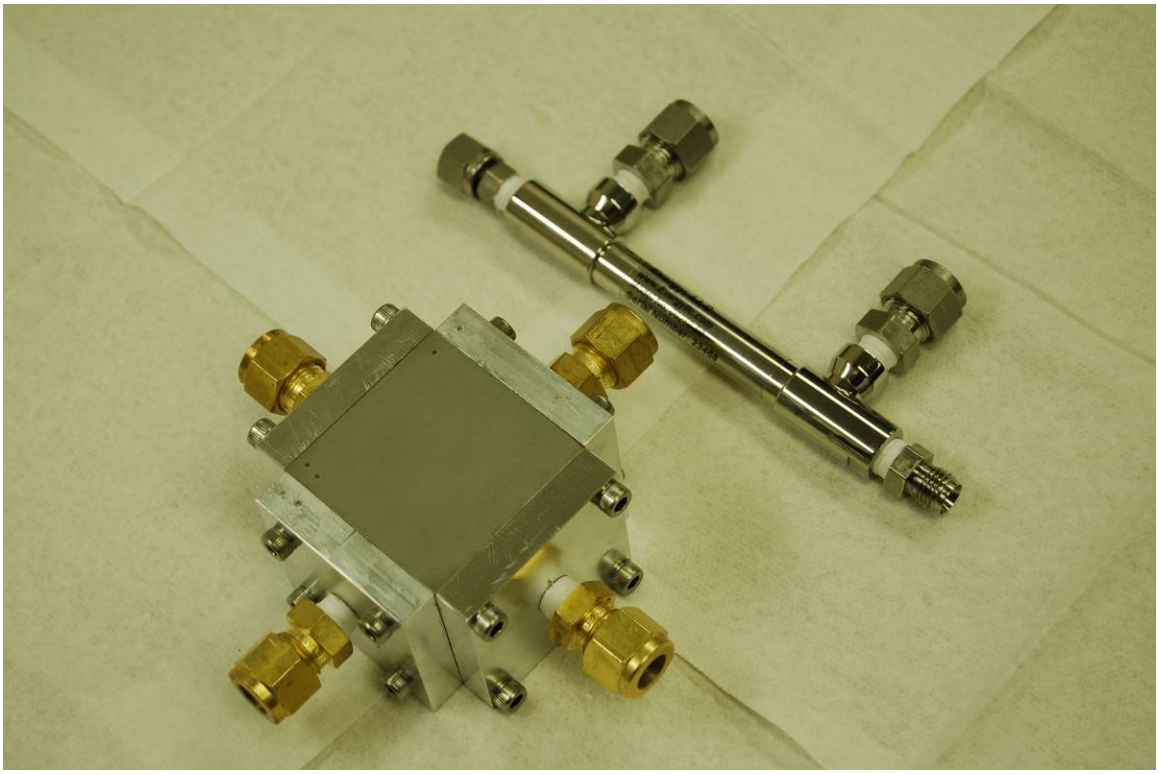

Figure 40: Both heat exchangers with manifolds

It is desirable that the recirculating system operates at the lowest temperature and pressure possible. This minimizes stresses on all components in the system. The operational limits of the shell and tube heat exchanger, primarily the MATD, put it in the desired range for the integrated recirculating system. In order to better compare the cross

flow and the shell and tube heat exchangers, the designs should be compared at equivalent levels of exertion. One way to do this is to simulate the performance of the heat exchangers at identical MATD levels. This will cause inlet temperatures to be similar and will give a better comparison of their performance differences. It is also useful to compare the built designs to the design 3 cross flow and the Exergy model 00268-1 shell and tube heat exchangers simulated in this study at the same MATD. In the future, these heat exchangers could be built and operated if feasible. Table 15 shows general dimensions, capacities, and performance of both built heat exchangers as well as the design 3 cross flow and Exergy model 00268-1 heat exchangers.

Table 15: Comparison of four heat exchanger designs

| | **Built Prototypes** | | **Additional Designs** | |
|---|---|---|---|---|
| | Shell and Tube Model 00268-2 | Cross Flow (Design 2) | Shell and Tube Model 00268-1 | Cross Flow (Design 3) |
| Primary Volume (mL) = | 2.01 | 4.48 | 4.00 | 5.56 |
| Manifold Volume (mL) = | 0.40 | 2.00 | 0.40 | 2.00 |
| Total Primary Volume (mL) = | 2.81 | 8.48 | 4.80 | 9.56 |
| Primary Flow Rate (LPM) = | 3.47 | 3.33 | 3.46 | 3.41 |
| Secondary Flow Rate (LPM) = | 12.59 | 12.17 | 6.66 | 13.28 |
| | MATD = 125 °F for a pump speed of 5500 RPM | | | |
| Heat Transfer (kW) = | 4.49 | 3.26 | 8.54 | 5.52 |
| Load Density, *excluding manifold volume* (kW/mL) = | 2.23 | 0.73 | 2.14 | 0.99 |
| Load Density, *including manifold volume* (kW/mL) = | 1.60 | 0.38 | 1.78 | 0.58 |
| Primary Inlet Temperature (°F) = | 231.9 | 226.6 | 260.0 | 237.2 |

It can be seen that all four heat exchangers have similar values for primary and secondary flow rates. The primary side inlet temperature is strongly dependent upon the heat transfer rate, thus the model 00268-1 shell and tube heat exchanger has the highest primary inlet temperature. The primary side flow rates are similar because the heat exchangers are being simulated in operation with the testing apparatus where the majority of the pressure drop is present in the test equipment rather than the heat exchanger.

There are several differences between the four heat exchangers. The primary side volumes are higher for the cross flow heat exchangers across the board. Not only the actual channels of the cross flow heat exchangers have more volume than the tubes in the shell and tube heat exchangers, the manifolds have a higher volume as well. The volume of one cross flow manifold is equal to the volume of the primary side of the model 00268-2 shell and tube heat exchanger. The cross flow heat exchangers have roughly

300% more primary side volume than the model 0026802 shell and tube heat exchanger when including manifold volumes. As far as heat transfer, the model 00268-2 shell and tube heat exchanger has 31% more capacity that the prototype cross flow heat exchanger and has approximately 1 kW less capacity than the design 3 cross flow heat exchanger. When load densities are compared, the shell and tube heat exchangers are proven to be far more efficient than both cross flow heat exchanger designs.

As mentioned before, the wall thickness of heat exchangers plays an important part in regulating the heat transfer rate. The wall thickness also sets how much of an affect inputs such as flow rates and inlet temperatures have on the performance of a heat exchanger. Figure 41 shows a thermal performance simulation of the built cross flow and the shell and tube heat exchangers as well as the other two compared design under laboratory testing conditions. Notice the difference in slope as well as magnitude throughout the primary side flow rate span.

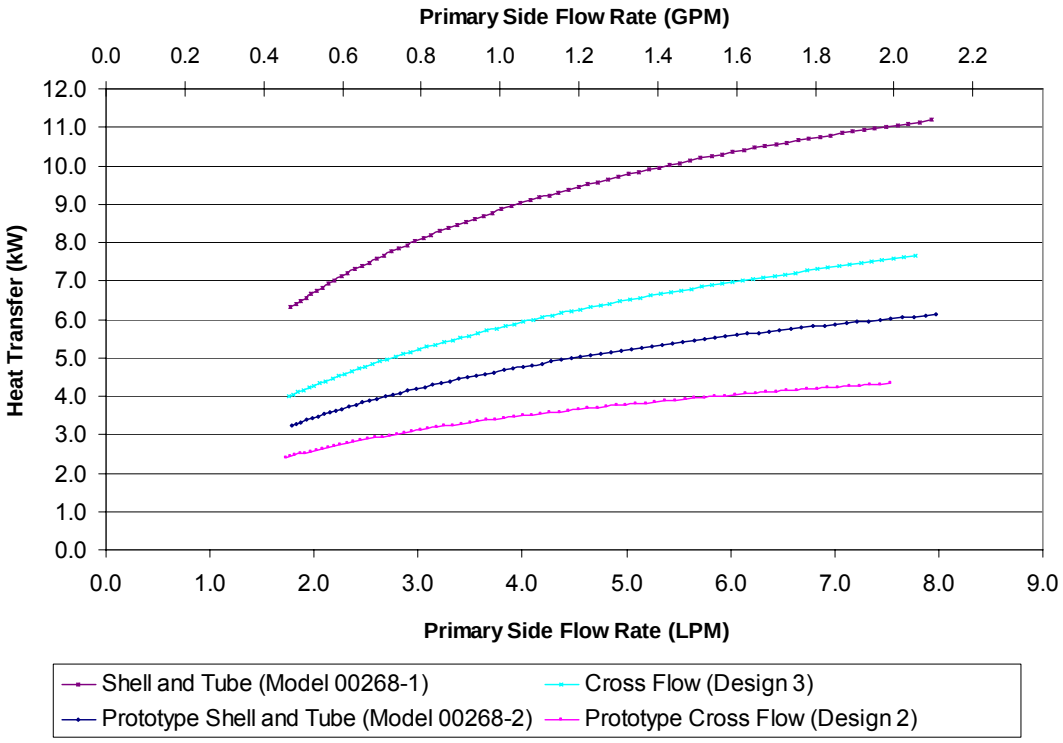


Figure 41: Comparison of built and alternate heat exchanger designs at an MATD of 125 °F

Based on previous findings and the comparison of the four heat exchangers at a common operational level, definitive performance differences have been uncovered. The

shell and tube heat exchangers show favorable results in all design categories. In comparison to the built and the design 3 cross flow heat exchangers the shell and tube heat exchangers have higher heat transfer rate per unit volume. The shell and tube heat exchangers are also less than a quarter of the weight and have a much smaller footprint in the integrated recirculating target system. Even though the cross flow heat exchanger could be revised and a new prototype built, this study indicates that the shell and tube heat exchanger is still the best choice.

The two considered shell and tube heat exchanger designs are essentially the same except that the model 00268-1 is twice as long as the model 00268-2. Because manifolds volume is the same for both models, the volume difference between the models is less than half. When including manifold volume, the model 00268-1 has a higher load density than the model 00268-2 heat exchanger. For a space restricted system, the model 00268-2 heat exchanger would work better due to its smaller footprint. Using the model 00268-2 heat exchanger also allows for easy configuration for different heat loads by simply changing the number of heat exchangers present in the system. Though for higher heat load systems (10+ kW), it may be necessary to use a larger shell and tube heat exchanger according to system flow rate. Because of the versatility of both of these heat exchangers, they should both be considered for use with the integrated recirculating target system and selected based upon the heat load required, and the space available. Simulations of systems with both heat exchangers will be performed.

## 4.3 System Modeling and Performance Simulation

In order to model the integrated target system, simple additions to the existing code were made. Previously, when only simulating the performance of a heat exchanger, there was no need to account for pressure drops of the other components that would exist in the integrated system. Additional components such as the target and pressurizer exist in the integrated recirculating target system that must now be accounted for.

Simulations were performed on the integrated system with different tubing sizes and with either a single or a set of series heat exchangers. Tubing options are 1/16” or 1/8” ID tubes. These sizes are commonly used with all devices in the system. An estimated 20 inches of tubing is required to piece the prototype system together, though that length will likely decrease with future systems.

The initial simulation for the prototype system was performed using ΔP vs. flow data on the 10 mm target body. The 10 mm target adds minimal pressure drop to the system amounting to around 1 psi at 2.20 LPM. Pressure drop data for the connection tubing can be calculated directly. The pressurizer acts to control system pressure and as a surge volume. The pressurizer does not contribute to the pressure drop in the system and therefore is not considered in the pressure drop calculations.

### 4.3.1 Single Shell and Tube Heat Exchanger System

The normal operating speed of the regenerative turbine pump during product production is anticipated to be between 4000 and 6000 RPM. Therefore, the performance of the system was considered only at that level. Two simulations were made for systems using a single shell and tube heat exchanger with 1/16" and 1/8" tubes. Figures 42 and 43 show the thermal performance data for these simulations. Table 16 displays the breakdown of volume for the systems as well as performance data at a pump speed of 5500 RPM and an MATD level of 125 °F.

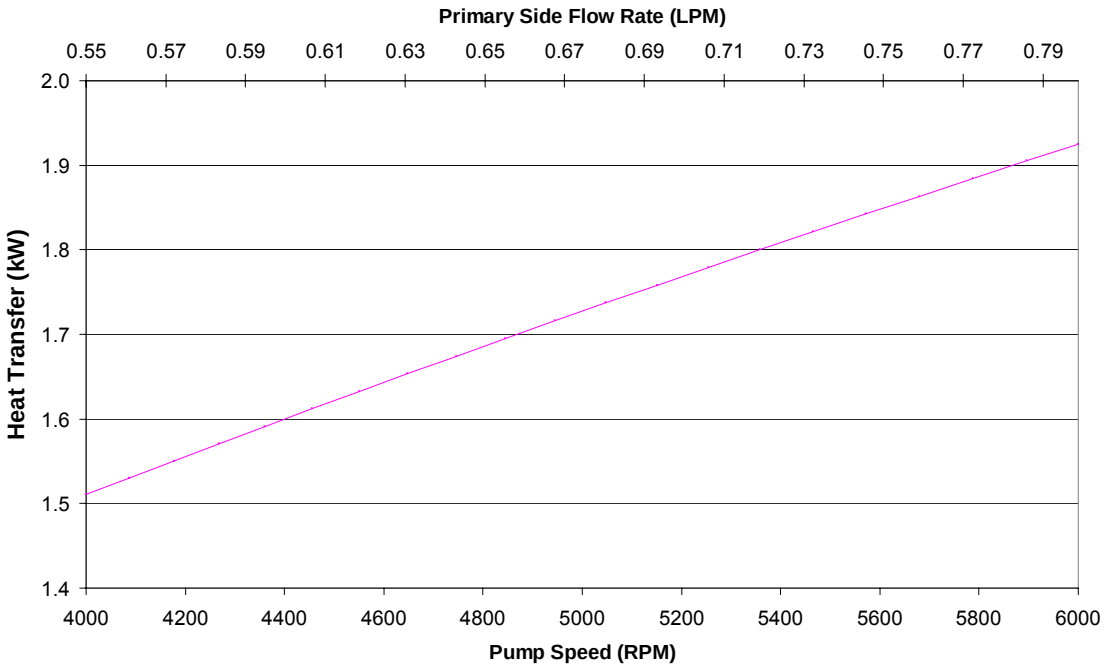


Figure 42: Simulation data for system with single heat exchanger system and 1/16" ID tubes, MATD = 125 °F

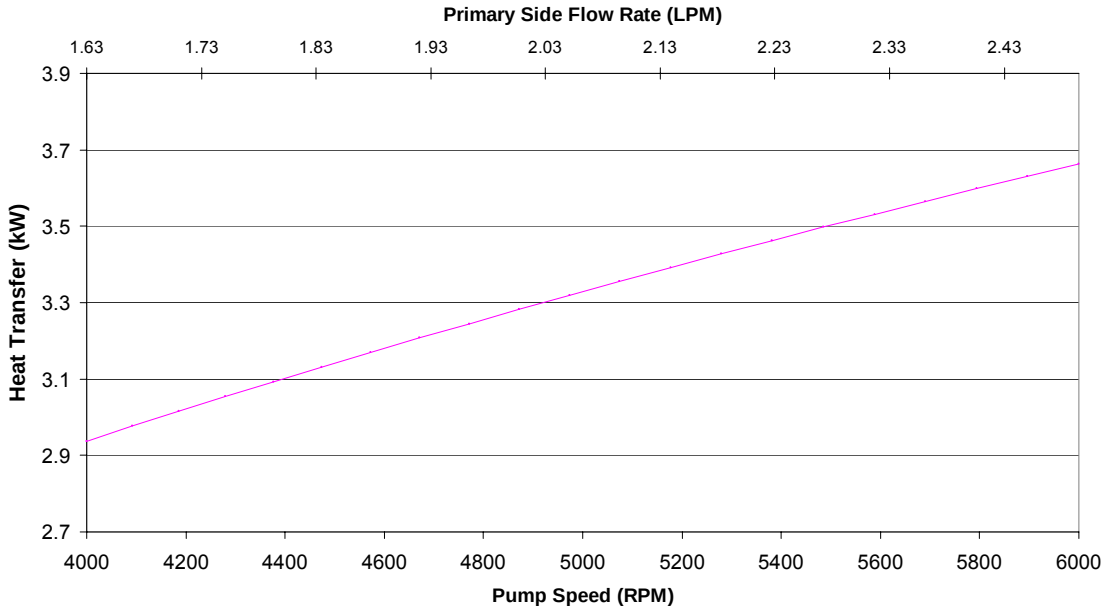


Figure 43: Simulation data for system with single heat exchanger system and 1/8" ID tubes, MATD = 125 °F

Table 16: Integrated system volume breakdown

| | | |
|---|---|---|
| Length of connection tubing (in) = | 20 | |
| Tube Diameter (in) = | 1/16 | 1/8 |
| System Volume Breakdown (mL): | | |
| Connection tubing = | 1.01 | 4.02 |
| Primary side of heat exchanger = | 2.01 | |
| Heat exchanger manifolds = | 0.40 | |
| Target (10mm) = | 0.70 | |
| Pressurizer = | 2.50 | |
| Pump = | 2.50 | |
| Misc: Fittings, etc. = | 3.00 | |
| TOTAL VOLUME = | 12.52 | 15.53 |
| Primary side flow rate (LPM) = | 0.73 | 2.27 |
| Heat transfer rate (kW) = | 1.82 | 3.50 |

From Table 15 it can be seen that the systems are within 3 mL of each other. Using a 15 mm target instead of a 10 mm target would increase the system volume by 0.90 mL. Performance varies greatly between the two simulated systems though the only difference is the connecting tube diameter. With nearly twice the heat transfer rate, over

3 times the flow rate, and only a 25% increase in volume the system with 1/8" connection tube diameter is more efficient. The increase in heat transfer rate is directly related to the lower pressure drop and higher flow rate associated with the larger tubes.

### 4.3.2 Multiple Shell and Tube Heat Exchanger System

In cases where higher heat transfer rates are required, it may be necessary to use a set of heat exchangers in series. This will increase thermal performance of the system while only increasing volume by around 2.81 mL with 1/8" diameter tubes. Table 17 shows basic information for this system at a pump speed of 5500 RPM and an MATD level of 125 °F. Figure 44 shows the thermal performance data for this system between 4000 and 6000 RPM.

Table 17: Basic system information for two Exergy model 00268-2 shell and tube heat exchangers in series

| | |
|---|---|
| TOTAL VOLUME (mL) = | 18.34 |
| Primary side flow rate (LPM) = | 2.16 |
| Heat transfer rate (kW) = | 5.66 |

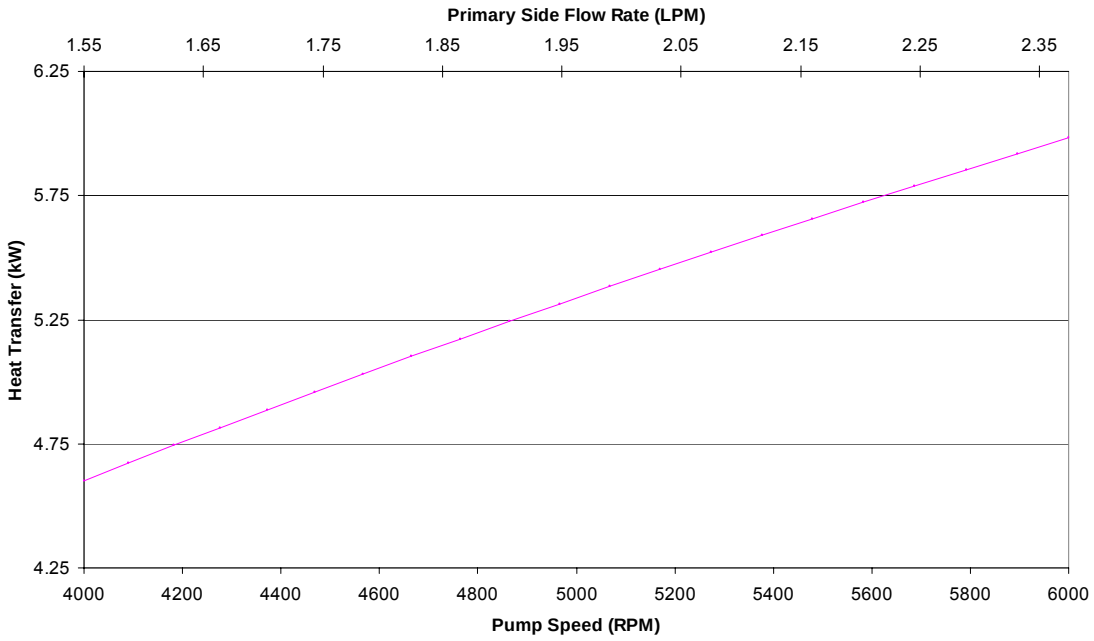


Figure 44: Simulation data for system with two Exergy model 00268-2 shell and tube heat exchangers in series and 1/8" ID tubes, MATD = 125 °F

If even higher heat transfer rates are needed, it is possible to use a different model Exergy shell and tube heat exchanger. The Exergy model 00268-1 is the next size larger shell and tube heat exchanger built in the 10 series. Its performance is discussed in detail in chapter 2. Using two of these heat exchangers in series has a predicted heat transfer rate of 10.35 kW at a primary side flow rate of 2.37 LPM. Table 18 displays the basic information for this system at a pump speed of 5500 RPM and an MATD level of 125 °F. Figure 45 shows the thermal performance data for this system between 4000 and 6000 RPM.

Table 18: Basic system information for two Exergy model 00268-1 shell and tube heat exchangers in series

| | |
|---|---|
| TOTAL VOLUME (mL) = | 22.35 |
| Primary side flow rate (LPM) = | 2.16 |
| Heat transfer rate (kW) = | 9.75 |

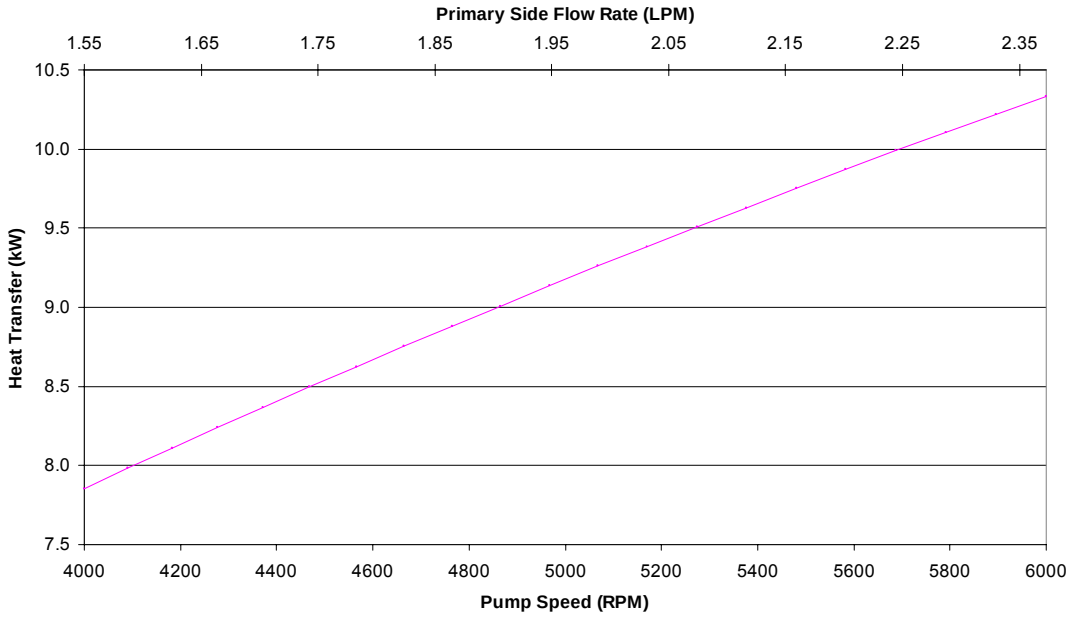


Figure 45: Simulation data for system with two Exergy model 00268-1 shell and tube heat exchangers in series and 1/8" ID tubes, MATD = 125 °F

### 4.3.3 Performance Prediction for a Commercially Available System

It is useful to consider the differences in construction and performance of a recirculating target system built for commercial use. One possible difference in a commercial system is the elimination of some primary side connective tubing. Small ID tubes contribute a large portion of the total primary side pressure drop. The fittings used

to connect components also add to the primary side pressure drop. A commercial system would likely include shortened tubes and welded connection points, thus decreasing the primary side pressure drop and increasing flow rate and heat transfer.

An estimated 4 inches of tubing is assumed necessary to connect the pump, heat exchangers, and target. This simulation considers the use two Exergy 00268-2 shell and tube heat exchangers in series, with 4 inches of 1/8" ID connective tubing. Table 19 displays the basic information for this system at a pump speed of 5500 RPM and an MATD level of 125 °F. Figure 46 shows the thermal performance of this system for pump speeds between 4000 and 6000 RPM.

Table 19: Basic system information for a commercially available system using two Exergy model 00268-2 shell and tube heat exchangers in series

| | |
|---|---|
| TOTAL VOLUME (mL) = | 15.12 |
| Primary side flow rate (LPM) = | 2.66 |
| Heat transfer rate (kW) = | 6.38 |

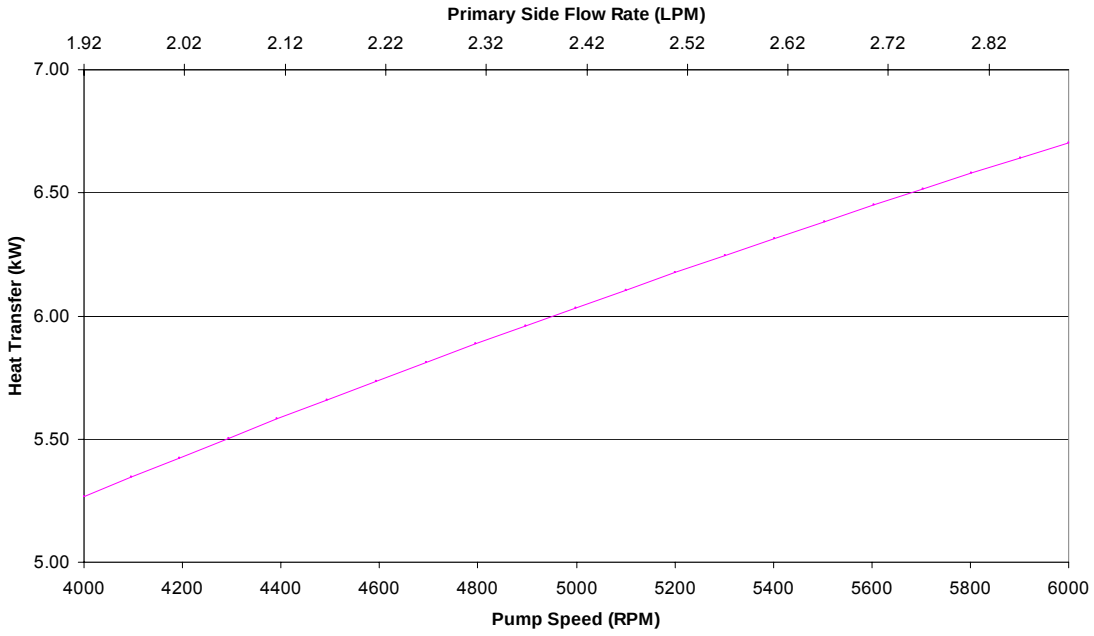


Figure 46: Simulation data for commercially available system using two Exergy model 00268-2 shell and tube heat exchangers in series and 1/8" ID, 4" long connective tubes, MATD = 125 °F

Upon comparison to a system with 20 inches of 1/8" ID connective tubing and Swagelok fittings, this system removes approximately 13% more heat with a 23% higher primary side flow rate. The data for the compared system is displayed in Table 17.

# Chapter 5

# Conclusions

This study examines two new heat exchangers for the integrated recirculating target system capable of providing sufficient heat removal capacity for high powered targets up to 10 kW. The experimental tests for both the shell and tube heat exchanger and the cross flow heat exchanger show that the simulations are accurate and can be considered valid for future system simulations and heat exchanger designs.

Optimization studies identified the design characteristics desired in a prototype shell and tube heat exchanger. It was found that the commercially available Exergy 10 series shell and tube heat exchangers were equivalent in size scale to the optimized designs. The Exergy heat exchangers also incorporate materials that are compatible with the integrated recirculating target system. Even with the limitation of the maximum average temperature difference (MATD), which reduces maximum possible heat transfer rates, the Exergy heat exchangers still satisfy the design goals for a low system temperature and pressure. The Exergy model 00268-2 shell and tube heat exchanger was tested up to 5.9 kW with a primary side flow rate and volume of 6.7 LPM and 2.81 mL (with manifolds). It has a peak performance of 6.0 kW at a primary side flow rate of 7.5 LPM. Using a set of these heat exchangers in series allows for a maximum heat transfer rate of 10.5 kW with a primary side flow rate of 6.5 LPM.

Highly efficient designs such as the micro cross flow heat exchanger represent the best case scenario for a cross flow heat exchanger. For this study it was impractical to construct this type of heat exchanger due to complications with the construction techniques necessary to fabricate it. Future research and design of the integrated recirculating target system could include the development of a micro cross flow heat exchanger that may represent the most efficient design for a commercially available system.

The constructed prototype cross flow heat exchanger represents a trade off between maximum heat transfer and practicality. It was experimentally tested up to 7.2 kW at a primary side flow rate of 6.0 LPM. It has a peak performance prediction of 10.0 kW at a primary side flow rate of 7.5 LPM. The cross flow design relies on a high inlet temperature and system pressure in order to achieve maximum heat transfer. This means that the integrated recirculating target system would have to run hotter as a whole and higher pressures would be required to prevent boiling. In the future, it might be possible to construct a cross heat exchanger with smaller channel diameter and channel spacing as discussed with the design 3 cross flow heat exchanger. This will increase the performance of the heat exchanger and allow for a reduced inlet temperature and system pressure. The design 3 cross flow heat exchanger presented in this study with 0.030" channel diameter and 0.010" channel spacing has a peak predicted performance approaching 14 kW. If the cross flow heat exchanger design is pursued further, this is a viable design for construction and use.

The shell and tube heat exchanger was selected for use with the prototype integrated recirculating target system. Its selection was based on its performance and size. It out performs the current prototype cross flow heat exchanger at a moderate system pressure and temperature with less volume. Though the use of the Exergy model 00268-2 shell and tube heat exchanger requires two units to perform at higher heat loads, it is still more volume efficient that than the prototype cross flow heat exchanger.

At a maximum pump speed of 6000 RPM it is estimated that the integrated system can reject 3.65 kW of heat with one shell and tube heat exchanger at a primary side flow rate of 2.5 LPM and 6.0 kW with a set of shell and tube heat exchangers in series at a primary side flow rate of 2.37 LPM. For a higher capacity system using two larger Exergy shell and tube heat exchangers the integrated system could reject 10.35 kW of heat at a primary side flow rate of 2.37 LPM. These heat transfer rates are strongly dependent on primary side flow rate and could be sharply increased for both systems if pump performance is increased.

## 5.1 Recommendations and Future Work

This study provides information for the design and optimization of two types of heat exchangers. It also provides the ability to model and predict performance of prototype systems using either heat exchanger design. This tool can be used in the future

to model systems that are to be tested as well as assess different designs regarding the arrangement and size of the heat exchangers and components used.

The heat exchangers tested showed strong dependence on the primary side flow rate. This is expected as the majority of the heat transfer resistance is on the primary side. Therefore, it is essential that the pump used to drive primary side flow has sufficient capacity to operate the heat exchangers optimally. Suggested flow rates between 4 and 8 LPM are necessary to maximize performance in the heat exchangers. Currently, it is expected that the prototype regenerative turbine pump will only be able to drive around 2 to 3 LPM in the integrated system. Along with increasing the flow rate, it is also necessary to design and test a more robust pump that can operate for extended periods of time. During heat exchanger experiments, numerous failures were experienced from the prototype regenerative turbine pump. Many of these issues are being resolved with the magnetic drive regenerative turbine pump, though little to no increases in flow rates are expected from this new design.

The current recirculating target is a 15 mm diameter design. It is based on the 10 mm target which was experimentally tested in past work. This design has worked well but has not been subjected to high heat loads. Once the magnetic drive pump is finished and incorporated into the recirculating system, the system will be evaluated in actual beam tests.

# Bibliography


[1] Clark J.C. High-Powered Cyclotron Recirculating Targets for Production of the $^{18}F$ Radionuclide. Masters Thesis. Department of Nuclear Engineering, North Carolina State University. December 2004.

[2] Ehrfeld W., Hessel V., Lowe H. Microreactors, New Technology for Modern Chemistry. Wiley-VCH, July 2000.

[3] El-Wakil M. Nuclear Heat Transport. International Textbook Company, Fourth Printing, 1971.

[4] Exergy, LLC. Miniature Heat Exchangers. Garden City, NY. <http://www.exergyinc.com/> January 24, 2006.

[5] Holman J.P. Heat Transfer. McGraw-Hill Companies, Inc., Ninth Edition, 2002.

[6] Hess E., Takàcs S., Scholten B., Tàrkànyi F., Coenen H. H., and Qaim S. M. "Excitation function of the $^{18}O(p,n)^{18}F$ nuclear reaction from threshold up to 30 MeV." Radiochimica Acta. 89:357-362, 2001.

[7] Idelchik I.E. Handbook of Hydraulic Resistance. CRC Press, Inc., Third Edition, 1994.

[8] Incropera F.P., Dewitt D.P. Heat and Mass Transfer. John Wiley & Sons, Inc., Fifth Edition, 2002.

[9] Kakac S., Liu H. Heat Exchangers, Selection, Rating, and Thermal Design. CRC Press, Inc., 1998.

**[10] Peeples J.L. Design and Optimization of Thermosyphon Bath Targets for Production of $^{18}F$. Masters Thesis. Department of Nuclear Engineering, North Carolina State University. December 2006.**

**[11] Phelps M.E. PET: Molecular Imaging and Its Biological Applications. New York: Springer-Verlag, 2004.**

**[12] Schubert K., Bier W., Linder G., and Seidel D. Profiled Micro Diamonds for Producing Microstructures. Precision Machining, 1990.**

**[13] Wright B. Regenerative Turbine Pumps: Unsung heroes for volatile fluids. *Chemical Engineering*, 106(4):116, April 1999.**

**[14] XACT Wire EDM Corp. Cary, Illinois < http://www.xactedm.com/index.html> January 24, 2006.**

# APPENDICES

# Appendix A

## Shell and Tube Heat Exchanger Simulation and Experimental Data

This appendix contains the simulation data for all three Exergy 10 series shell and tube heat exchangers. It also contains the experimental data that was recorded for the Exergy model 00268-2 shell and tube heat exchanger.

Table 20: Simulation data for the Exergy model 00268-2 shell and tube heat exchanger

| | | Primary Side | | | | Secondary Side | | | |
|---|---|---|---|---|---|---|---|---|---|
| **Heat Transfer** | **MATD** | **Flow Rate** | **Press. Drop** | **Inlet Temp.** | **Outlet Temp.** | **Flow Rate** | **Press. Drop** | **Inlet Temp.** | **Outlet Temp.** |
| kW | °F | LPM | psig | °F | °F | LPM | psig | °F | °F |
| | | | | | | | | | |
| 3.21 | 124.94 | 1.78 | 1.00 | 234.69 | 186.17 | 40.05 | 12.57 | 82.19 | 88.78 |
| 3.30 | 124.97 | 1.88 | 1.11 | 234.24 | 186.86 | 40.05 | 12.57 | 82.19 | 88.96 |
| 3.39 | 124.94 | 1.98 | 1.23 | 233.70 | 187.53 | 40.05 | 12.57 | 82.19 | 89.15 |
| 3.49 | 124.99 | 2.09 | 1.38 | 233.25 | 188.27 | 40.05 | 12.57 | 82.19 | 89.35 |
| 3.59 | 124.96 | 2.21 | 1.53 | 232.71 | 188.95 | 40.05 | 12.57 | 82.19 | 89.55 |
| 3.69 | 125.00 | 2.33 | 1.71 | 232.26 | 189.69 | 40.05 | 12.57 | 82.19 | 89.76 |
| 3.79 | 124.96 | 2.47 | 1.91 | 231.72 | 190.36 | 40.05 | 12.57 | 82.19 | 89.97 |
| 3.90 | 124.98 | 2.61 | 2.13 | 231.27 | 191.06 | 40.05 | 12.57 | 82.19 | 90.18 |
| 4.00 | 124.99 | 2.75 | 2.37 | 230.82 | 191.74 | 40.05 | 12.57 | 82.19 | 90.39 |
| 4.10 | 124.98 | 2.90 | 2.64 | 230.37 | 192.39 | 40.05 | 12.57 | 82.19 | 90.60 |
| 4.20 | 124.97 | 3.06 | 2.93 | 229.92 | 193.01 | 40.05 | 12.57 | 82.19 | 90.80 |
| 4.30 | 124.94 | 3.22 | 3.25 | 229.47 | 193.60 | 40.05 | 12.57 | 82.19 | 91.00 |
| 4.40 | 124.97 | 3.39 | 3.59 | 229.11 | 194.22 | 40.05 | 12.57 | 82.19 | 91.21 |
| 4.49 | 124.98 | 3.56 | 3.95 | 228.75 | 194.81 | 40.05 | 12.57 | 82.19 | 91.40 |
| 4.59 | 124.98 | 3.73 | 4.35 | 228.39 | 195.37 | 40.05 | 12.57 | 82.19 | 91.60 |
| 4.68 | 124.97 | 3.91 | 4.77 | 228.03 | 195.89 | 40.05 | 12.57 | 82.19 | 91.78 |
| 4.76 | 124.95 | 4.09 | 5.22 | 227.67 | 196.38 | 40.05 | 12.57 | 82.19 | 91.96 |
| 4.85 | 124.99 | 4.28 | 5.70 | 227.40 | 196.91 | 40.05 | 12.57 | 82.19 | 92.14 |
| 4.93 | 124.94 | 4.46 | 6.21 | 227.04 | 197.34 | 40.05 | 12.57 | 82.19 | 92.31 |
| 5.02 | 124.95 | 4.65 | 6.75 | 226.77 | 197.81 | 40.05 | 12.57 | 82.19 | 92.48 |
| 5.10 | 124.96 | 4.85 | 7.32 | 226.50 | 198.25 | 40.05 | 12.57 | 82.19 | 92.65 |
| 5.18 | 124.95 | 5.04 | 7.92 | 226.23 | 198.67 | 40.05 | 12.57 | 82.19 | 92.81 |
| 5.25 | 124.93 | 5.24 | 8.55 | 225.96 | 199.06 | 40.05 | 12.57 | 82.19 | 92.96 |
| 5.33 | 124.98 | 5.44 | 9.21 | 225.78 | 199.49 | 40.05 | 12.57 | 82.19 | 93.12 |
| 5.40 | 124.95 | 5.64 | 9.90 | 225.51 | 199.84 | 40.05 | 12.57 | 82.19 | 93.26 |
| 5.47 | 124.98 | 5.85 | 10.63 | 225.33 | 200.23 | 40.05 | 12.57 | 82.19 | 93.41 |
| 5.53 | 124.93 | 6.05 | 11.39 | 225.06 | 200.52 | 40.05 | 12.57 | 82.19 | 93.54 |
| 5.60 | 124.94 | 6.26 | 12.18 | 224.88 | 200.87 | 40.05 | 12.57 | 82.19 | 93.68 |
| 5.66 | 124.95 | 6.47 | 13.00 | 224.70 | 201.21 | 40.05 | 12.57 | 82.19 | 93.81 |
| 5.73 | 124.95 | 6.68 | 13.86 | 224.52 | 201.52 | 40.05 | 12.57 | 82.19 | 93.94 |
| 5.79 | 124.95 | 6.89 | 14.75 | 224.34 | 201.81 | 40.05 | 12.57 | 82.19 | 94.06 |
| 5.84 | 124.94 | 7.11 | 15.67 | 224.16 | 202.09 | 40.05 | 12.57 | 82.19 | 94.18 |
| 5.90 | 124.92 | 7.32 | 16.63 | 223.98 | 202.35 | 40.05 | 12.57 | 82.19 | 94.30 |
| 5.96 | 124.98 | 7.54 | 17.62 | 223.89 | 202.68 | 40.05 | 12.57 | 82.19 | 94.42 |
| 6.01 | 124.95 | 7.76 | 18.64 | 223.71 | 202.91 | 40.05 | 12.57 | 82.19 | 94.52 |
| 6.07 | 125.00 | 7.97 | 19.70 | 223.62 | 203.20 | 40.05 | 12.57 | 82.19 | 94.64 |

Table 21: Simulation data for the Exergy model 00268-1 shell and tube heat exchanger

| | | Primary Side | | | | Secondary Side | | | |
|---|---|---|---|---|---|---|---|---|---|
| **Heat Transfer** | **MATD** | **Flow Rate** | **Press. Drop** | **Inlet Temp.** | **Outlet Temp.** | **Flow Rate** | **Press. Drop** | **Inlet Temp.** | **Outlet Temp.** |
| kW | °F | LPM | psig | °F | °F | LPM | psig | °F | °F |
| | | | | | | | | | |
| 6.26 | 124.97 | 1.78 | 1.05 | 267.18 | 171.42 | 6.64 | 56.94 | 82.19 | 106.48 |
| 6.42 | 124.96 | 1.87 | 1.16 | 266.28 | 172.94 | 6.64 | 56.94 | 82.19 | 107.11 |
| 6.59 | 124.96 | 1.97 | 1.29 | 265.38 | 174.51 | 6.64 | 56.94 | 82.19 | 107.78 |
| 6.77 | 124.97 | 2.08 | 1.43 | 264.48 | 176.12 | 6.64 | 56.94 | 82.19 | 108.47 |
| 6.95 | 124.98 | 2.20 | 1.60 | 263.58 | 177.74 | 6.64 | 56.94 | 82.19 | 109.17 |
| 7.13 | 124.98 | 2.32 | 1.78 | 262.68 | 179.35 | 6.64 | 56.94 | 82.19 | 109.88 |
| 7.31 | 124.97 | 2.46 | 1.99 | 261.78 | 180.94 | 6.64 | 56.94 | 82.19 | 110.59 |
| 7.50 | 124.94 | 2.59 | 2.21 | 260.88 | 182.49 | 6.64 | 56.94 | 82.19 | 111.29 |
| 7.68 | 124.96 | 2.74 | 2.47 | 260.07 | 184.03 | 6.64 | 56.94 | 82.19 | 111.99 |
| 7.85 | 124.96 | 2.89 | 2.74 | 259.26 | 185.52 | 6.64 | 56.94 | 82.19 | 112.68 |
| 8.03 | 124.99 | 3.05 | 3.04 | 258.54 | 187.00 | 6.64 | 56.94 | 82.19 | 113.37 |
| 8.20 | 124.95 | 3.21 | 3.36 | 257.73 | 188.37 | 6.64 | 56.94 | 82.19 | 114.02 |
| 8.37 | 125.00 | 3.37 | 3.71 | 257.10 | 189.77 | 6.64 | 56.94 | 82.19 | 114.69 |
| 8.53 | 124.97 | 3.54 | 4.09 | 256.38 | 191.06 | 6.64 | 56.94 | 82.19 | 115.31 |
| 8.69 | 124.98 | 3.71 | 4.50 | 255.75 | 192.33 | 6.64 | 56.94 | 82.19 | 115.93 |
| 8.84 | 124.97 | 3.89 | 4.93 | 255.12 | 193.53 | 6.64 | 56.94 | 82.19 | 116.52 |
| 8.99 | 124.94 | 4.07 | 5.40 | 254.49 | 194.66 | 6.64 | 56.94 | 82.19 | 117.09 |
| 9.13 | 124.95 | 4.25 | 5.89 | 253.95 | 195.79 | 6.64 | 56.94 | 82.19 | 117.65 |
| 9.27 | 124.94 | 4.44 | 6.41 | 253.41 | 196.86 | 6.64 | 56.94 | 82.19 | 118.19 |
| 9.41 | 124.98 | 4.63 | 6.96 | 252.96 | 197.92 | 6.64 | 56.94 | 82.19 | 118.73 |
| 9.54 | 125.00 | 4.82 | 7.55 | 252.51 | 198.92 | 6.64 | 56.94 | 82.19 | 119.24 |
| 9.66 | 124.94 | 5.02 | 8.16 | 251.97 | 199.81 | 6.64 | 56.94 | 82.19 | 119.71 |
| 9.79 | 124.99 | 5.21 | 8.81 | 251.61 | 200.77 | 6.64 | 56.94 | 82.19 | 120.21 |
| 9.91 | 124.97 | 5.41 | 9.49 | 251.16 | 201.61 | 6.64 | 56.94 | 82.19 | 120.66 |
| 10.02 | 124.99 | 5.61 | 10.20 | 250.80 | 202.47 | 6.64 | 56.94 | 82.19 | 121.11 |
| 10.14 | 125.00 | 5.81 | 10.94 | 250.44 | 203.28 | 6.64 | 56.94 | 82.19 | 121.54 |
| 10.24 | 125.00 | 6.02 | 11.72 | 250.08 | 204.05 | 6.64 | 56.94 | 82.19 | 121.95 |
| 10.34 | 124.98 | 6.22 | 12.53 | 249.72 | 204.78 | 6.64 | 56.94 | 82.19 | 122.35 |
| 10.44 | 124.96 | 6.43 | 13.37 | 249.36 | 205.46 | 6.64 | 56.94 | 82.19 | 122.73 |
| 10.54 | 124.98 | 6.64 | 14.25 | 249.09 | 206.18 | 6.64 | 56.94 | 82.19 | 123.11 |
| 10.63 | 124.94 | 6.85 | 15.16 | 248.73 | 206.79 | 6.64 | 56.94 | 82.19 | 123.46 |
| 10.72 | 124.94 | 7.06 | 16.10 | 248.46 | 207.43 | 6.64 | 56.94 | 82.19 | 123.81 |
| 10.81 | 124.94 | 7.28 | 17.08 | 248.19 | 208.04 | 6.64 | 56.94 | 82.19 | 124.16 |
| 10.90 | 125.00 | 7.49 | 18.09 | 248.01 | 208.68 | 6.64 | 56.94 | 82.19 | 124.51 |
| 10.98 | 124.98 | 7.71 | 19.14 | 247.74 | 209.23 | 6.64 | 56.94 | 82.19 | 124.82 |
| 11.06 | 124.96 | 7.92 | 20.22 | 247.47 | 209.75 | 6.64 | 56.94 | 82.19 | 125.12 |

Table 22: Simulation data for the Exergy model 00268-3 shell and tube heat exchanger

| | | Primary Side | | | | Secondary Side | | | |
|---|---|---|---|---|---|---|---|---|---|
| **Heat Transfer** | **MATD** | **Flow Rate** | **Press. Drop** | **Inlet Temp.** | **Outlet Temp.** | **Flow Rate** | **Press. Drop** | **Inlet Temp.** | **Outlet Temp.** |
| kW | °F | LPM | psig | °F | °F | LPM | psig | °F | °F |
| | | | | | | | | | |
| 9.26 | 125.00 | 1.77 | 1.08 | 307.41 | 163.52 | 4.22 | 60.95 | 82.19 | 138.74 |
| 9.51 | 124.97 | 1.87 | 1.19 | 306.33 | 166.04 | 4.22 | 60.95 | 82.19 | 140.24 |
| 9.76 | 124.96 | 1.97 | 1.32 | 305.25 | 168.66 | 4.22 | 60.95 | 82.19 | 141.80 |
| 10.02 | 124.97 | 2.08 | 1.47 | 304.17 | 171.37 | 4.22 | 60.95 | 82.19 | 143.40 |
| 10.29 | 124.99 | 2.20 | 1.64 | 303.09 | 174.11 | 4.22 | 60.95 | 82.19 | 145.03 |
| 10.55 | 124.97 | 2.32 | 1.83 | 301.92 | 176.83 | 4.22 | 60.95 | 82.19 | 146.62 |
| 10.81 | 125.00 | 2.45 | 2.04 | 300.84 | 179.57 | 4.22 | 60.95 | 82.19 | 148.23 |
| 11.07 | 124.97 | 2.59 | 2.27 | 299.67 | 182.22 | 4.22 | 60.95 | 82.19 | 149.77 |
| 11.32 | 124.98 | 2.73 | 2.53 | 298.59 | 184.85 | 4.22 | 60.95 | 82.19 | 151.30 |
| 11.56 | 124.97 | 2.88 | 2.81 | 297.51 | 187.40 | 4.22 | 60.95 | 82.19 | 152.78 |
| 11.79 | 124.95 | 3.04 | 3.12 | 296.43 | 189.87 | 4.22 | 60.95 | 82.19 | 154.20 |
| 12.02 | 124.97 | 3.20 | 3.45 | 295.44 | 192.27 | 4.22 | 60.95 | 82.19 | 155.60 |
| 12.24 | 124.96 | 3.36 | 3.81 | 294.45 | 194.58 | 4.22 | 60.95 | 82.19 | 156.93 |
| 12.45 | 124.98 | 3.53 | 4.19 | 293.55 | 196.82 | 4.22 | 60.95 | 82.19 | 158.23 |
| 12.65 | 124.98 | 3.70 | 4.61 | 292.65 | 198.96 | 4.22 | 60.95 | 82.19 | 159.46 |
| 12.85 | 124.96 | 3.88 | 5.05 | 291.75 | 200.99 | 4.22 | 60.95 | 82.19 | 160.63 |
| 13.03 | 124.97 | 4.06 | 5.53 | 290.94 | 202.96 | 4.22 | 60.95 | 82.19 | 161.77 |
| 13.21 | 124.96 | 4.24 | 6.03 | 290.13 | 204.82 | 4.22 | 60.95 | 82.19 | 162.84 |
| 13.38 | 124.98 | 4.43 | 6.56 | 289.41 | 206.63 | 4.22 | 60.95 | 82.19 | 163.90 |
| 13.54 | 124.98 | 4.62 | 7.13 | 288.70 | 208.35 | 4.22 | 60.95 | 82.19 | 164.89 |
| 13.70 | 124.97 | 4.81 | 7.72 | 287.98 | 209.97 | 4.22 | 60.95 | 82.19 | 165.82 |
| 13.85 | 124.98 | 5.00 | 8.35 | 287.35 | 211.55 | 4.22 | 60.95 | 82.19 | 166.74 |
| 13.99 | 124.98 | 5.20 | 9.01 | 286.72 | 213.04 | 4.22 | 60.95 | 82.19 | 167.61 |
| 14.12 | 124.96 | 5.40 | 9.70 | 286.09 | 214.45 | 4.22 | 60.95 | 82.19 | 168.43 |
| 14.26 | 124.98 | 5.60 | 10.42 | 285.55 | 215.84 | 4.22 | 60.95 | 82.19 | 169.24 |
| 14.38 | 124.98 | 5.80 | 11.18 | 285.01 | 217.15 | 4.22 | 60.95 | 82.19 | 170.00 |
| 14.50 | 124.97 | 6.00 | 11.97 | 284.47 | 218.38 | 4.22 | 60.95 | 82.19 | 170.72 |
| 14.62 | 125.00 | 6.21 | 12.80 | 284.02 | 219.61 | 4.22 | 60.95 | 82.19 | 171.44 |
| 14.72 | 124.96 | 6.41 | 13.65 | 283.48 | 220.71 | 4.22 | 60.95 | 82.19 | 172.08 |
| 14.83 | 124.96 | 6.62 | 14.55 | 283.03 | 221.81 | 4.22 | 60.95 | 82.19 | 172.72 |
| 14.93 | 124.95 | 6.83 | 15.47 | 282.58 | 222.85 | 4.22 | 60.95 | 82.19 | 173.33 |
| 15.03 | 124.98 | 7.04 | 16.43 | 282.22 | 223.89 | 4.22 | 60.95 | 82.19 | 173.95 |
| 15.12 | 124.95 | 7.25 | 17.43 | 281.77 | 224.82 | 4.22 | 60.95 | 82.19 | 174.50 |
| 15.21 | 124.96 | 7.47 | 18.46 | 281.41 | 225.76 | 4.22 | 60.95 | 82.19 | 175.05 |
| 15.29 | 124.96 | 7.68 | 19.53 | 281.05 | 226.65 | 4.22 | 60.95 | 82.19 | 175.58 |
| 15.38 | 124.95 | 7.90 | 20.63 | 280.69 | 227.50 | 4.22 | 60.95 | 82.19 | 176.08 |

Table 23: Experimental data for the Exergy model 00268–2 shell and tube heat exchanger

| | | | | | Primary Side | | | Secondary Side | | | |
|---|---|---|---|---|---|---|---|---|---|---|---|
| **Relative MATD Level** | **Pump Speed** | **Heat Transfer** | **MATD** | **System Press. Drop** | **Flow Rate** | **Inlet Temp.** | **Outlet Temp.** | **Flow Rate** | **Press. Drop** | **Inlet Temp.** | **Outlet Temp.** |
| °F | RPM | kW | °F | psig | LPM | °F | °F | LPM | psig | °F | °F |
| | | | | | | | | | | | |
| 125 | 3000 | 3.64 | 124.85 | 2.81 | 2.11 | 231.19 | 188.21 | 12.14 | 41.38 | 81.60 | 88.10 |
| | 4000 | 4.06 | 124.87 | 4.47 | 2.64 | 228.85 | 191.88 | 12.08 | 40.96 | 81.66 | 89.33 |
| | 5000 | 4.41 | 124.96 | 6.35 | 3.18 | 226.89 | 194.16 | 12.15 | 41.44 | 81.34 | 89.79 |
| | 5900 | 4.73 | 125.17 | 8.47 | 3.72 | 225.82 | 196.09 | 12.12 | 41.24 | 81.19 | 90.39 |
| | 7050 | 5.07 | 124.97 | 12.41 | 4.46 | 225.05 | 198.44 | 12.14 | 41.37 | 81.85 | 91.70 |
| | 8000 | 5.30 | 124.97 | 15.78 | 5.15 | 223.70 | 199.27 | 12.12 | 41.28 | 81.38 | 91.66 |
| | 9010 | 5.58 | 124.95 | 19.78 | 5.89 | 223.38 | 200.77 | 12.16 | 41.54 | 81.74 | 92.53 |
| | 10080 | 5.80 | 124.62 | 24.38 | 6.71 | 221.72 | 200.89 | 12.11 | 41.18 | 81.10 | 92.27 |
| | 10240 | 5.84 | 124.67 | 25.13 | 6.83 | 222.13 | 201.50 | 12.11 | 41.17 | 81.50 | 92.78 |
| 100 | 3075 | 2.81 | 100.36 | 2.87 | 2.14 | 201.42 | 168.69 | 12.01 | 40.56 | 82.12 | 87.25 |
| | 4100 | 3.11 | 99.59 | 4.52 | 2.67 | 198.08 | 170.13 | 11.96 | 40.22 | 81.51 | 87.53 |
| | 5000 | 3.38 | 99.94 | 6.21 | 3.19 | 197.16 | 172.03 | 12.10 | 41.07 | 81.38 | 87.94 |
| | 6075 | 3.66 | 100.02 | 8.88 | 3.87 | 196.12 | 173.71 | 12.13 | 41.28 | 81.32 | 88.46 |
| | 7025 | 3.87 | 100.09 | 11.85 | 4.48 | 195.77 | 175.23 | 12.05 | 40.76 | 81.60 | 89.22 |
| | 7978 | 4.07 | 99.64 | 15.36 | 5.15 | 194.54 | 175.70 | 12.17 | 41.58 | 81.48 | 89.47 |
| | 9100 | 4.29 | 99.63 | 19.97 | 6.01 | 194.17 | 176.96 | 12.07 | 40.94 | 81.73 | 90.14 |
| | 9900 | 4.43 | 99.98 | 23.32 | 6.64 | 194.05 | 177.72 | 12.04 | 40.70 | 81.58 | 90.22 |
| 75 | 3100 | 1.92 | 75.00 | 2.90 | 2.12 | 169.85 | 146.88 | 12.29 | 42.18 | 81.60 | 85.13 |
| | 4150 | 2.19 | 75.11 | 4.33 | 2.71 | 168.56 | 148.62 | 12.12 | 41.08 | 81.38 | 85.58 |
| | 5200 | 2.40 | 74.83 | 6.18 | 3.22 | 167.44 | 149.79 | 12.23 | 42.06 | 81.43 | 86.14 |
| | 6000 | 2.55 | 75.22 | 8.47 | 3.81 | 167.44 | 151.42 | 11.75 | 39.01 | 81.60 | 86.81 |
| | 7000 | 2.72 | 74.94 | 11.37 | 4.48 | 166.55 | 151.92 | 12.07 | 40.98 | 81.60 | 86.98 |
| | 8100 | 2.90 | 74.83 | 15.18 | 5.25 | 165.82 | 152.48 | 12.18 | 41.46 | 81.43 | 87.21 |
| | 9000 | 3.05 | 75.05 | 18.80 | 5.92 | 165.70 | 153.15 | 12.12 | 41.33 | 81.38 | 87.37 |
| | 10100 | 3.20 | 74.94 | 23.61 | 6.83 | 165.26 | 153.60 | 12.07 | 40.95 | 81.32 | 87.65 |

# Appendix B

## Cross Flow Heat Exchanger Simulation and Experimental Data

This appendix contains all simulation data for the four cross flow heat exchanger designs. It also contains experimental data that was recorded for the design 2 cross flow heat exchanger which had a channel diameter of 0.040" and channel thickness of 0.020".

Table 24: Simulation data for design 1 of chapter 3, channel diameter = 0.125", channel spacing of 0.063"

| | | Primary Side | | | | Secondary Side | | | |
|---|---|---|---|---|---|---|---|---|---|
| **Heat Transfer** | **MATD** | **Flow Rate** | **Press. Drop** | **Inlet Temp.** | **Outlet Temp.** | **Flow Rate** | **Press. Drop** | **Inlet Temp.** | **Outlet Temp.** |
| kW | °F | LPM | psig | °F | °F | LPM | psig | °F | °F |
| | | | | | | | | | |
| 0.72 | 125.00 | 1.75 | 0.65 | 216.19 | 205.22 | 13.34 | 38.62 | 85.01 | 86.40 |
| 0.74 | 124.99 | 1.84 | 0.72 | 216.05 | 205.37 | 13.34 | 38.62 | 85.01 | 86.43 |
| 0.75 | 124.99 | 1.94 | 0.80 | 215.92 | 205.54 | 13.34 | 38.62 | 85.01 | 86.47 |
| 0.77 | 125.00 | 2.05 | 0.89 | 215.79 | 205.72 | 13.34 | 38.62 | 85.01 | 86.51 |
| 0.79 | 124.99 | 2.17 | 0.99 | 215.65 | 205.88 | 13.34 | 38.62 | 85.01 | 86.54 |
| 0.81 | 124.99 | 2.29 | 1.10 | 215.52 | 206.05 | 13.34 | 38.62 | 85.01 | 86.58 |
| 0.83 | 124.99 | 2.42 | 1.23 | 215.40 | 206.22 | 13.34 | 38.62 | 85.01 | 86.62 |
| 0.85 | 124.99 | 2.56 | 1.37 | 215.27 | 206.38 | 13.34 | 38.62 | 85.01 | 86.66 |
| 0.87 | 124.99 | 2.70 | 1.53 | 215.15 | 206.53 | 13.34 | 38.62 | 85.01 | 86.69 |
| 0.89 | 125.00 | 2.85 | 1.70 | 215.04 | 206.69 | 13.34 | 38.62 | 85.01 | 86.73 |
| 0.91 | 125.00 | 3.00 | 1.89 | 214.93 | 206.85 | 13.34 | 38.62 | 85.01 | 86.76 |
| 0.92 | 125.00 | 3.16 | 2.09 | 214.82 | 206.99 | 13.34 | 38.62 | 85.01 | 86.80 |
| 0.94 | 124.99 | 3.32 | 2.31 | 214.71 | 207.12 | 13.34 | 38.62 | 85.01 | 86.83 |
| 0.96 | 124.98 | 3.48 | 2.54 | 214.60 | 207.24 | 13.34 | 38.62 | 85.01 | 86.87 |
| 0.98 | 124.99 | 3.65 | 2.80 | 214.51 | 207.37 | 13.34 | 38.62 | 85.01 | 86.90 |
| 0.99 | 124.99 | 3.83 | 3.07 | 214.42 | 207.49 | 13.34 | 38.62 | 85.01 | 86.93 |
| 1.01 | 125.00 | 4.00 | 3.35 | 214.35 | 207.62 | 13.34 | 38.62 | 85.01 | 86.96 |
| 1.02 | 124.99 | 4.18 | 3.66 | 214.26 | 207.72 | 13.34 | 38.62 | 85.01 | 86.99 |
| 1.04 | 124.99 | 4.36 | 3.98 | 214.19 | 207.83 | 13.34 | 38.62 | 85.01 | 87.02 |
| 1.05 | 125.00 | 4.55 | 4.33 | 214.12 | 207.93 | 13.34 | 38.62 | 85.01 | 87.05 |
| 1.07 | 124.99 | 4.74 | 4.69 | 214.05 | 208.03 | 13.34 | 38.62 | 85.01 | 87.07 |
| 1.08 | 124.99 | 4.93 | 5.07 | 213.97 | 208.11 | 13.34 | 38.62 | 85.01 | 87.10 |
| 1.09 | 125.00 | 5.12 | 5.47 | 213.92 | 208.21 | 13.34 | 38.62 | 85.01 | 87.12 |
| 1.10 | 124.99 | 5.31 | 5.89 | 213.85 | 208.28 | 13.34 | 38.62 | 85.01 | 87.15 |
| 1.12 | 124.99 | 5.51 | 6.33 | 213.79 | 208.37 | 13.34 | 38.62 | 85.01 | 87.17 |
| 1.13 | 124.99 | 5.70 | 6.80 | 213.74 | 208.45 | 13.34 | 38.62 | 85.01 | 87.19 |
| 1.14 | 124.99 | 5.90 | 7.28 | 213.69 | 208.52 | 13.34 | 38.62 | 85.01 | 87.22 |
| 1.15 | 124.99 | 6.10 | 7.78 | 213.63 | 208.59 | 13.34 | 38.62 | 85.01 | 87.24 |
| 1.16 | 125.00 | 6.31 | 8.30 | 213.60 | 208.67 | 13.34 | 38.62 | 85.01 | 87.26 |
| 1.17 | 124.99 | 6.51 | 8.84 | 213.54 | 208.73 | 13.34 | 38.62 | 85.01 | 87.28 |
| 1.18 | 125.00 | 6.71 | 9.41 | 213.51 | 208.80 | 13.34 | 38.62 | 85.01 | 87.30 |
| 1.19 | 124.99 | 6.92 | 9.99 | 213.45 | 208.85 | 13.34 | 38.62 | 85.01 | 87.32 |
| 1.20 | 124.99 | 7.13 | 10.60 | 213.42 | 208.91 | 13.34 | 38.62 | 85.01 | 87.33 |
| 1.21 | 124.99 | 7.33 | 11.22 | 213.38 | 208.97 | 13.34 | 38.62 | 85.01 | 87.35 |
| 1.22 | 125.00 | 7.54 | 11.87 | 213.34 | 209.03 | 13.34 | 38.62 | 85.01 | 87.37 |
| 1.23 | 125.00 | 7.75 | 12.54 | 213.31 | 209.08 | 13.34 | 38.62 | 85.01 | 87.38 |

Table 25: Simulation data for the design 2 of chapter 3, channel diameter = 0.040", channel spacing of 0.020"

| | | Primary Side | | | | Secondary Side | | | |
|---|---|---|---|---|---|---|---|---|---|
| **Heat Transfer** | **MATD** | **Flow Rate** | **Press. Drop** | **Inlet Temp.** | **Outlet Temp.** | **Flow Rate** | **Press. Drop** | **Inlet Temp.** | **Outlet Temp.** |
| kW | °F | LPM | psig | °F | °F | LPM | psig | °F | °F |
| | | | | | | | | | |
| 2.42 | 124.99 | 1.75 | 0.80 | 231.17 | 193.96 | 39.80 | 12.18 | 85.01 | 90.14 |
| 2.48 | 124.99 | 1.84 | 0.88 | 230.78 | 194.50 | 39.80 | 12.18 | 85.01 | 90.28 |
| 2.55 | 124.99 | 1.94 | 0.98 | 230.36 | 195.05 | 39.80 | 12.18 | 85.01 | 90.42 |
| 2.62 | 124.99 | 2.05 | 1.09 | 229.95 | 195.60 | 39.80 | 12.18 | 85.01 | 90.56 |
| 2.69 | 124.99 | 2.16 | 1.21 | 229.53 | 196.16 | 39.80 | 12.18 | 85.01 | 90.71 |
| 2.76 | 124.99 | 2.29 | 1.36 | 229.14 | 196.72 | 39.80 | 12.18 | 85.01 | 90.86 |
| 2.83 | 125.00 | 2.42 | 1.51 | 228.74 | 197.27 | 39.80 | 12.18 | 85.01 | 91.01 |
| 2.90 | 124.99 | 2.55 | 1.68 | 228.34 | 197.80 | 39.80 | 12.18 | 85.01 | 91.16 |
| 2.97 | 125.00 | 2.69 | 1.88 | 227.98 | 198.34 | 39.80 | 12.18 | 85.01 | 91.31 |
| 3.04 | 124.98 | 2.84 | 2.08 | 227.61 | 198.83 | 39.80 | 12.18 | 85.01 | 91.46 |
| 3.11 | 124.99 | 2.99 | 2.31 | 227.26 | 199.33 | 39.80 | 12.18 | 85.01 | 91.61 |
| 3.18 | 125.00 | 3.15 | 2.56 | 226.94 | 199.82 | 39.80 | 12.18 | 85.01 | 91.75 |
| 3.25 | 124.99 | 3.31 | 2.82 | 226.61 | 200.27 | 39.80 | 12.18 | 85.01 | 91.89 |
| 3.31 | 124.99 | 3.47 | 3.11 | 226.31 | 200.72 | 39.80 | 12.18 | 85.01 | 92.03 |
| 3.37 | 124.99 | 3.64 | 3.42 | 226.00 | 201.14 | 39.80 | 12.18 | 85.01 | 92.16 |
| 3.43 | 124.99 | 3.81 | 3.75 | 225.71 | 201.56 | 39.80 | 12.18 | 85.01 | 92.29 |
| 3.49 | 125.00 | 3.99 | 4.10 | 225.44 | 201.97 | 39.80 | 12.18 | 85.01 | 92.41 |
| 3.54 | 125.00 | 4.17 | 4.47 | 225.17 | 202.36 | 39.80 | 12.18 | 85.01 | 92.52 |
| 3.60 | 125.00 | 4.35 | 4.85 | 224.92 | 202.72 | 39.80 | 12.18 | 85.01 | 92.64 |
| 3.65 | 125.00 | 4.53 | 5.27 | 224.69 | 203.07 | 39.80 | 12.18 | 85.01 | 92.75 |
| 3.70 | 124.99 | 4.72 | 5.71 | 224.45 | 203.39 | 39.80 | 12.18 | 85.01 | 92.86 |
| 3.76 | 125.00 | 4.91 | 6.18 | 224.25 | 203.72 | 39.80 | 12.18 | 85.01 | 92.97 |
| 3.81 | 124.99 | 5.10 | 6.66 | 224.06 | 204.03 | 39.80 | 12.18 | 85.01 | 93.08 |
| 3.86 | 124.98 | 5.29 | 7.18 | 223.86 | 204.31 | 39.80 | 12.18 | 85.01 | 93.19 |
| 3.90 | 125.00 | 5.49 | 7.71 | 223.70 | 204.60 | 39.80 | 12.18 | 85.01 | 93.29 |
| 3.95 | 124.99 | 5.68 | 8.27 | 223.52 | 204.86 | 39.80 | 12.18 | 85.01 | 93.39 |
| 4.00 | 125.00 | 5.88 | 8.86 | 223.37 | 205.13 | 39.80 | 12.18 | 85.01 | 93.49 |
| 4.04 | 124.99 | 6.08 | 9.47 | 223.21 | 205.37 | 39.80 | 12.18 | 85.01 | 93.58 |
| 4.09 | 124.99 | 6.28 | 10.10 | 223.06 | 205.61 | 39.80 | 12.18 | 85.01 | 93.68 |
| 4.13 | 124.99 | 6.48 | 10.76 | 222.92 | 205.84 | 39.80 | 12.18 | 85.01 | 93.77 |
| 4.17 | 124.98 | 6.69 | 11.44 | 222.78 | 206.05 | 39.80 | 12.18 | 85.01 | 93.85 |
| 4.21 | 124.99 | 6.89 | 12.15 | 222.65 | 206.27 | 39.80 | 12.18 | 85.01 | 93.93 |
| 4.25 | 124.99 | 7.10 | 12.89 | 222.52 | 206.47 | 39.80 | 12.18 | 85.01 | 94.02 |
| 4.28 | 125.00 | 7.30 | 13.65 | 222.42 | 206.68 | 39.80 | 12.18 | 85.01 | 94.10 |
| 4.32 | 124.99 | 7.51 | 14.44 | 222.29 | 206.86 | 39.80 | 12.18 | 85.01 | 94.17 |
| 4.36 | 124.99 | 7.72 | 15.25 | 222.18 | 207.05 | 39.80 | 12.18 | 85.01 | 94.25 |

Table 26: Simulation data for design 3 of chapter 3, channel diameter = 0.040", channel spacing of 0.040"

| | | Primary Side | | | | Secondary Side | | | |
|---|---|---|---|---|---|---|---|---|---|
| **Heat Transfer** | **MATD** | **Flow Rate** | **Press. Drop** | **Inlet Temp.** | **Outlet Temp.** | **Flow Rate** | **Press. Drop** | **Inlet Temp.** | **Outlet Temp.** |
| kW | °F | LPM | psig | °F | °F | LPM | psig | °F | °F |
| | | | | | | | | | |
| 3.98 | 124.99 | 1.76 | 0.66 | 244.51 | 183.24 | 13.29 | 38.89 | 85.01 | 92.75 |
| 4.10 | 124.99 | 1.85 | 0.73 | 243.91 | 184.05 | 13.29 | 38.89 | 85.01 | 92.97 |
| 4.21 | 124.99 | 1.95 | 0.81 | 243.28 | 184.91 | 13.29 | 38.89 | 85.01 | 93.20 |
| 4.33 | 124.99 | 2.06 | 0.90 | 242.63 | 185.78 | 13.29 | 38.89 | 85.01 | 93.43 |
| 4.46 | 124.99 | 2.17 | 1.00 | 242.00 | 186.66 | 13.29 | 38.89 | 85.01 | 93.67 |
| 4.58 | 124.99 | 2.30 | 1.12 | 241.37 | 187.54 | 13.29 | 38.89 | 85.01 | 93.92 |
| 4.71 | 125.00 | 2.43 | 1.25 | 240.76 | 188.41 | 13.29 | 38.89 | 85.01 | 94.16 |
| 4.84 | 124.99 | 2.56 | 1.39 | 240.15 | 189.26 | 13.29 | 38.89 | 85.01 | 94.41 |
| 4.97 | 125.00 | 2.71 | 1.55 | 239.57 | 190.09 | 13.29 | 38.89 | 85.01 | 94.66 |
| 5.09 | 124.99 | 2.85 | 1.72 | 238.99 | 190.90 | 13.29 | 38.89 | 85.01 | 94.90 |
| 5.22 | 124.99 | 3.01 | 1.91 | 238.45 | 191.69 | 13.29 | 38.89 | 85.01 | 95.15 |
| 5.34 | 124.99 | 3.16 | 2.11 | 237.93 | 192.45 | 13.29 | 38.89 | 85.01 | 95.39 |
| 5.46 | 124.99 | 3.33 | 2.33 | 237.43 | 193.19 | 13.29 | 38.89 | 85.01 | 95.62 |
| 5.58 | 124.99 | 3.49 | 2.57 | 236.94 | 193.90 | 13.29 | 38.89 | 85.01 | 95.85 |
| 5.70 | 125.00 | 3.66 | 2.82 | 236.51 | 194.58 | 13.29 | 38.89 | 85.01 | 96.09 |
| 5.82 | 124.99 | 3.84 | 3.09 | 236.07 | 195.23 | 13.29 | 38.89 | 85.01 | 96.31 |
| 5.93 | 125.00 | 4.01 | 3.38 | 235.68 | 195.86 | 13.29 | 38.89 | 85.01 | 96.54 |
| 6.04 | 124.99 | 4.19 | 3.69 | 235.28 | 196.46 | 13.29 | 38.89 | 85.01 | 96.75 |
| 6.15 | 124.99 | 4.37 | 4.02 | 234.92 | 197.04 | 13.29 | 38.89 | 85.01 | 96.97 |
| 6.26 | 125.00 | 4.56 | 4.36 | 234.58 | 197.61 | 13.29 | 38.89 | 85.01 | 97.18 |
| 6.37 | 124.99 | 4.75 | 4.73 | 234.24 | 198.14 | 13.29 | 38.89 | 85.01 | 97.38 |
| 6.47 | 124.99 | 4.94 | 5.11 | 233.91 | 198.66 | 13.29 | 38.89 | 85.01 | 97.58 |
| 6.57 | 125.00 | 5.13 | 5.51 | 233.61 | 199.16 | 13.29 | 38.89 | 85.01 | 97.77 |
| 6.66 | 124.99 | 5.32 | 5.94 | 233.30 | 199.63 | 13.29 | 38.89 | 85.01 | 97.95 |
| 6.75 | 125.00 | 5.52 | 6.38 | 233.03 | 200.11 | 13.29 | 38.89 | 85.01 | 98.13 |
| 6.84 | 125.00 | 5.72 | 6.84 | 232.76 | 200.55 | 13.29 | 38.89 | 85.01 | 98.31 |
| 6.93 | 124.99 | 5.92 | 7.32 | 232.49 | 200.98 | 13.29 | 38.89 | 85.01 | 98.48 |
| 7.02 | 124.99 | 6.12 | 7.83 | 232.24 | 201.39 | 13.29 | 38.89 | 85.01 | 98.64 |
| 7.10 | 124.99 | 6.32 | 8.35 | 232.00 | 201.80 | 13.29 | 38.89 | 85.01 | 98.80 |
| 7.18 | 124.99 | 6.53 | 8.90 | 231.77 | 202.18 | 13.29 | 38.89 | 85.01 | 98.96 |
| 7.26 | 124.99 | 6.73 | 9.44 | 231.55 | 202.55 | 13.29 | 38.89 | 85.01 | 99.11 |
| 7.34 | 125.00 | 6.94 | 10.03 | 231.35 | 202.92 | 13.29 | 38.89 | 85.01 | 99.27 |
| 7.42 | 125.00 | 7.15 | 10.63 | 231.17 | 203.25 | 13.29 | 38.89 | 85.01 | 99.42 |
| 7.50 | 124.99 | 7.35 | 11.26 | 230.99 | 203.58 | 13.29 | 38.89 | 85.01 | 99.58 |
| 7.58 | 124.99 | 7.56 | 11.91 | 230.83 | 203.90 | 13.29 | 38.89 | 85.01 | 99.73 |
| 7.65 | 124.99 | 7.78 | 12.58 | 230.67 | 204.21 | 13.29 | 38.89 | 85.01 | 99.88 |

Table 27: Simulation data for design 4 of chapter 3, channel dimensions = 150 μm X 150 μm, channel spacing = 25 μm

| | | Primary Side | | | | Secondary Side | | | |
|---|---|---|---|---|---|---|---|---|---|
| **Heat Transfer** | **MATD** | **Flow Rate** | **Press. Drop** | **Inlet Temp.** | **Outlet Temp.** | **Flow Rate** | **Press. Drop** | **Inlet Temp.** | **Outlet Temp.** |
| kW | °F | LPM | psig | °F | °F | LPM | psig | °F | °F |
| | | | | | | | | | |
| 9.38 | 124.99 | 1.73 | 0.76 | 293.82 | 145.24 | 12.72 | 40.69 | 85.01 | 104.06 |
| 9.69 | 125.00 | 1.82 | 0.84 | 292.70 | 146.99 | 12.72 | 40.69 | 85.01 | 104.69 |
| 10.01 | 125.00 | 1.92 | 0.92 | 291.53 | 148.82 | 12.72 | 40.69 | 85.01 | 105.34 |
| 10.35 | 125.00 | 2.03 | 1.02 | 290.36 | 150.68 | 12.72 | 40.69 | 85.01 | 106.03 |
| 10.70 | 125.00 | 2.15 | 1.13 | 289.19 | 152.57 | 12.72 | 40.69 | 85.01 | 106.75 |
| 11.06 | 124.99 | 2.27 | 1.26 | 288.00 | 154.48 | 12.72 | 40.69 | 85.01 | 107.48 |
| 11.43 | 125.00 | 2.40 | 1.39 | 286.83 | 156.40 | 12.72 | 40.69 | 85.01 | 108.22 |
| 11.79 | 125.00 | 2.53 | 1.54 | 285.66 | 158.31 | 12.72 | 40.69 | 85.01 | 108.96 |
| 12.15 | 125.00 | 2.67 | 1.71 | 284.50 | 160.20 | 12.72 | 40.69 | 85.01 | 109.70 |
| 12.52 | 125.00 | 2.82 | 1.89 | 283.37 | 162.07 | 12.72 | 40.69 | 85.01 | 110.43 |
| 12.87 | 124.99 | 2.97 | 2.09 | 282.25 | 163.91 | 12.72 | 40.69 | 85.01 | 111.16 |
| 13.23 | 125.00 | 3.13 | 2.30 | 281.17 | 165.71 | 12.72 | 40.69 | 85.01 | 111.87 |
| 13.57 | 125.00 | 3.29 | 2.53 | 280.12 | 167.46 | 12.72 | 40.69 | 85.01 | 112.58 |
| 13.91 | 124.99 | 3.46 | 2.78 | 279.10 | 169.17 | 12.72 | 40.69 | 85.01 | 113.27 |
| 14.24 | 124.99 | 3.62 | 3.05 | 278.11 | 170.83 | 12.72 | 40.69 | 85.01 | 113.94 |
| 14.53 | 124.99 | 3.80 | 3.33 | 276.95 | 172.55 | 12.72 | 40.69 | 85.01 | 114.52 |
| 14.82 | 124.99 | 3.97 | 3.63 | 275.93 | 174.18 | 12.72 | 40.69 | 85.01 | 115.11 |
| 15.11 | 125.00 | 4.15 | 3.95 | 275.01 | 175.71 | 12.72 | 40.69 | 85.01 | 115.71 |
| 15.42 | 124.99 | 4.33 | 4.29 | 274.18 | 177.15 | 12.72 | 40.69 | 85.01 | 116.33 |
| 15.73 | 124.99 | 4.52 | 4.65 | 273.44 | 178.52 | 12.72 | 40.69 | 85.01 | 116.96 |
| 16.03 | 124.99 | 4.70 | 5.03 | 272.72 | 179.85 | 12.72 | 40.69 | 85.01 | 117.57 |
| 16.32 | 125.00 | 4.89 | 5.42 | 272.03 | 181.14 | 12.72 | 40.69 | 85.01 | 118.17 |
| 16.61 | 125.00 | 5.08 | 5.84 | 271.39 | 182.38 | 12.72 | 40.69 | 85.01 | 118.75 |
| 16.89 | 125.00 | 5.28 | 6.28 | 270.75 | 183.57 | 12.72 | 40.69 | 85.01 | 119.33 |
| 17.17 | 125.00 | 5.47 | 6.73 | 270.16 | 184.73 | 12.72 | 40.69 | 85.01 | 119.89 |
| 17.44 | 124.99 | 5.67 | 7.21 | 269.58 | 185.84 | 12.72 | 40.69 | 85.01 | 120.44 |
| 17.70 | 124.99 | 5.87 | 7.71 | 269.04 | 186.93 | 12.72 | 40.69 | 85.01 | 120.97 |
| 17.96 | 124.99 | 6.07 | 8.23 | 268.52 | 187.97 | 12.72 | 40.69 | 85.01 | 121.50 |
| 18.21 | 124.99 | 6.27 | 8.77 | 268.02 | 188.98 | 12.72 | 40.69 | 85.01 | 122.01 |
| 18.46 | 125.00 | 6.47 | 9.33 | 267.55 | 189.97 | 12.72 | 40.69 | 85.01 | 122.51 |
| 18.70 | 125.00 | 6.68 | 9.91 | 267.10 | 190.91 | 12.72 | 40.69 | 85.01 | 123.01 |
| 18.94 | 124.99 | 6.88 | 10.51 | 266.65 | 191.82 | 12.72 | 40.69 | 85.01 | 123.48 |
| 19.16 | 124.99 | 7.09 | 11.13 | 266.21 | 192.72 | 12.72 | 40.69 | 85.01 | 123.94 |
| 19.39 | 124.99 | 7.30 | 11.78 | 265.80 | 193.58 | 12.72 | 40.69 | 85.01 | 124.39 |
| 19.60 | 125.00 | 7.51 | 12.44 | 265.40 | 194.43 | 12.72 | 40.69 | 85.01 | 124.82 |
| 19.81 | 125.00 | 7.72 | 13.13 | 265.01 | 195.24 | 12.72 | 40.69 | 85.01 | 125.25 |

Table 28: Experimental data for design 2 of chapter 3 with channel diameter = 0.040", and channel spacing = 0.020"

| | | | | | Primary Side | | | Secondary Side | | | |
|---|---|---|---|---|---|---|---|---|---|---|---|
| **Relative MATD Level** | **Pump Speed** | **Heat Transfer** | **MATD** | **System Press. Drop** | **Flow Rate** | **Inlet Temp.** | **Outlet Temp.** | **Flow Rate** | **Press. Drop** | **Inlet Temp.** | **Outlet Temp.** |
| °F | RPM | kW | °F | psig | LPM | °F | °F | LPM | psig | °F | °F |
| | | | | | | | | | | | |
| 200 | 3100 | 4.94 | 200.26 | 4.50 | 1.95 | 318.94 | 261.79 | 12.89 | 38.19 | 85.60 | 94.62 |
| | 4050 | 5.26 | 200.20 | 5.74 | 2.38 | 315.00 | 266.49 | 12.74 | 37.31 | 85.52 | 95.56 |
| | 5020 | 5.65 | 200.17 | 8.02 | 2.85 | 312.45 | 269.71 | 12.92 | 38.38 | 85.47 | 96.36 |
| | 6060 | 6.08 | 200.30 | 11.00 | 3.42 | 310.98 | 272.63 | 12.98 | 38.71 | 85.61 | 97.38 |
| | 6930 | 6.39 | 199.95 | 13.86 | 3.94 | 309.26 | 274.13 | 12.78 | 37.56 | 85.48 | 98.02 |
| | 8060 | 6.76 | 199.92 | 17.72 | 4.62 | 307.87 | 275.96 | 12.98 | 38.73 | 85.45 | 98.54 |
| | 9080 | 7.06 | 199.91 | 21.56 | 5.30 | 306.71 | 277.33 | 12.86 | 38.04 | 85.27 | 98.95 |
| | 10010 | 7.40 | 201.16 | 25.27 | 5.96 | 307.51 | 279.83 | 12.88 | 38.12 | 85.41 | 99.61 |
| 175 | 3100 | 4.19 | 175.21 | 3.91 | 1.97 | 289.14 | 239.98 | 12.77 | 37.50 | 85.47 | 93.23 |
| | 4200 | 4.53 | 175.29 | 5.33 | 2.52 | 285.50 | 245.03 | 12.75 | 37.38 | 85.58 | 94.37 |
| | 4900 | 4.74 | 175.29 | 6.87 | 2.86 | 284.25 | 247.19 | 12.88 | 38.14 | 85.84 | 95.03 |
| | 6000 | 5.07 | 175.37 | 9.96 | 3.48 | 282.22 | 249.66 | 12.84 | 37.89 | 85.58 | 95.56 |
| | 7000 | 5.37 | 175.28 | 13.14 | 4.10 | 280.90 | 251.38 | 12.68 | 37.01 | 85.53 | 96.19 |
| | 8040 | 5.67 | 175.53 | 16.76 | 4.76 | 280.22 | 253.15 | 12.79 | 37.63 | 85.58 | 96.74 |
| | 8900 | 5.87 | 175.13 | 19.96 | 5.33 | 279.09 | 253.67 | 12.80 | 37.69 | 85.49 | 97.00 |
| | 10000 | 6.19 | 175.31 | 24.29 | 6.11 | 278.41 | 254.87 | 12.96 | 38.56 | 85.38 | 97.28 |
| 150 | 3300 | 3.53 | 150.21 | 3.70 | 2.11 | 258.66 | 219.31 | 12.85 | 38.00 | 85.48 | 92.07 |
| | 4000 | 3.67 | 150.37 | 4.55 | 2.43 | 257.09 | 222.38 | 12.91 | 38.32 | 85.85 | 92.89 |
| | 5040 | 3.94 | 150.35 | 6.70 | 3.00 | 254.85 | 224.94 | 12.89 | 38.21 | 85.70 | 93.40 |
| | 6000 | 4.20 | 150.74 | 9.31 | 3.52 | 254.20 | 227.17 | 12.92 | 38.37 | 85.81 | 94.08 |
| | 7040 | 4.45 | 150.33 | 12.63 | 4.19 | 252.55 | 228.46 | 12.94 | 38.45 | 85.80 | 94.55 |
| | 8020 | 4.70 | 150.77 | 16.27 | 4.87 | 252.08 | 229.94 | 12.92 | 38.36 | 85.62 | 94.85 |
| | 9030 | 4.92 | 150.82 | 20.12 | 5.54 | 251.41 | 230.92 | 12.93 | 38.41 | 85.53 | 95.16 |
| | 10000 | 5.11 | 150.29 | 24.22 | 6.27 | 250.03 | 231.05 | 12.96 | 38.59 | 85.28 | 95.22 |
| 125 | 4000 | 3.01 | 125.63 | 4.27 | 2.47 | 228.52 | 199.93 | 12.92 | 38.39 | 85.70 | 91.49 |
| | 5100 | 3.25 | 125.43 | 6.49 | 3.07 | 226.34 | 201.91 | 13.17 | 39.81 | 85.55 | 91.84 |
| | 5950 | 3.40 | 125.35 | 8.83 | 3.57 | 225.02 | 203.00 | 13.01 | 38.85 | 85.30 | 92.03 |
| | 7080 | 3.65 | 125.56 | 12.44 | 4.28 | 224.02 | 204.25 | 13.16 | 39.77 | 85.01 | 92.14 |
| | 8040 | 3.80 | 125.01 | 15.88 | 4.97 | 222.65 | 204.70 | 12.87 | 38.04 | 84.86 | 92.45 |
| | 9000 | 3.97 | 125.22 | 20.05 | 5.63 | 222.39 | 205.73 | 12.82 | 37.78 | 84.87 | 92.80 |
| | 10040 | 4.10 | 125.14 | 24.76 | 6.40 | 221.98 | 206.49 | 12.86 | 37.99 | 85.02 | 93.16 |
| 100 | 3990 | 2.27 | 100.43 | 4.35 | 2.49 | 198.61 | 176.81 | 13.06 | 39.16 | 85.09 | 89.48 |
| | 5000 | 2.43 | 100.38 | 6.23 | 3.04 | 197.42 | 178.73 | 12.69 | 37.06 | 85.23 | 90.15 |
| | 6050 | 2.57 | 100.24 | 8.82 | 3.68 | 196.31 | 179.86 | 12.80 | 37.64 | 85.24 | 90.46 |
| | 7070 | 2.73 | 100.24 | 12.07 | 4.35 | 195.58 | 180.74 | 12.78 | 37.54 | 85.15 | 90.70 |
| | 8000 | 2.88 | 100.64 | 15.40 | 4.97 | 195.88 | 182.04 | 12.86 | 38.03 | 85.43 | 91.21 |
| | 9000 | 2.98 | 100.82 | 19.29 | 5.70 | 195.70 | 182.99 | 12.20 | 34.27 | 85.38 | 91.67 |
| | 10040 | 3.08 | 100.33 | 24.02 | 6.52 | 194.74 | 183.06 | 11.93 | 32.80 | 85.25 | 91.89 |

# Appendix C

## Prototype Integrated Recirculating System Simulation Data

This appendix contains all data for the four simulated configurations of the integrated recirculating target system using both the Exergy model 00268-1 and 00268-2 shell and tube heat exchangers.

Table 29: Simulation data for integrated recirculating target system with one Exergy model 00268-2 shell and tube heat exchanger with 1/16" diameter tubes

| | | | Primary Side | | | | Secondary Side | | | |
|---|---|---|---|---|---|---|---|---|---|---|
| **Pump Speed** | **Heat Transfer** | **MATD** | **Flow Rate** | **Press. Drop** | **Inlet Temp.** | **Outlet Temp.** | **Flow Rate** | **Press. Drop** | **Inlet Temp.** | **Outlet Temp.** |
| RPM | kW | °F | LPM | psig | °F | °F | LPM | psig | °F | °F |
| | | | | | | | | | | |
| 4000 | 1.51 | 124.99 | 0.55 | 9.36 | 231.47 | 157.38 | 13.58 | 47.25 | 68.00 | 70.87 |
| 4100 | 1.53 | 125.00 | 0.56 | 9.73 | 231.25 | 157.65 | 13.58 | 47.25 | 68.00 | 70.90 |
| 4200 | 1.55 | 124.99 | 0.57 | 10.10 | 231.02 | 157.92 | 13.58 | 47.25 | 68.00 | 70.94 |
| 4300 | 1.57 | 124.99 | 0.58 | 10.49 | 230.78 | 158.18 | 13.58 | 47.25 | 68.00 | 70.98 |
| 4400 | 1.59 | 125.00 | 0.59 | 10.90 | 230.57 | 158.45 | 13.58 | 47.25 | 68.00 | 71.02 |
| 4500 | 1.61 | 124.99 | 0.61 | 11.32 | 230.33 | 158.71 | 13.58 | 47.25 | 68.00 | 71.06 |
| 4600 | 1.63 | 124.99 | 0.62 | 11.75 | 230.11 | 158.97 | 13.58 | 47.25 | 68.00 | 71.10 |
| 4700 | 1.65 | 125.00 | 0.63 | 12.20 | 229.90 | 159.23 | 13.58 | 47.25 | 68.00 | 71.14 |
| 4800 | 1.67 | 125.00 | 0.64 | 12.66 | 229.68 | 159.49 | 13.58 | 47.25 | 68.00 | 71.18 |
| 4900 | 1.70 | 125.00 | 0.65 | 13.13 | 229.47 | 159.75 | 13.58 | 47.25 | 68.00 | 71.22 |
| 5000 | 1.72 | 125.00 | 0.67 | 13.62 | 229.25 | 160.00 | 13.58 | 47.25 | 68.00 | 71.26 |
| 5100 | 1.74 | 124.99 | 0.68 | 14.13 | 229.03 | 160.25 | 13.58 | 47.25 | 68.00 | 71.30 |
| 5200 | 1.76 | 124.99 | 0.69 | 14.64 | 228.82 | 160.50 | 13.58 | 47.25 | 68.00 | 71.34 |
| 5300 | 1.78 | 125.00 | 0.70 | 15.18 | 228.62 | 160.75 | 13.58 | 47.25 | 68.00 | 71.38 |
| 5400 | 1.80 | 124.99 | 0.72 | 15.72 | 228.40 | 160.99 | 13.58 | 47.25 | 68.00 | 71.42 |
| 5500 | 1.82 | 124.99 | 0.73 | 16.29 | 228.20 | 161.23 | 13.58 | 47.25 | 68.00 | 71.46 |
| 5600 | 1.84 | 124.99 | 0.74 | 16.86 | 228.01 | 161.47 | 13.58 | 47.25 | 68.00 | 71.50 |
| 5700 | 1.86 | 124.99 | 0.76 | 17.45 | 227.81 | 161.71 | 13.58 | 47.25 | 68.00 | 71.54 |
| 5800 | 1.88 | 124.99 | 0.77 | 18.06 | 227.61 | 161.94 | 13.58 | 47.25 | 68.00 | 71.57 |
| 5900 | 1.91 | 125.00 | 0.78 | 18.68 | 227.43 | 162.18 | 13.58 | 47.25 | 68.00 | 71.61 |
| 6000 | 1.92 | 125.00 | 0.80 | 19.42 | 227.25 | 162.40 | 13.58 | 47.25 | 68.00 | 71.65 |

Table 30: Simulation data for integrated recirculating target system with one Exergy model 00268-2 shell and tube heat exchanger with 1/8" diameter tubes

| | | | Primary Side | | | | Secondary Side | | | |
|---|---|---|---|---|---|---|---|---|---|---|
| **Pump Speed** | **Heat Transfer** | **MATD** | **Flow Rate** | **Press. Drop** | **Inlet Temp.** | **Outlet Temp.** | **Flow Rate** | **Press. Drop** | **Inlet Temp.** | **Outlet Temp.** |
| RPM | kW | °F | LPM | psig | °F | °F | LPM | psig | °F | °F |
| | | | | | | | | | | |
| 4000 | 2.94 | 124.99 | 1.63 | 5.36 | 219.90 | 171.66 | 13.58 | 47.25 | 68.00 | 73.57 |
| 4100 | 2.98 | 125.00 | 1.67 | 5.61 | 219.68 | 171.96 | 13.58 | 47.25 | 68.00 | 73.65 |
| 4200 | 3.02 | 124.99 | 1.71 | 5.88 | 219.45 | 172.25 | 13.58 | 47.25 | 68.00 | 73.72 |
| 4300 | 3.05 | 124.99 | 1.75 | 6.16 | 219.23 | 172.55 | 13.58 | 47.25 | 68.00 | 73.80 |
| 4400 | 3.09 | 124.99 | 1.80 | 6.45 | 219.02 | 172.84 | 13.58 | 47.25 | 68.00 | 73.87 |
| 4500 | 3.13 | 124.99 | 1.84 | 6.75 | 218.80 | 173.13 | 13.58 | 47.25 | 68.00 | 73.94 |
| 4600 | 3.17 | 124.99 | 1.88 | 7.07 | 218.58 | 173.40 | 13.58 | 47.25 | 68.00 | 74.01 |
| 4700 | 3.21 | 124.99 | 1.92 | 7.40 | 218.39 | 173.68 | 13.58 | 47.25 | 68.00 | 74.09 |
| 4800 | 3.25 | 124.99 | 1.97 | 7.75 | 218.19 | 173.96 | 13.58 | 47.25 | 68.00 | 74.16 |
| 4900 | 3.28 | 124.99 | 2.01 | 8.11 | 217.99 | 174.23 | 13.58 | 47.25 | 68.00 | 74.23 |
| 5000 | 3.32 | 124.99 | 2.05 | 8.48 | 217.79 | 174.48 | 13.58 | 47.25 | 68.00 | 74.30 |
| 5100 | 3.36 | 124.99 | 2.10 | 8.86 | 217.61 | 174.75 | 13.58 | 47.25 | 68.00 | 74.37 |
| 5200 | 3.39 | 125.00 | 2.14 | 9.26 | 217.43 | 175.00 | 13.58 | 47.25 | 68.00 | 74.44 |
| 5300 | 3.43 | 125.00 | 2.19 | 9.68 | 217.25 | 175.25 | 13.58 | 47.25 | 68.00 | 74.50 |
| 5400 | 3.46 | 124.99 | 2.23 | 10.11 | 217.07 | 175.49 | 13.58 | 47.25 | 68.00 | 74.57 |
| 5500 | 3.50 | 125.00 | 2.27 | 10.55 | 216.91 | 175.73 | 13.58 | 47.25 | 68.00 | 74.64 |
| 5600 | 3.53 | 124.99 | 2.32 | 11.01 | 216.73 | 175.95 | 13.58 | 47.25 | 68.00 | 74.70 |
| 5700 | 3.57 | 124.99 | 2.36 | 11.48 | 216.57 | 176.18 | 13.58 | 47.25 | 68.00 | 74.76 |
| 5800 | 3.60 | 124.99 | 2.41 | 11.97 | 216.40 | 176.40 | 13.58 | 47.25 | 68.00 | 74.83 |
| 5900 | 3.63 | 125.00 | 2.45 | 12.47 | 216.26 | 176.62 | 13.58 | 47.25 | 68.00 | 74.89 |
| 6000 | 3.66 | 124.99 | 2.50 | 12.98 | 216.10 | 176.83 | 13.58 | 47.25 | 68.00 | 74.95 |

Table 31: Primary side simulation data for integrated recirculating target system with two Exergy model 00268-2 shell and tube heat exchanger with 1/8" diameter tubes in series

| | | Primary Side | | | | | | | |
|---|---|---|---|---|---|---|---|---|---|
| | | | | First Heat Exchanger | | | Second Heat Exchanger | | |
| **Pump Speed** | **Heat Transfer** | **Flow Rate** | **Press. Drop** | **MATD** | **Inlet Temp.** | **Outlet Temp.** | **MATD** | **Inlet Temp.** | **Outlet Temp.** |
| RPM | kW | LPM | psig | °F | °F | °F | °F | °F | °F |
| | | | | | | | | | |
| 4000 | 4.60 | 1.55 | 5.58 | 125.00 | 220.38 | 171.04 | 86.57 | 171.04 | 141.41 |
| 4100 | 4.67 | 1.59 | 5.84 | 124.99 | 220.14 | 171.34 | 86.91 | 171.34 | 141.84 |
| 4200 | 4.74 | 1.63 | 6.11 | 125.00 | 219.93 | 171.64 | 87.24 | 171.64 | 142.28 |
| 4300 | 4.82 | 1.67 | 6.40 | 124.99 | 219.69 | 171.92 | 87.57 | 171.92 | 142.71 |
| 4400 | 4.89 | 1.71 | 6.69 | 124.99 | 219.48 | 172.21 | 87.90 | 172.21 | 143.15 |
| 4500 | 4.96 | 1.75 | 7.00 | 124.99 | 219.26 | 172.50 | 88.23 | 172.50 | 143.58 |
| 4600 | 5.03 | 1.79 | 7.32 | 125.00 | 219.06 | 172.79 | 88.56 | 172.79 | 144.01 |
| 4700 | 5.10 | 1.83 | 7.66 | 124.99 | 218.84 | 173.06 | 88.87 | 173.06 | 144.43 |
| 4800 | 5.17 | 1.87 | 8.01 | 125.00 | 218.65 | 173.34 | 89.19 | 173.34 | 144.85 |
| 4900 | 5.24 | 1.91 | 8.37 | 125.00 | 218.45 | 173.61 | 89.50 | 173.61 | 145.27 |
| 5000 | 5.31 | 1.95 | 8.74 | 124.99 | 218.25 | 173.87 | 89.80 | 173.87 | 145.67 |
| 5100 | 5.38 | 1.99 | 9.13 | 124.99 | 218.05 | 174.13 | 90.10 | 174.13 | 146.07 |
| 5200 | 5.45 | 2.04 | 9.53 | 124.99 | 217.87 | 174.39 | 90.39 | 174.39 | 146.47 |
| 5300 | 5.52 | 2.08 | 9.95 | 125.00 | 217.69 | 174.64 | 90.68 | 174.64 | 146.87 |
| 5400 | 5.59 | 2.12 | 10.38 | 125.00 | 217.51 | 174.88 | 90.97 | 174.88 | 147.26 |
| 5500 | 5.66 | 2.16 | 10.83 | 124.99 | 217.33 | 175.12 | 91.25 | 175.12 | 147.63 |
| 5600 | 5.72 | 2.21 | 11.28 | 125.00 | 217.17 | 175.36 | 91.52 | 175.36 | 148.01 |
| 5700 | 5.79 | 2.25 | 11.76 | 124.99 | 216.99 | 175.58 | 91.79 | 175.58 | 148.38 |
| 5800 | 5.86 | 2.29 | 12.25 | 124.99 | 216.83 | 175.81 | 92.05 | 175.81 | 148.74 |
| 5900 | 5.92 | 2.34 | 12.75 | 125.00 | 216.68 | 176.04 | 92.32 | 176.04 | 149.10 |
| 6000 | 5.98 | 2.38 | 13.26 | 124.99 | 216.52 | 176.25 | 92.57 | 176.25 | 149.45 |

Table 32: Secondary side simulation data for integrated recirculating target system with two Exergy model 00268-2 shell and tube heat exchanger with 1/8" diameter tubes in series

| | | Secondary Side | | | | | |
|---|---|---|---|---|---|---|---|
| | | | | First Heat Exchanger | | Second Heat Exchanger | |
| **Pump Speed** | **Heat Transfer** | **Flow Rate** | **Press. Drop** | **Inlet Temp.** | **Outlet Temp.** | **Inlet Temp.** | **Outlet Temp.** |
| RPM | kW | LPM | psig | °F | °F | °F | °F |
| | | | | | | | |
| 4000 | 4.60 | 13.58 | 47.25 | 68.00 | 73.42 | 68.00 | 71.30 |
| 4100 | 4.67 | 13.58 | 47.25 | 68.00 | 73.50 | 68.00 | 71.37 |
| 4200 | 4.74 | 13.58 | 47.25 | 68.00 | 73.57 | 68.00 | 71.43 |
| 4300 | 4.82 | 13.58 | 47.25 | 68.00 | 73.64 | 68.00 | 71.50 |
| 4400 | 4.89 | 13.58 | 47.25 | 68.00 | 73.71 | 68.00 | 71.56 |
| 4500 | 4.96 | 13.58 | 47.25 | 68.00 | 73.78 | 68.00 | 71.62 |
| 4600 | 5.03 | 13.58 | 47.25 | 68.00 | 73.85 | 68.00 | 71.69 |
| 4700 | 5.10 | 13.58 | 47.25 | 68.00 | 73.93 | 68.00 | 71.75 |
| 4800 | 5.17 | 13.58 | 47.25 | 68.00 | 74.00 | 68.00 | 71.82 |
| 4900 | 5.24 | 13.58 | 47.25 | 68.00 | 74.07 | 68.00 | 71.88 |
| 5000 | 5.31 | 13.58 | 47.25 | 68.00 | 74.13 | 68.00 | 71.95 |
| 5100 | 5.38 | 13.58 | 47.25 | 68.00 | 74.20 | 68.00 | 72.01 |
| 5200 | 5.45 | 13.58 | 47.25 | 68.00 | 74.27 | 68.00 | 72.08 |
| 5300 | 5.52 | 13.58 | 47.25 | 68.00 | 74.34 | 68.00 | 72.14 |
| 5400 | 5.59 | 13.58 | 47.25 | 68.00 | 74.40 | 68.00 | 72.20 |
| 5500 | 5.66 | 13.58 | 47.25 | 68.00 | 74.47 | 68.00 | 72.26 |
| 5600 | 5.72 | 13.58 | 47.25 | 68.00 | 74.53 | 68.00 | 72.33 |
| 5700 | 5.79 | 13.58 | 47.25 | 68.00 | 74.60 | 68.00 | 72.39 |
| 5800 | 5.86 | 13.58 | 47.25 | 68.00 | 74.66 | 68.00 | 72.45 |
| 5900 | 5.92 | 13.58 | 47.25 | 68.00 | 74.72 | 68.00 | 72.51 |
| 6000 | 5.98 | 13.58 | 47.25 | 68.00 | 74.78 | 68.00 | 72.57 |

Table 33: Primary Side simulation data for integrated recirculating target system with two Exergy model 00268-1 shell and tube heat exchanger with 1/8" diameter tubes in series

| | | Primary Side | | | | | | | |
|---|---|---|---|---|---|---|---|---|---|
| | | | | First Heat Exchanger | | | Second Heat Exchanger | | |
| **Pump Speed** | **Heat Transfer** | **Flow Rate** | **Press. Drop** | **MATD** | **Inlet Temp.** | **Outlet Temp.** | **MATD** | **Inlet Temp.** | **Outlet Temp.** |
| RPM | kW | LPM | psig | °F | °F | °F | °F | °F | °F |
| | | | | | | | | | |
| 4000 | 7.86 | 1.55 | 5.59 | 124.99 | 251.80 | 154.31 | 63.12 | 154.31 | 116.06 |
| 4100 | 7.98 | 1.59 | 5.85 | 124.99 | 251.39 | 154.99 | 63.67 | 154.99 | 116.69 |
| 4200 | 8.11 | 1.63 | 6.12 | 124.99 | 250.97 | 155.66 | 64.22 | 155.66 | 117.32 |
| 4300 | 8.24 | 1.67 | 6.41 | 124.99 | 250.56 | 156.32 | 64.76 | 156.32 | 117.95 |
| 4400 | 8.37 | 1.71 | 6.71 | 124.99 | 250.16 | 156.98 | 65.30 | 156.98 | 118.58 |
| 4500 | 8.50 | 1.75 | 7.02 | 125.00 | 249.76 | 157.63 | 65.84 | 157.63 | 119.21 |
| 4600 | 8.63 | 1.79 | 7.34 | 124.99 | 249.37 | 158.27 | 66.36 | 158.27 | 119.84 |
| 4700 | 8.75 | 1.83 | 7.68 | 125.00 | 248.99 | 158.90 | 66.89 | 158.90 | 120.46 |
| 4800 | 8.88 | 1.87 | 8.02 | 124.99 | 248.61 | 159.52 | 67.40 | 159.52 | 121.09 |
| 4900 | 9.01 | 1.91 | 8.39 | 124.99 | 248.23 | 160.13 | 67.91 | 160.13 | 121.70 |
| 5000 | 9.13 | 1.95 | 8.76 | 124.99 | 247.87 | 160.73 | 68.41 | 160.73 | 122.32 |
| 5100 | 9.26 | 1.99 | 9.15 | 125.00 | 247.53 | 161.33 | 68.91 | 161.33 | 122.93 |
| 5200 | 9.38 | 2.04 | 9.56 | 124.99 | 247.17 | 161.91 | 69.39 | 161.91 | 123.53 |
| 5300 | 9.51 | 2.08 | 9.97 | 125.00 | 246.84 | 162.48 | 69.87 | 162.48 | 124.13 |
| 5400 | 9.63 | 2.12 | 10.40 | 124.99 | 246.50 | 163.04 | 70.34 | 163.04 | 124.72 |
| 5500 | 9.75 | 2.16 | 10.85 | 124.99 | 246.18 | 163.58 | 70.80 | 163.58 | 125.30 |
| 5600 | 9.87 | 2.21 | 11.31 | 125.00 | 245.87 | 164.13 | 71.25 | 164.13 | 125.88 |
| 5700 | 9.99 | 2.25 | 11.78 | 125.00 | 245.57 | 164.65 | 71.70 | 164.65 | 126.45 |
| 5800 | 10.11 | 2.29 | 12.27 | 125.00 | 245.26 | 165.17 | 72.14 | 165.17 | 127.02 |
| 5900 | 10.22 | 2.33 | 12.78 | 125.00 | 244.97 | 165.67 | 72.57 | 165.67 | 127.57 |
| 6000 | 10.34 | 2.38 | 13.29 | 125.00 | 244.68 | 166.17 | 72.99 | 166.17 | 128.12 |

Table 34: Secondary side simulation data for integrated recirculating target system with two Exergy model 00268-1 shell and tube heat exchanger with 1/8" diameter tubes in series

| | | Secondary Side | | | | | |
|---|---|---|---|---|---|---|---|
| | | | | First Heat Exchanger | | Second Heat Exchanger | |
| **Pump Speed** | **Heat Transfer** | **Flow Rate** | **Press. Drop** | **Inlet Temp.** | **Outlet Temp.** | **Inlet Temp.** | **Outlet Temp.** |
| RPM | kW | LPM | psig | °F | °F | °F | °F |
| | | | | | | | |
| 4000 | 7.86 | 7.16 | 67.00 | 68.00 | 88.13 | 68.00 | 76.12 |
| 4100 | 7.98 | 7.16 | 67.00 | 68.00 | 88.39 | 68.00 | 76.33 |
| 4200 | 8.11 | 7.16 | 67.00 | 68.00 | 88.64 | 68.00 | 76.53 |
| 4300 | 8.24 | 7.16 | 67.00 | 68.00 | 88.89 | 68.00 | 76.74 |
| 4400 | 8.37 | 7.16 | 67.00 | 68.00 | 89.15 | 68.00 | 76.95 |
| 4500 | 8.50 | 7.16 | 67.00 | 68.00 | 89.40 | 68.00 | 77.16 |
| 4600 | 8.63 | 7.16 | 67.00 | 68.00 | 89.65 | 68.00 | 77.37 |
| 4700 | 8.75 | 7.16 | 67.00 | 68.00 | 89.90 | 68.00 | 77.59 |
| 4800 | 8.88 | 7.16 | 67.00 | 68.00 | 90.14 | 68.00 | 77.80 |
| 4900 | 9.01 | 7.16 | 67.00 | 68.00 | 90.38 | 68.00 | 78.02 |
| 5000 | 9.13 | 7.16 | 67.00 | 68.00 | 90.63 | 68.00 | 78.23 |
| 5100 | 9.26 | 7.16 | 67.00 | 68.00 | 90.86 | 68.00 | 78.44 |
| 5200 | 9.38 | 7.16 | 67.00 | 68.00 | 91.10 | 68.00 | 78.66 |
| 5300 | 9.51 | 7.16 | 67.00 | 68.00 | 91.33 | 68.00 | 78.87 |
| 5400 | 9.63 | 7.16 | 67.00 | 68.00 | 91.56 | 68.00 | 79.08 |
| 5500 | 9.75 | 7.16 | 67.00 | 68.00 | 91.78 | 68.00 | 79.29 |
| 5600 | 9.87 | 7.16 | 67.00 | 68.00 | 92.00 | 68.00 | 79.50 |
| 5700 | 9.99 | 7.16 | 67.00 | 68.00 | 92.22 | 68.00 | 79.71 |
| 5800 | 10.11 | 7.16 | 67.00 | 68.00 | 92.43 | 68.00 | 79.91 |
| 5900 | 10.22 | 7.16 | 67.00 | 68.00 | 92.65 | 68.00 | 80.12 |
| 6000 | 10.34 | 7.16 | 67.00 | 68.00 | 92.85 | 68.00 | 80.32 |